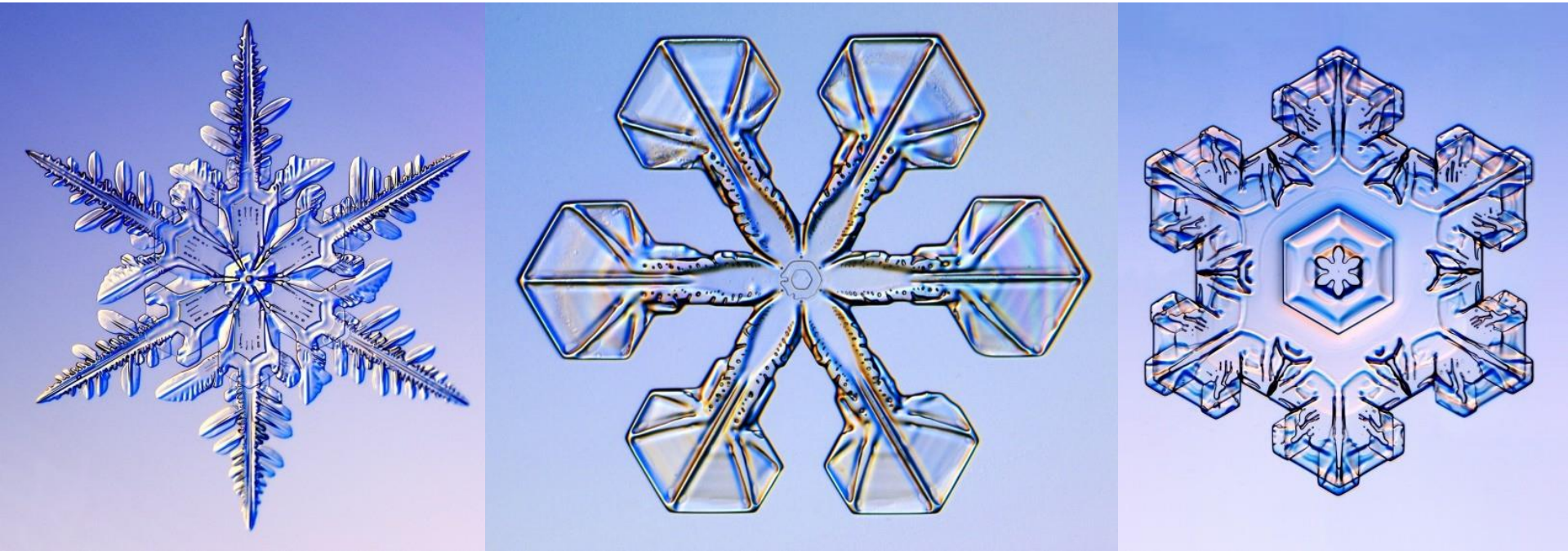
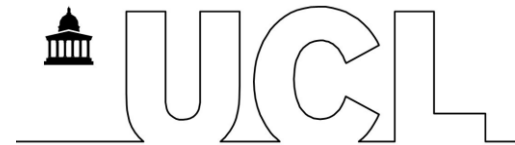


The many facets of experimental ice research

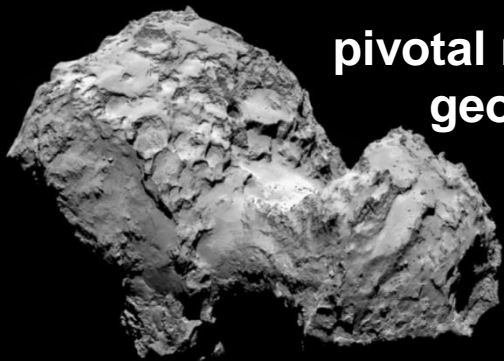
Erice summer school 2016 “Water and Water Systems”



*Dr Christoph G. Salzmann
Reader in Physical and Materials Chemistry
Department of Chemistry
University College London
c.salzmann@ucl.ac.uk*



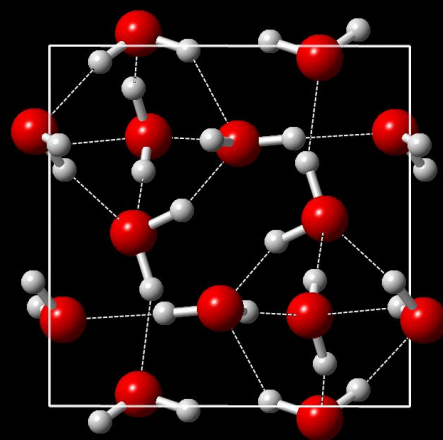
Interest in ice



pivotal role in cosmological & geological processes



key to understanding liquid water



scientific trailblazer

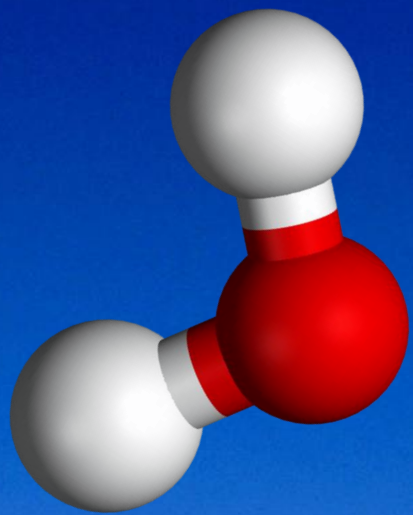


popular culture

influences & regulates our climate

energy storage in clathrate hydrates





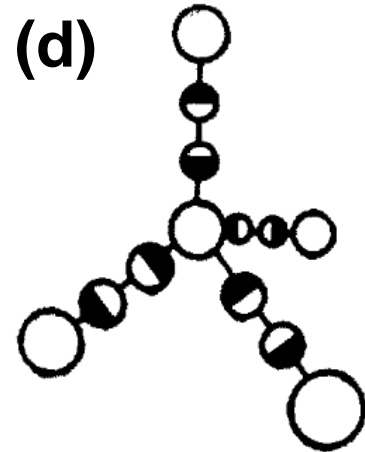
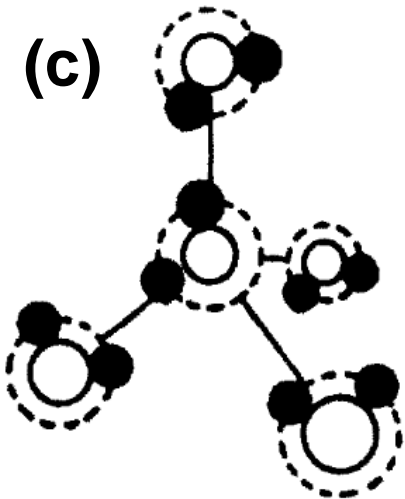
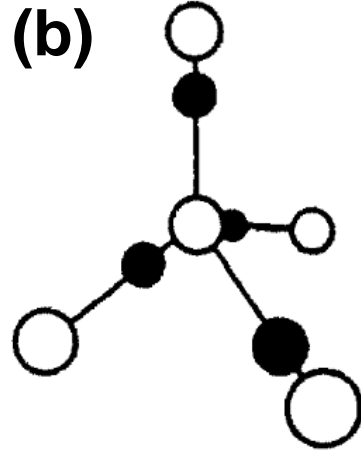
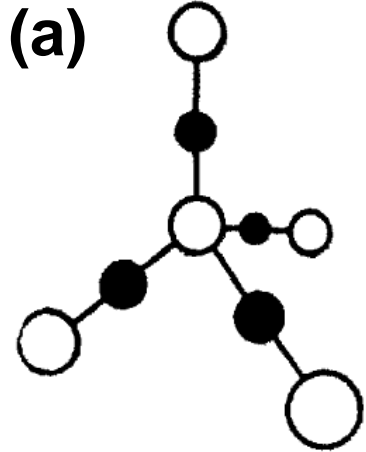
ice Ih



Early structural models

○ OXYGEN

● HYDROGEN



- (a) **Barnes model:** hydrogen atoms midway between oxygen atoms
- (b) **Bernal-Fowler model:** H₂O molecules with defined orientations
- (c) **Hydrogen molecules** rotating around oxygen atoms
- (d) **Pauling model:** two half-occupied hydrogen sites along each hydrogen bond

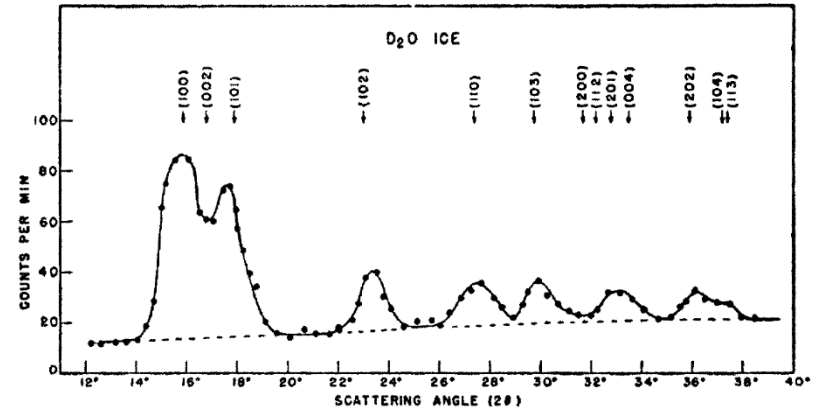
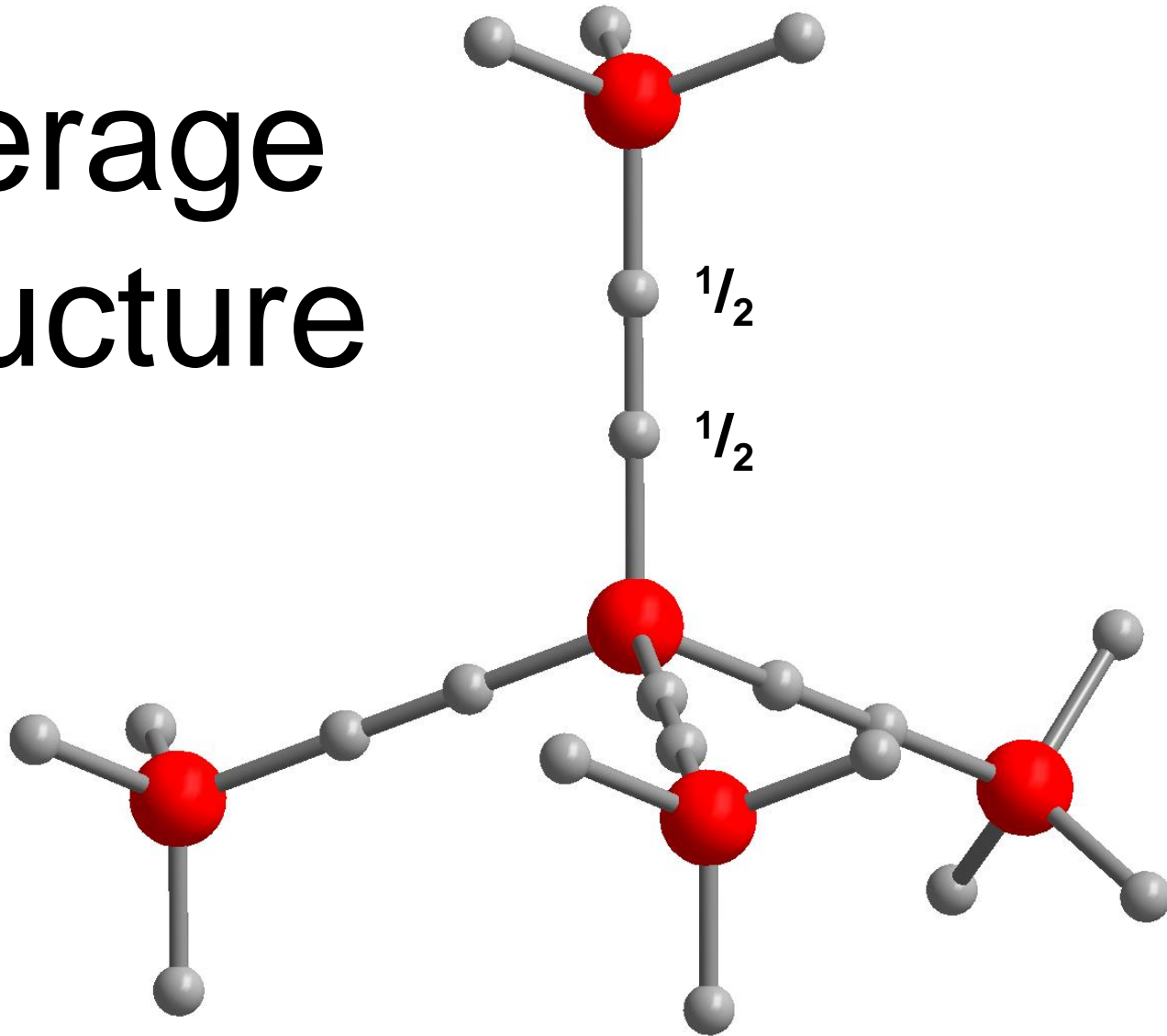


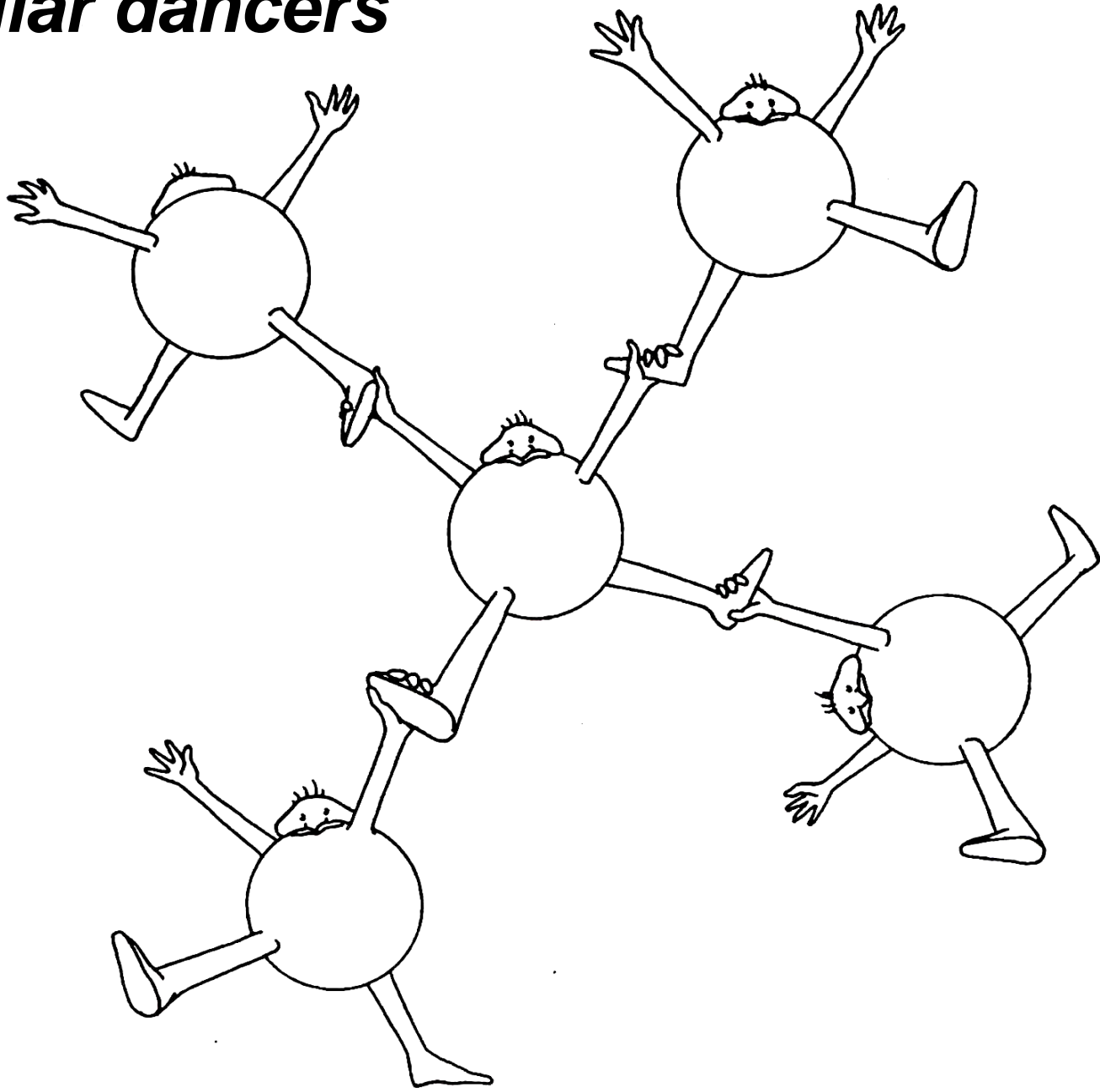
FIG. 1. Neutron diffraction powder pattern of heavy ice (D₂O) taken at -90°C with neutrons of wave-length 1.06Å.

Structure of ice

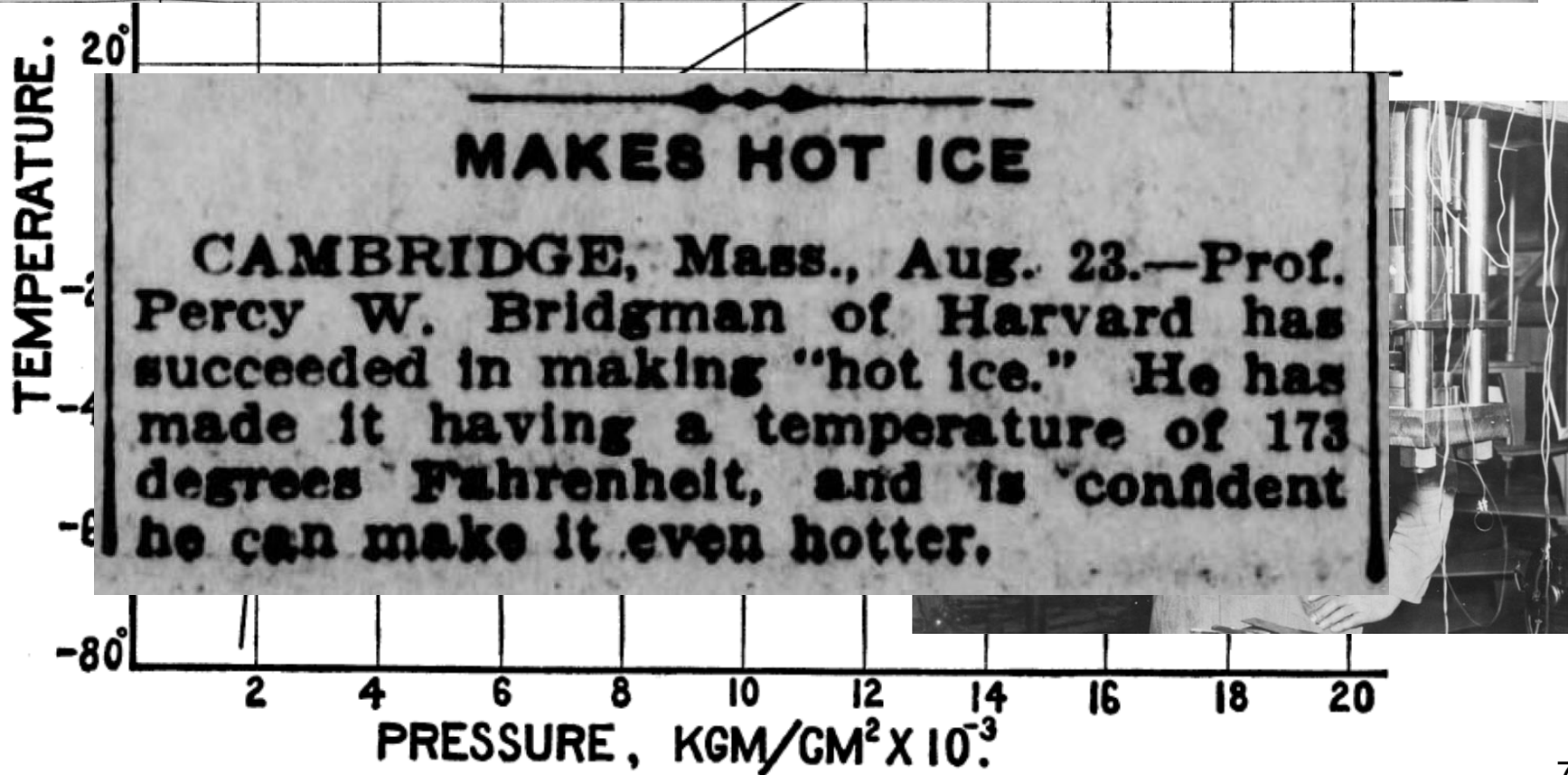
average
structure



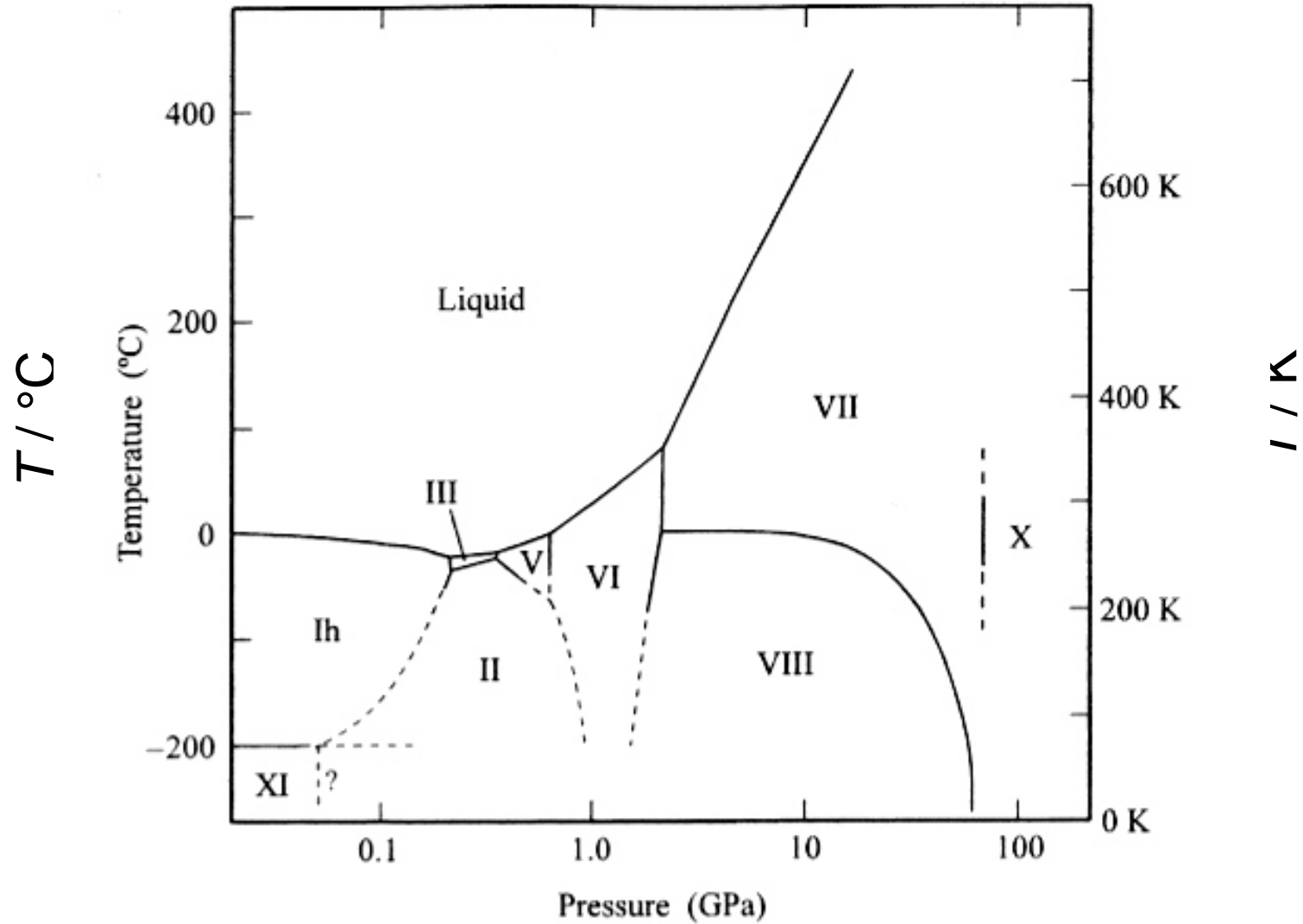
Molecular dancers



Ice under pressure (1912)



Ice under pressure (2016)



C. G. Salzmann, P. G. Radaelli, B. Slater, J. L. Finney, *Phys. Chem. Chem. Phys.*, **13** (2011) 18468

C. G. Salzmann, P. G. Radaelli, E. Mayer, J. L. Finney, *Phys. Rev. Lett.*, **103** (2009) 105701

C. G. Salzmann, P. G. Radaelli, A. Hallbrucker, E. Mayer, J. L. Finney, *Science*, **311** (2006) 1758

Heating ice VI at ambient pressure



'Strange' phases of ice in nature

(1) Stacking-disordered ice in Earth's atmosphere

B.J. Murray, D.A. Knopf, A.K. Bertram, *Nature* 434 (2005) 202.

(2) Ice VI inclusions in diamonds

H. Kagi, R. Lu, P. Davidson, A.F. Goncharov, H.K. Mao, R.J. Hemley, *Mineralogical Magazine* 64 (2000) 1089.

(3) Ice VII in cold subconducting slabs

C.R. Bina, A. Navrotsky, *Nature* 408 (2000) 844.

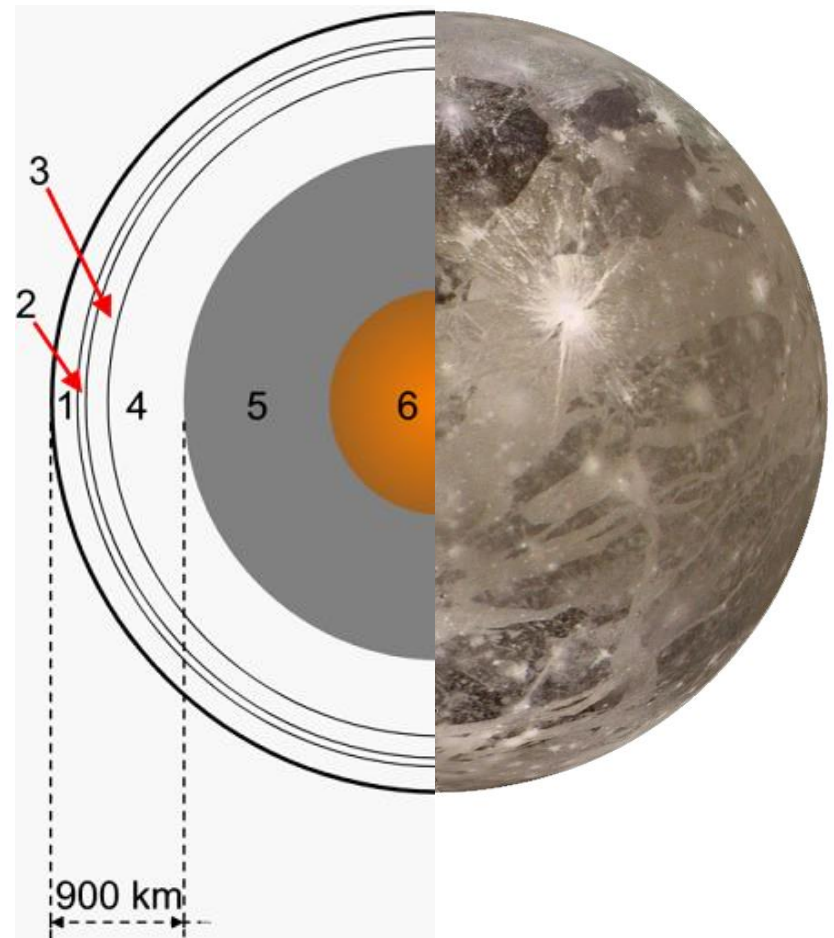
(4) High-pressure ices in icy moons

Jupiter's icy moon Ganymede

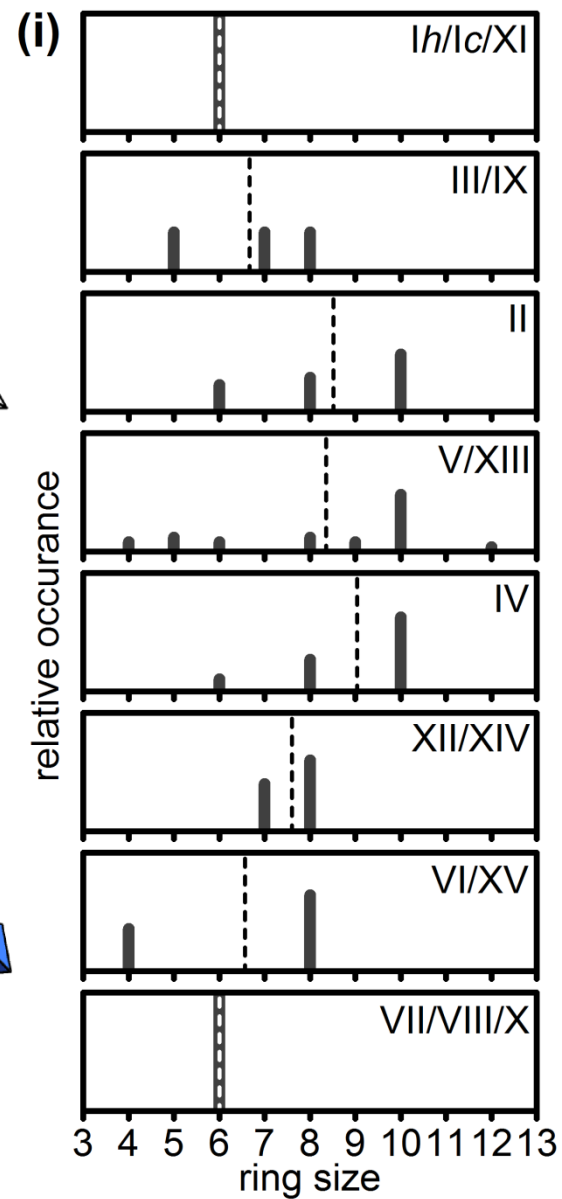
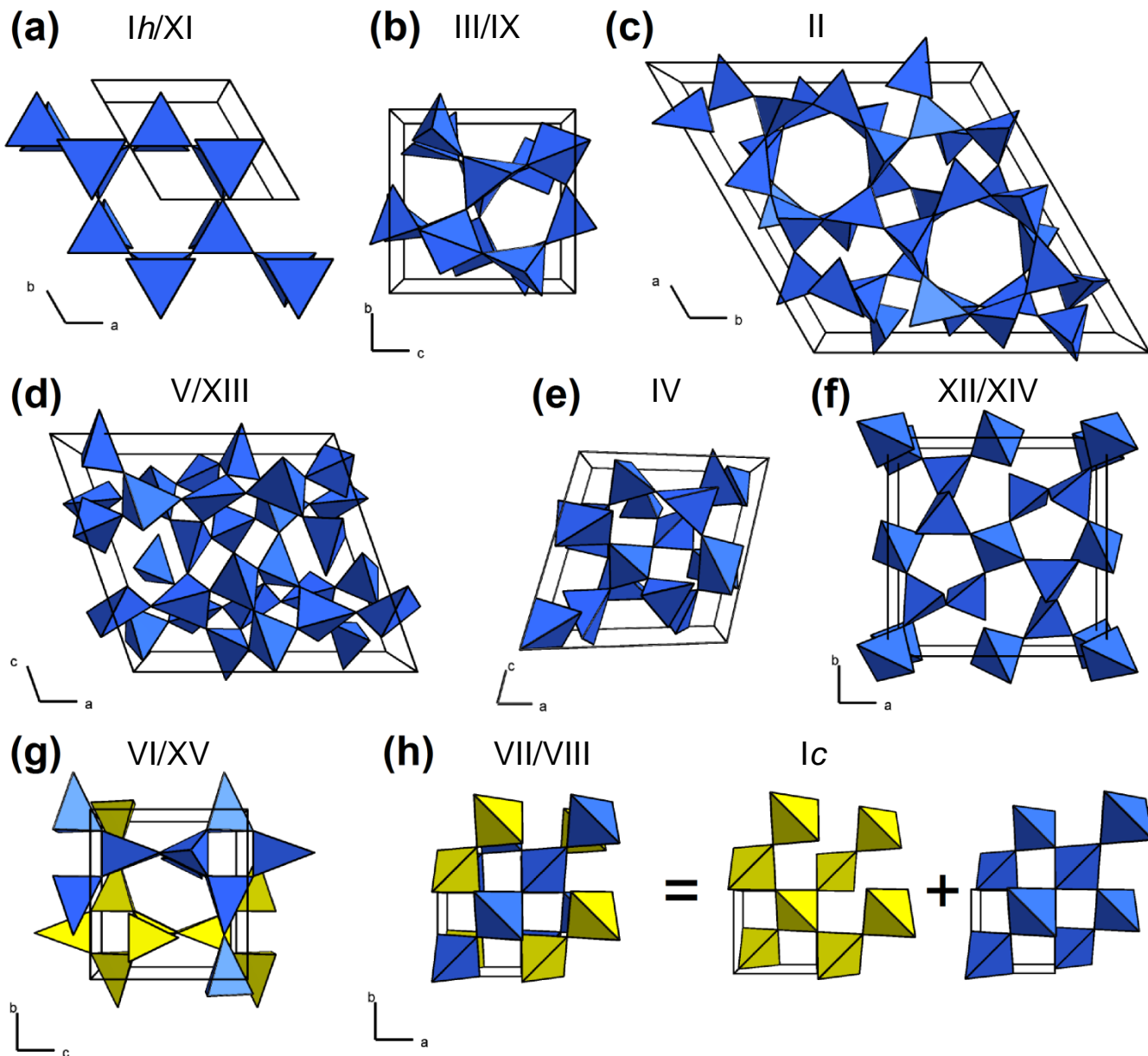
- 1 ice *I_h*
- 2 ice III
- 3 ice V
- 4 ice VI
- 5 silicates
- 6 Fe/FeS core

Antarctica: 1×10^{19} kg ice *I_h*

Ganymede: 3.5×10^{22} kg ice VI



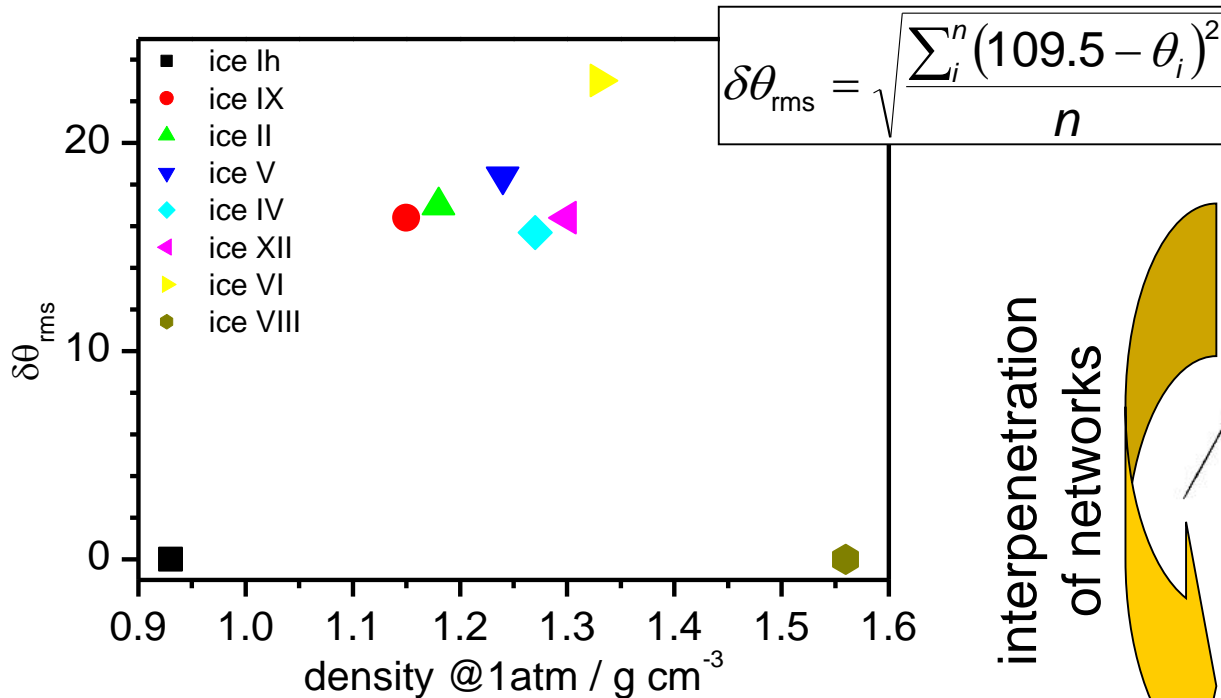
The crystal structures of ice



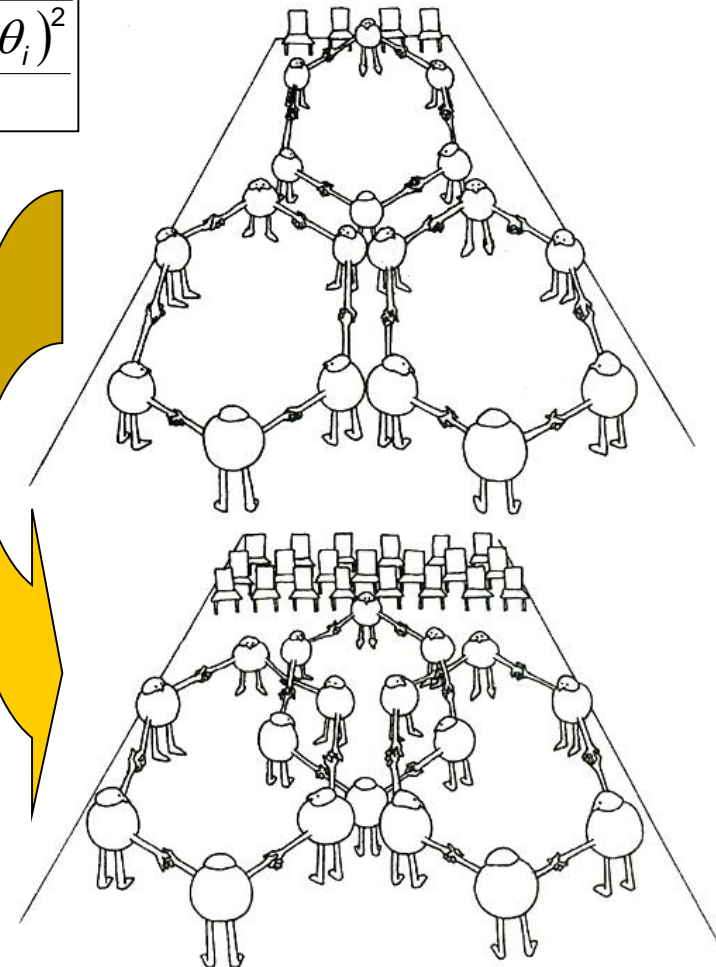
Structural trends

Higher density structures achieved by:

(1) Distortion of tetrahedral arrangement (bending of H-bonds)



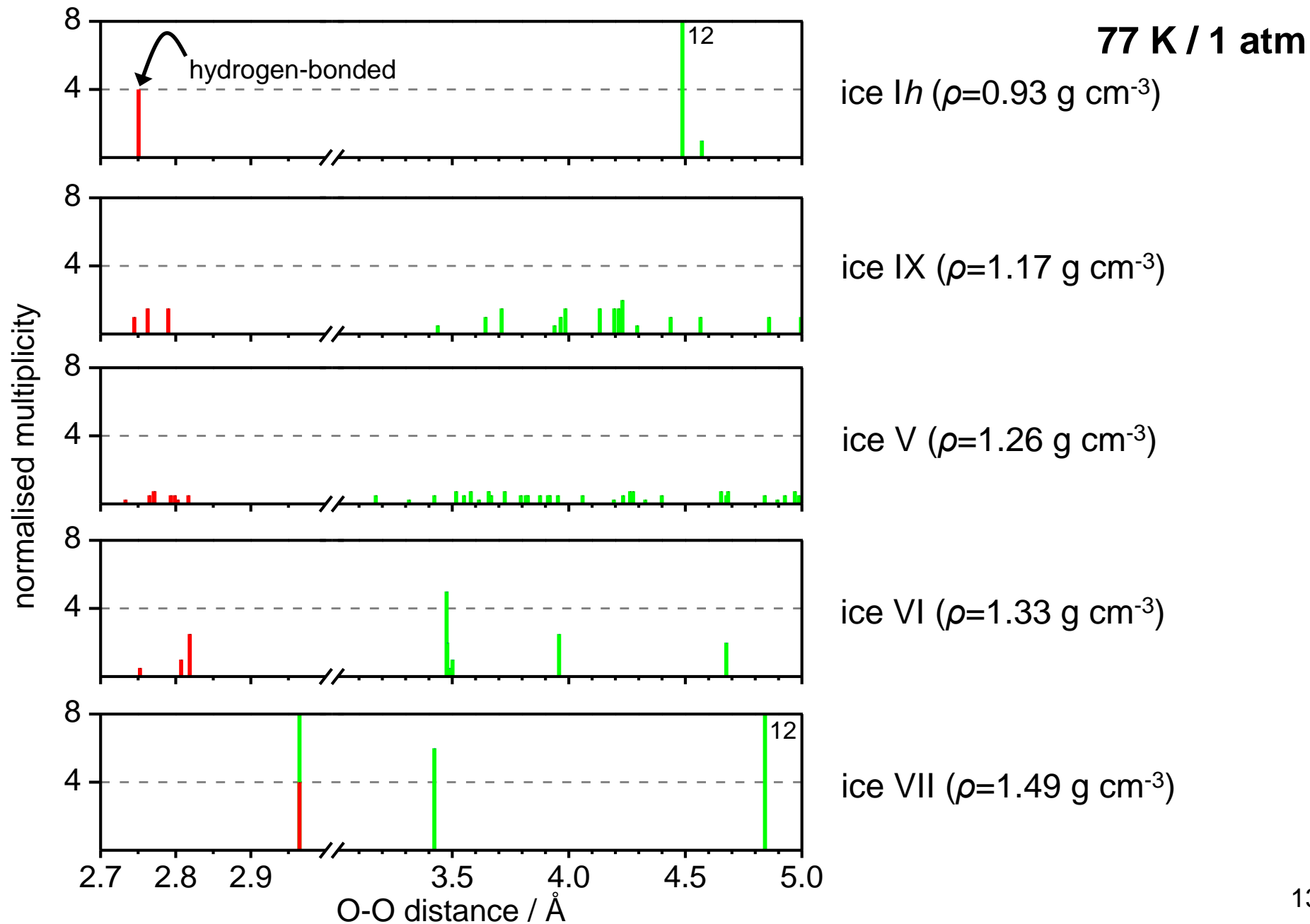
interpenetration
of networks



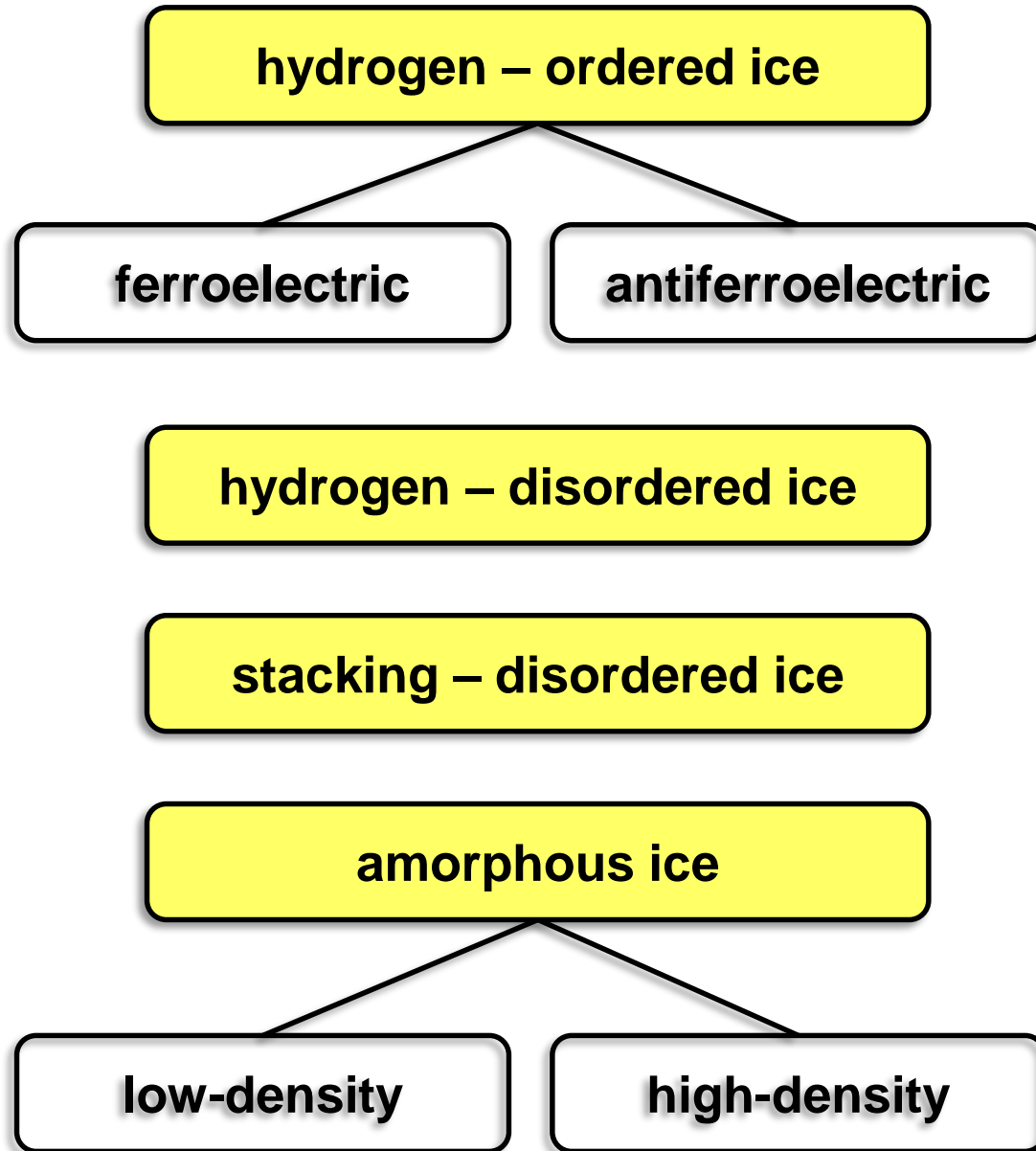
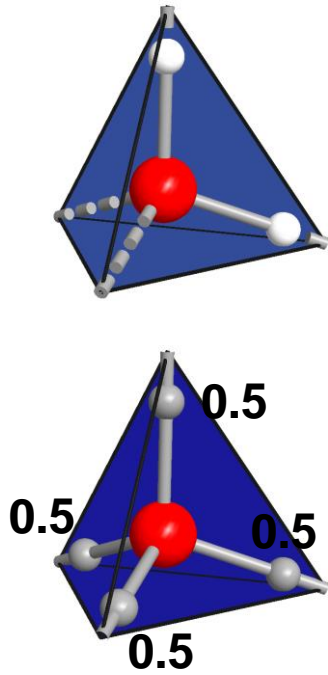
(2) Interpenetration of networks

Pressure distance paradox: Intermolecular distances increase in the higher density phases due to increase in coordination number.

Structural trends

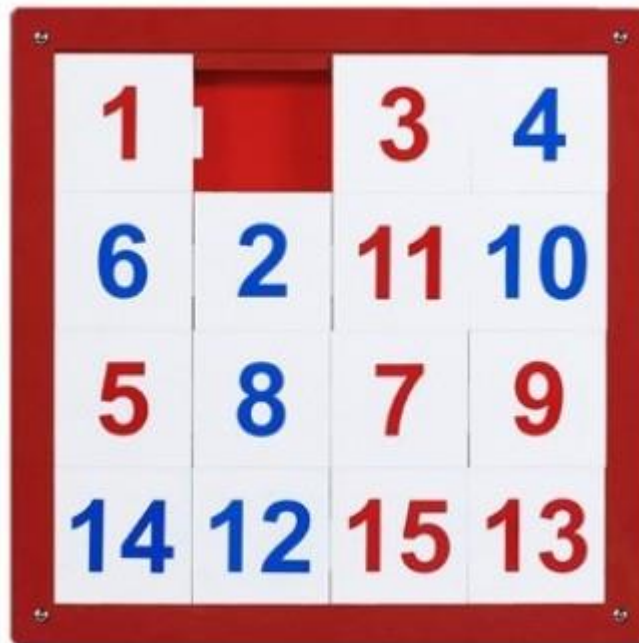


Structural classification of ice materials

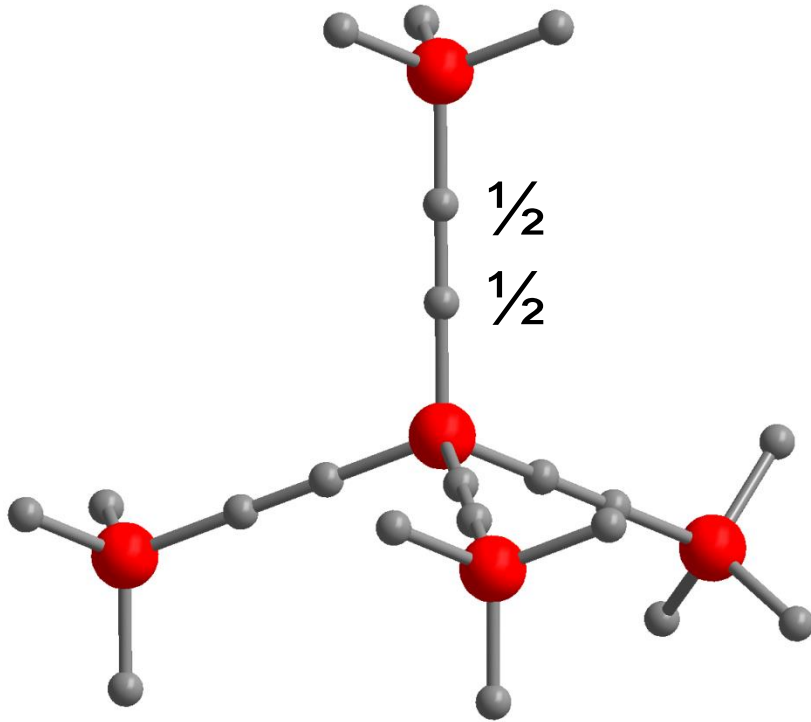


structural disorder

1. Hydrogen order / disorder

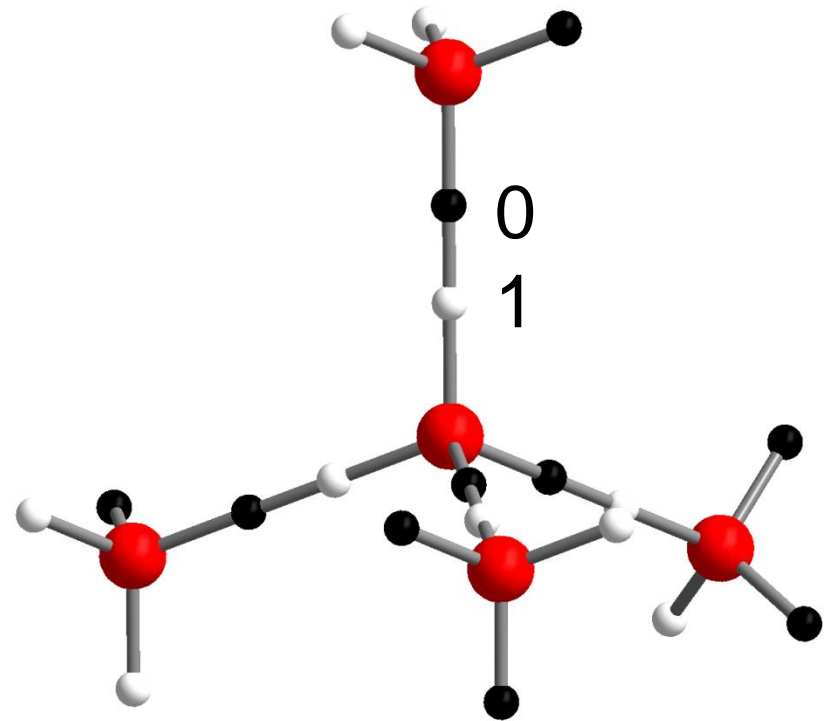


Hydrogen disorder / order in ice



hydrogen disorder

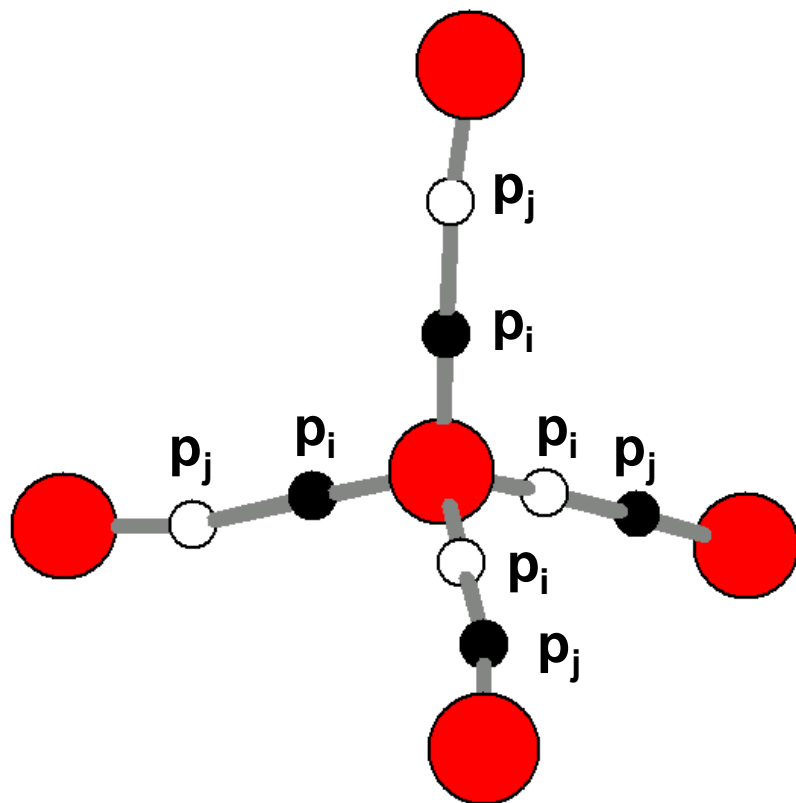
configurational entropy:
 $S = R \ln (3/2) = 3.37 \text{ J mol}^{-1} \text{ K}^{-1}$
(Pauling entropy)



hydrogen order

configurational entropy:
 $S = R \ln 1 = 0$
(3rd law of thermodynamics)

Bernal – Fowler ice rules / Pauling entropy



Bernal – Fowler rules preserve stoichiometry of the H_2O molecule:

$$(1) p_i + p_j = 1$$

$$(2) \sum p_i = 2$$

Pauling entropy for a completely disordered (dentric) ice:

$N H_2O$ molecules

Distribute hydrogen atoms randomly for each hydrogen bond.

$2N$ H atoms $\rightarrow 2^{2N}$ arrangements

$$W = 2^{2N} \cdot (6/16)^N = (3/2)^N$$

$$S = k \ln (W) \quad (\text{Boltzmann formula})$$

$$S = k \ln (3/2)^N = 3.38 \text{ J mol}^{-1} \text{ K}^{-1}$$

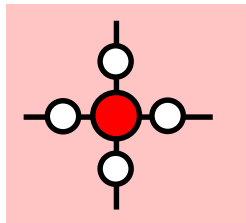
For completely ordered ices:

$$S = k \ln 1 = 0$$

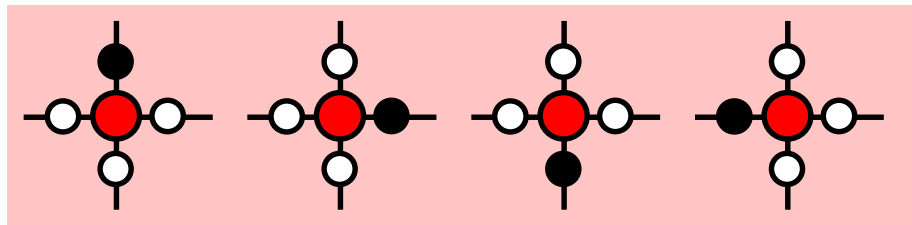
3rd law of thermodynamics

$(6/16)^N$ correction factor

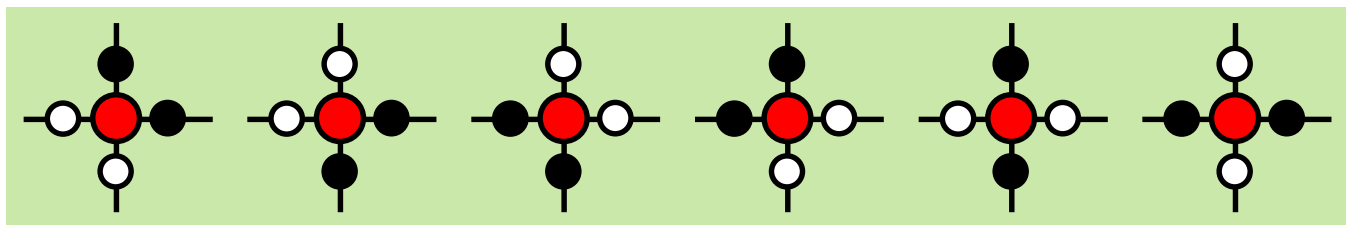
1



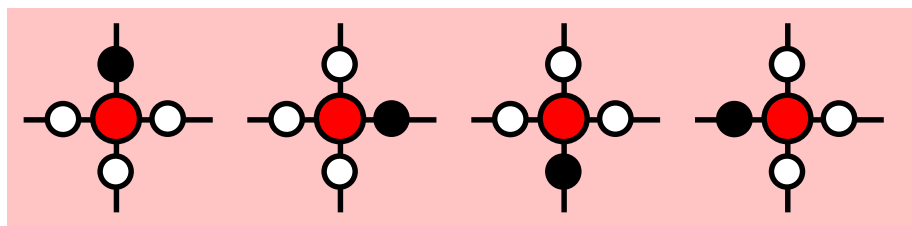
4



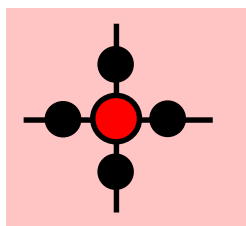
6



4

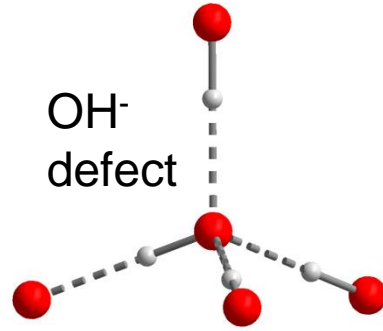
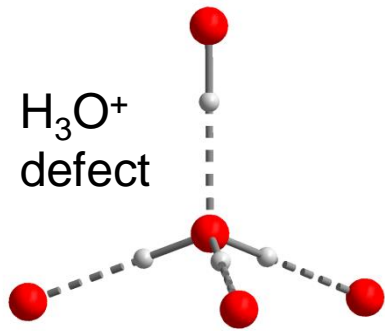


1

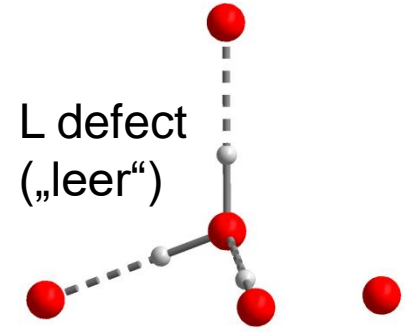
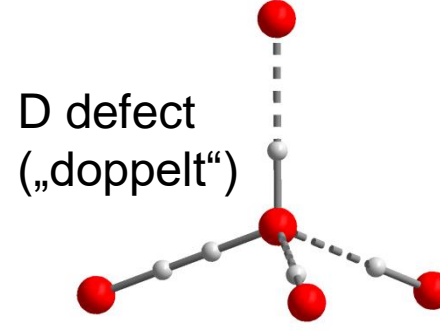


Point defects in ice

Molecular reorientation in ice requires point defects...



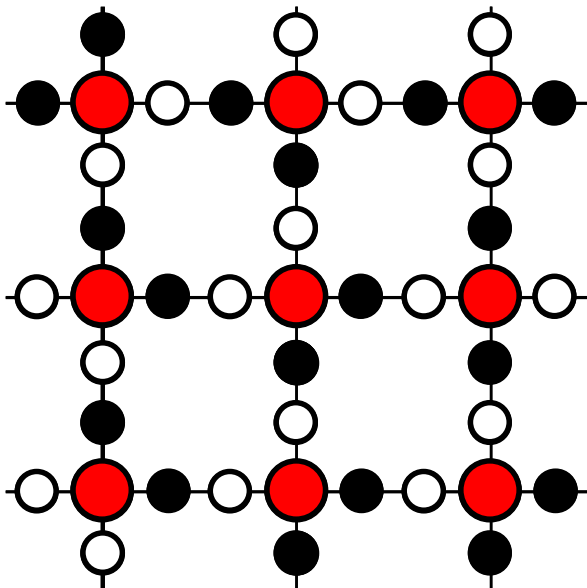
ionic defects



Bjerrum defects

... and their migration through the crystal.

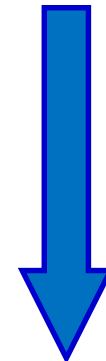
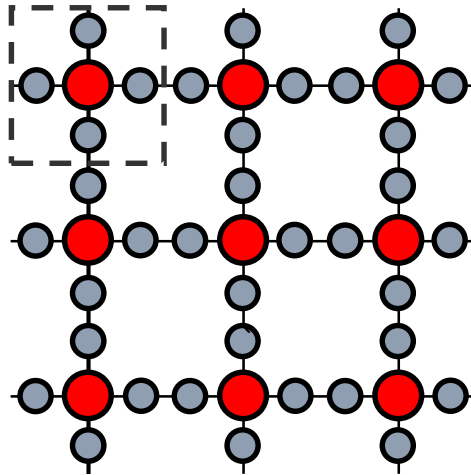
end configuration



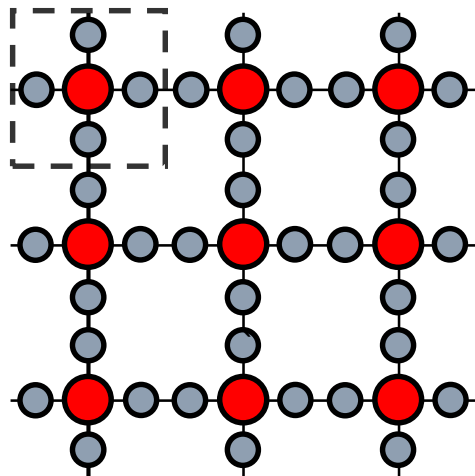
start configuration

Hydrogen-ordering phase transitions

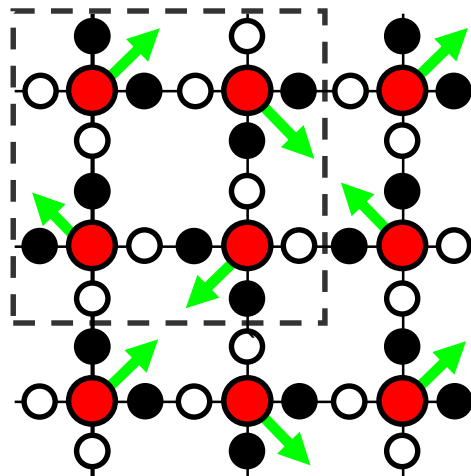
hydrogen disorder



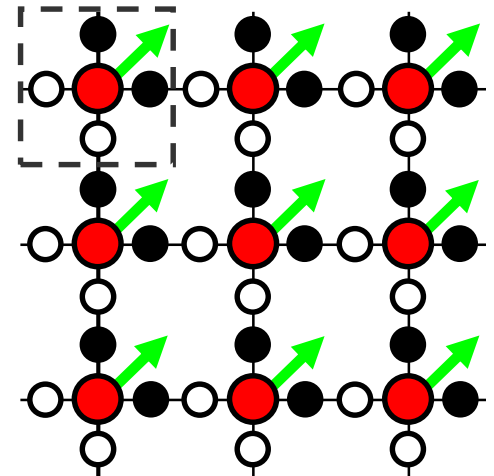
temperature decrease



hydrogen disorder
orientational glass



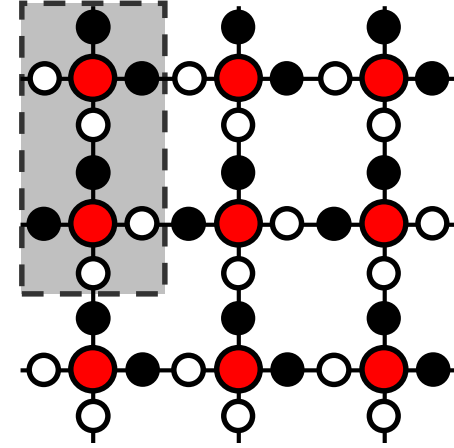
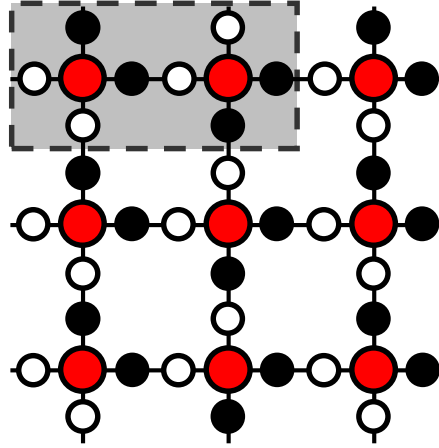
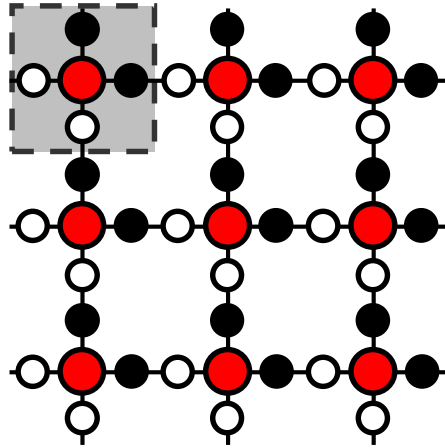
hydrogen order
antiferroelectric



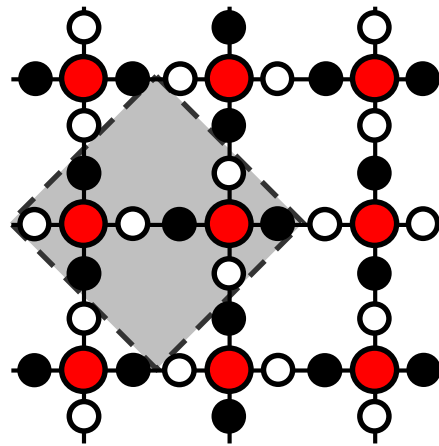
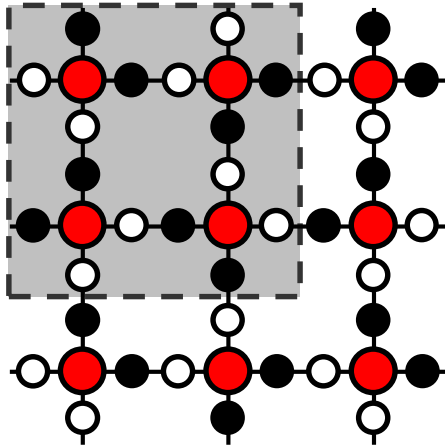
hydrogen order
ferroelectric

Possible hydrogen ordered structures

ferroelectric



antiferroelectric



Multitude of possible ordered structures

Different structures have different energies

Importance of the hydrogen-ordered phases

(1) Geophysics of icy moons and plane

Question of (anti)ferroelectricity is crucial.

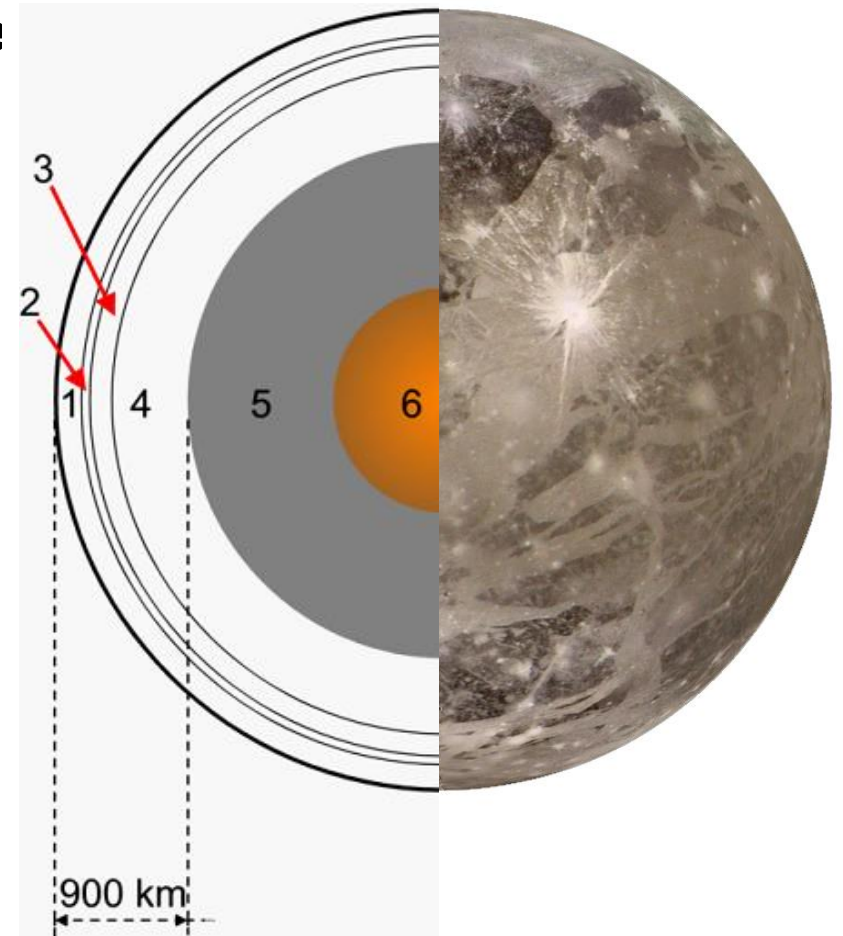
(2) Vibrational spectroscopy of condensed H₂O

Only condensed phases of H₂O with strictly defined selection rules.
Development of new structure - spectroscopy correlations.

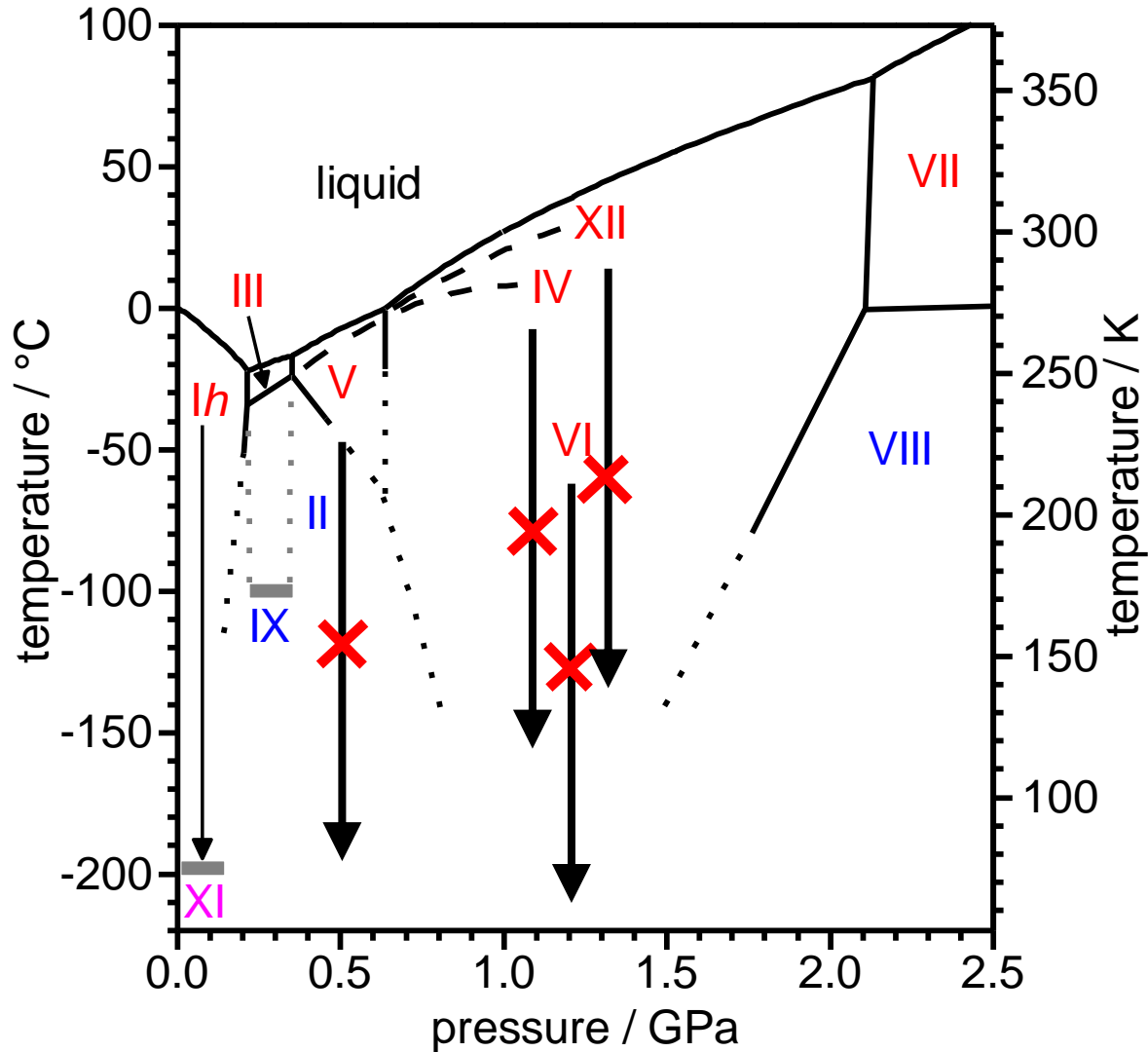
(3) Benchmark structures for computational methods

(4) New insights into defect dynamics

(5) Dynamics of the amorphous ices



Order / disorder in the phase diagram



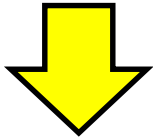
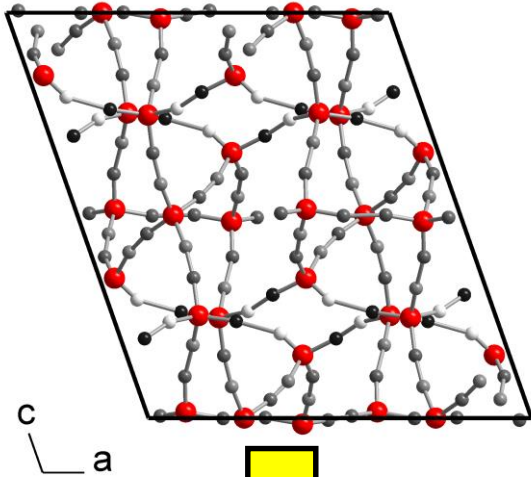
- hydrogen-disordered ice
- hydrogen-ordered ice (anti-ferroelectric)
- hydrogen-ordered ice (ferroelectric)

**Let's try
acid doping !**

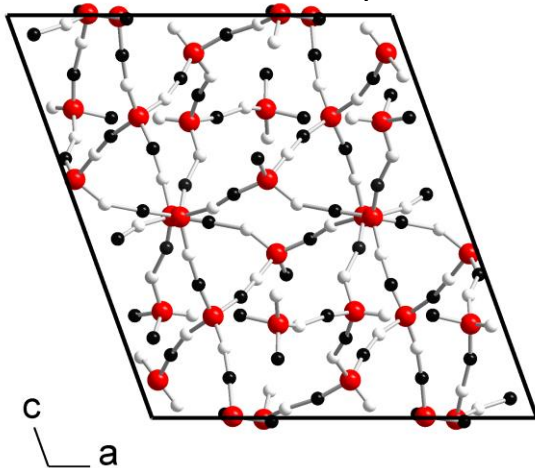
Upon cooling ices IV, V, VI and XII hydrogen disorder is frozen-in.
KOH doping has been tried for ices V and VI which showed no or little effect.

New hydrogen order / disorder pairs

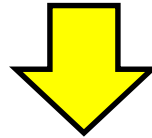
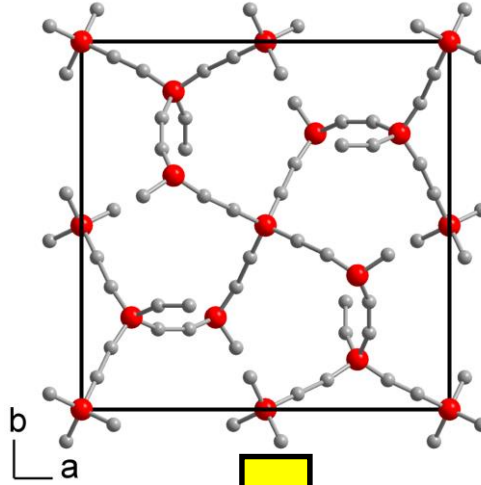
ice V ($A2/a$)



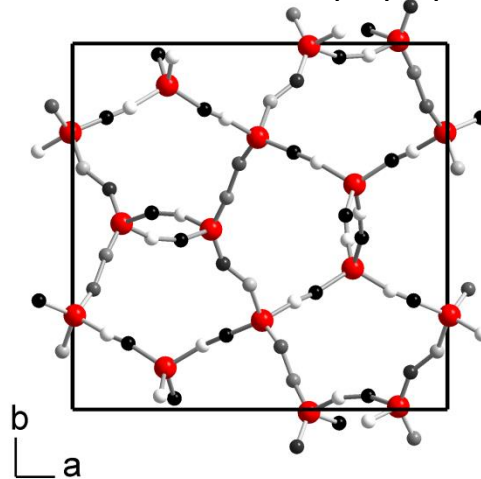
ice XIII ($P2_1/a$)



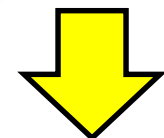
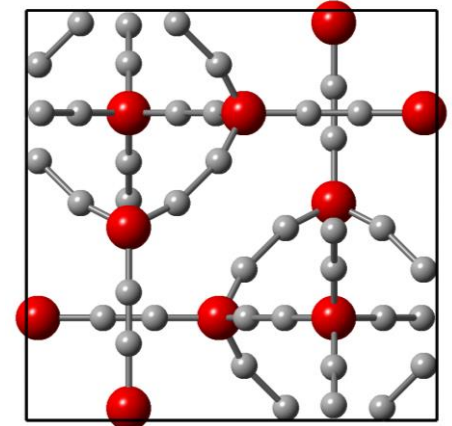
ice XII ($I4(\bar{1})2d$)



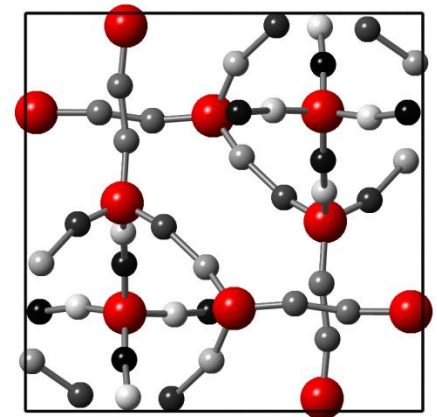
ice XIV ($P2_12_12_1$)



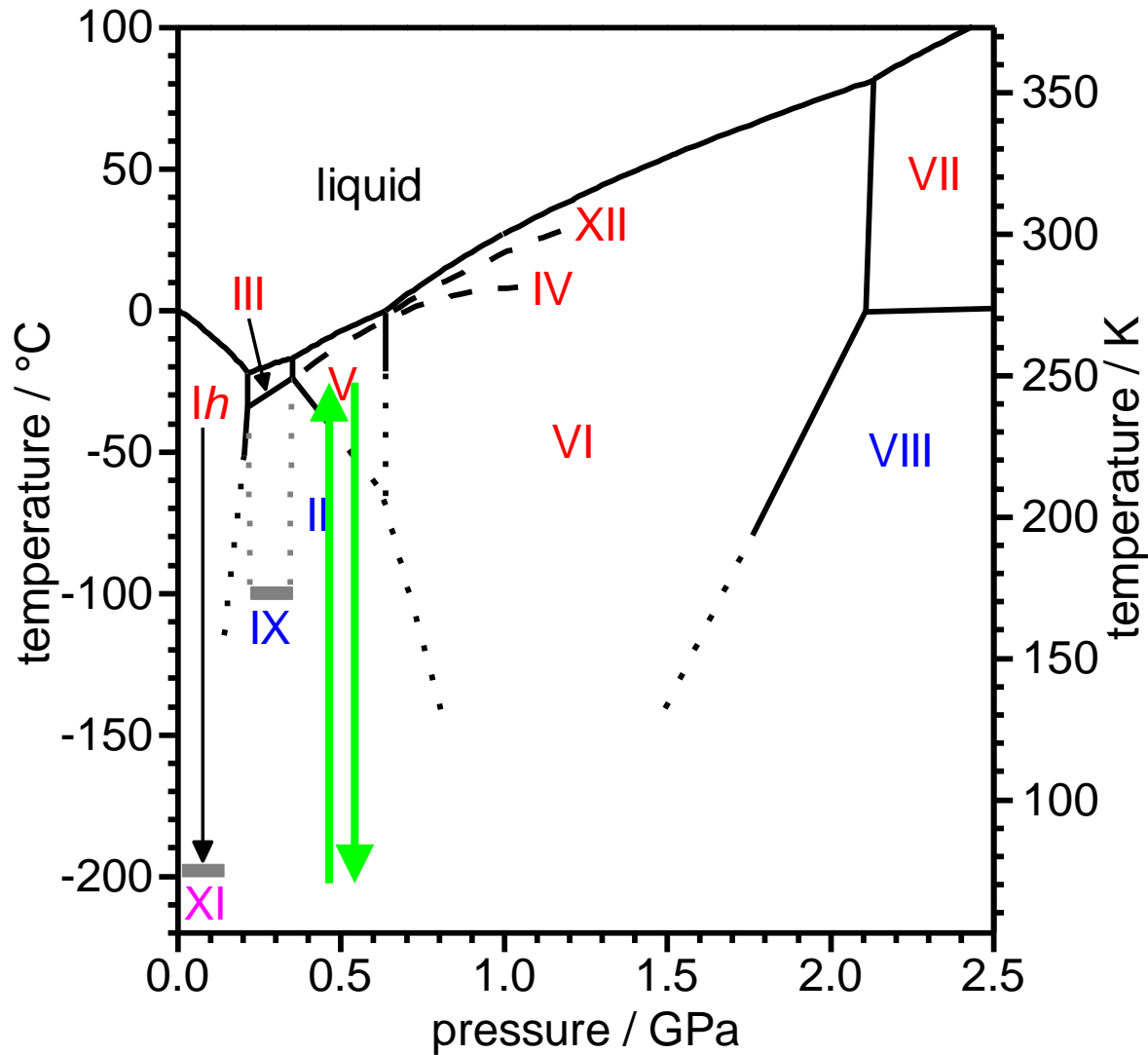
ice VI ($P4_2/nmc$)



ice XV ($P-1$)



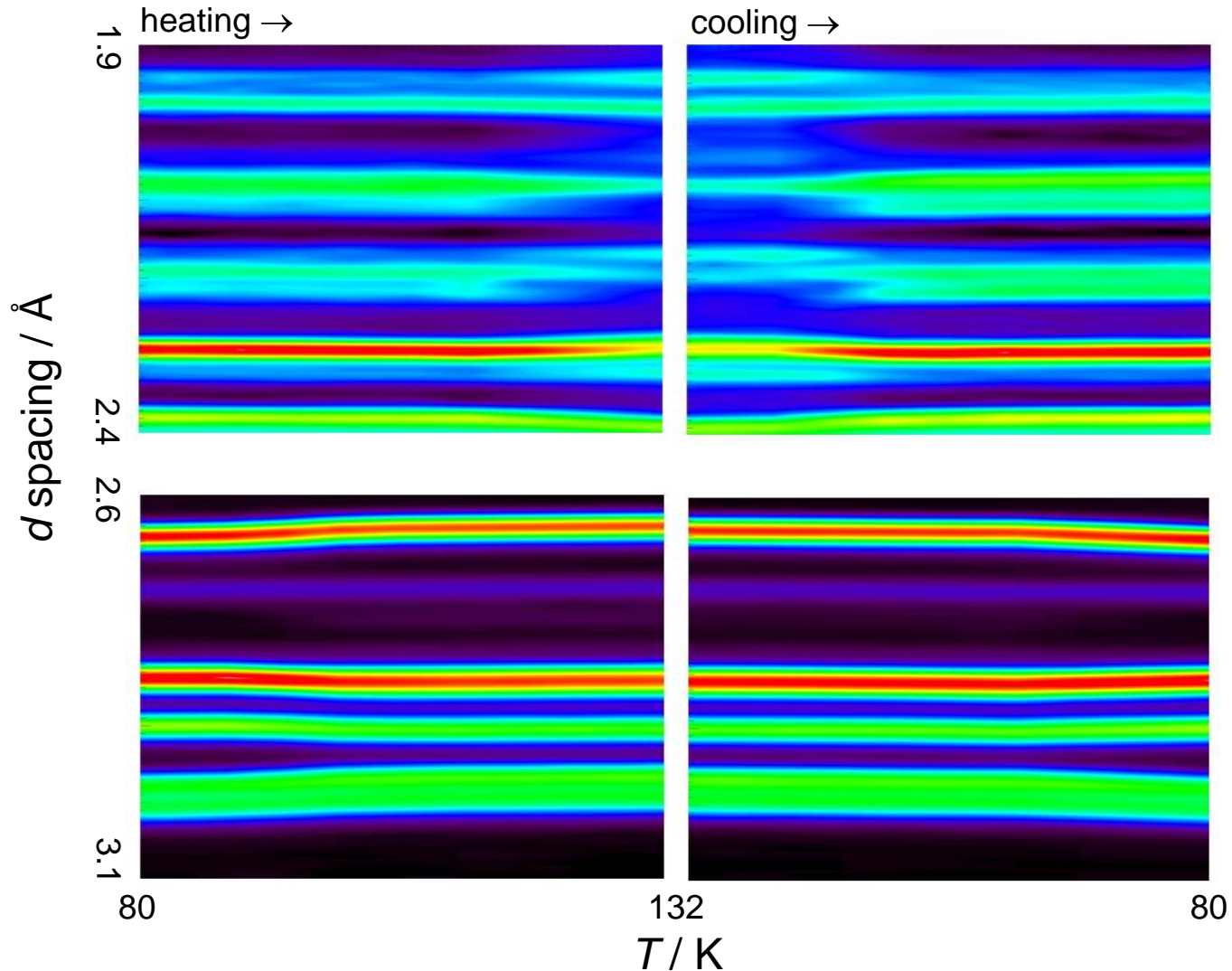
The ice V to ice XIII phase transition



Isobaric heating of doped ice *Ih* at 0.5 GPa followed by cooling back to 77 K.

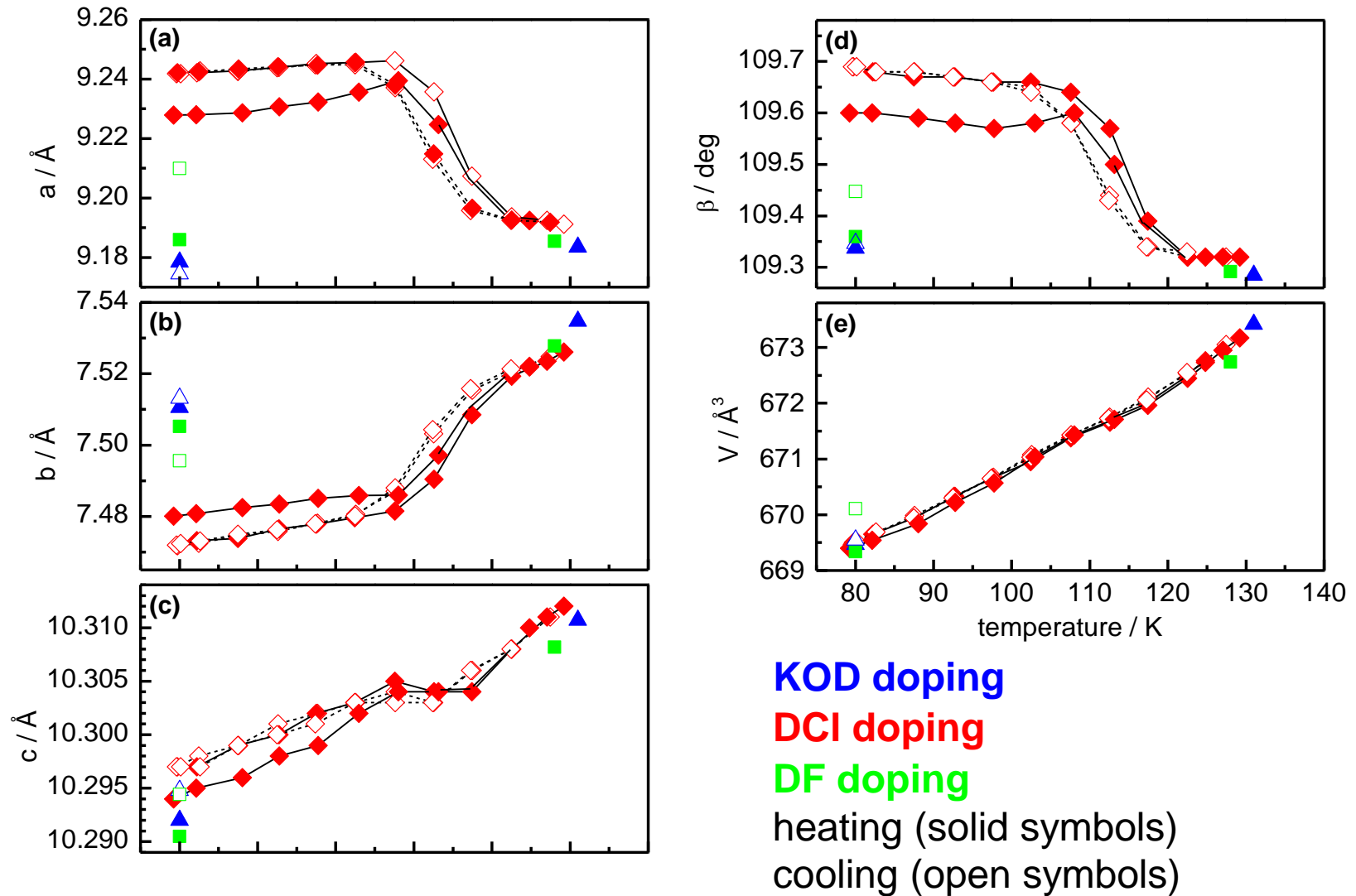
Neutron diffraction at ambient pressure

0.01 M DCI-doped slow-cooled D₂O sample at 0.5 GPa



Ice XIII to ice V phase transition can be seen reversibly.

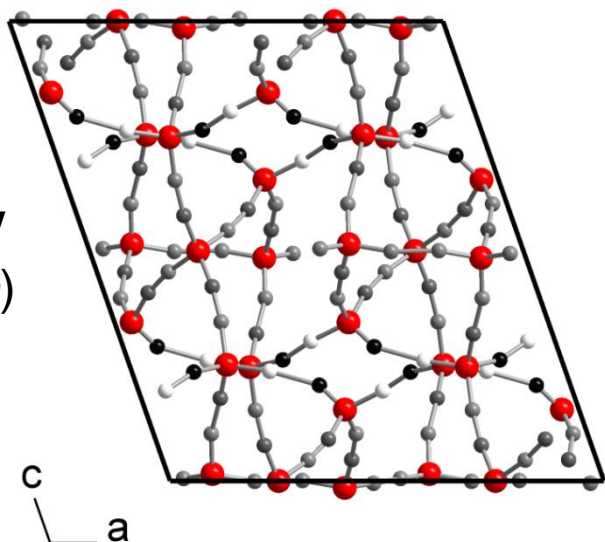
Changes in lattice constants



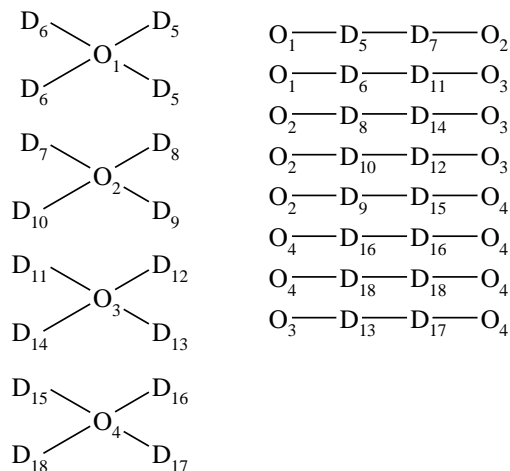
No detectable change of volume during the phase transition.

Structure of ice XIII

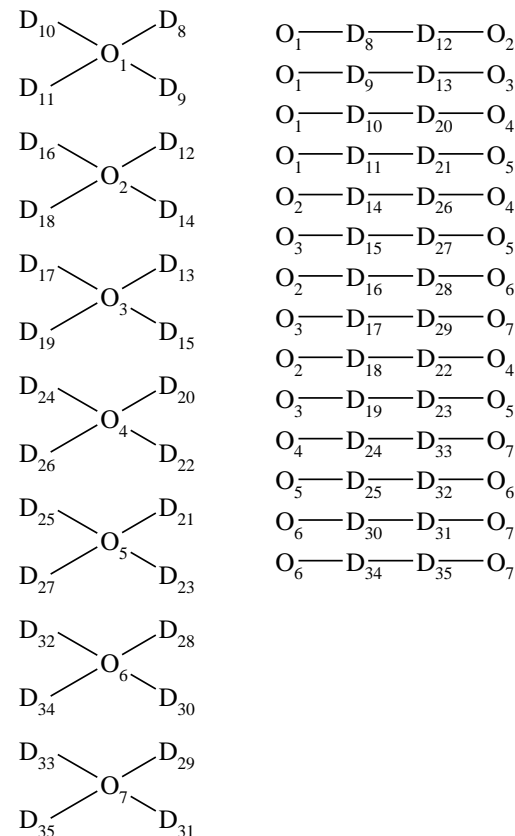
ice V
(A2/a)



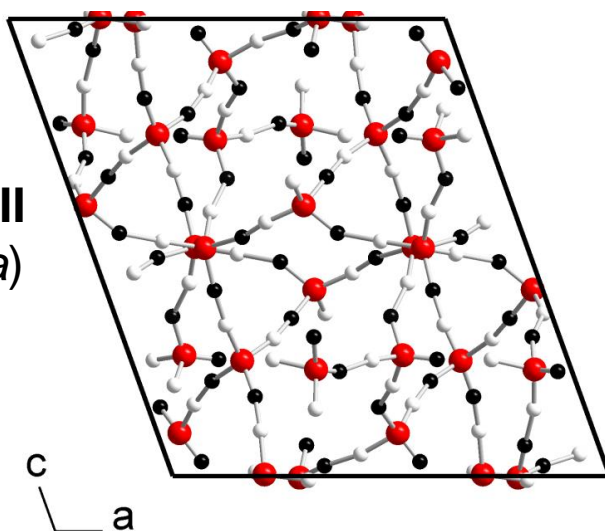
ice V (A2/a)



ice XIII (P2₁/a)



ice XIII
(P2₁/a)



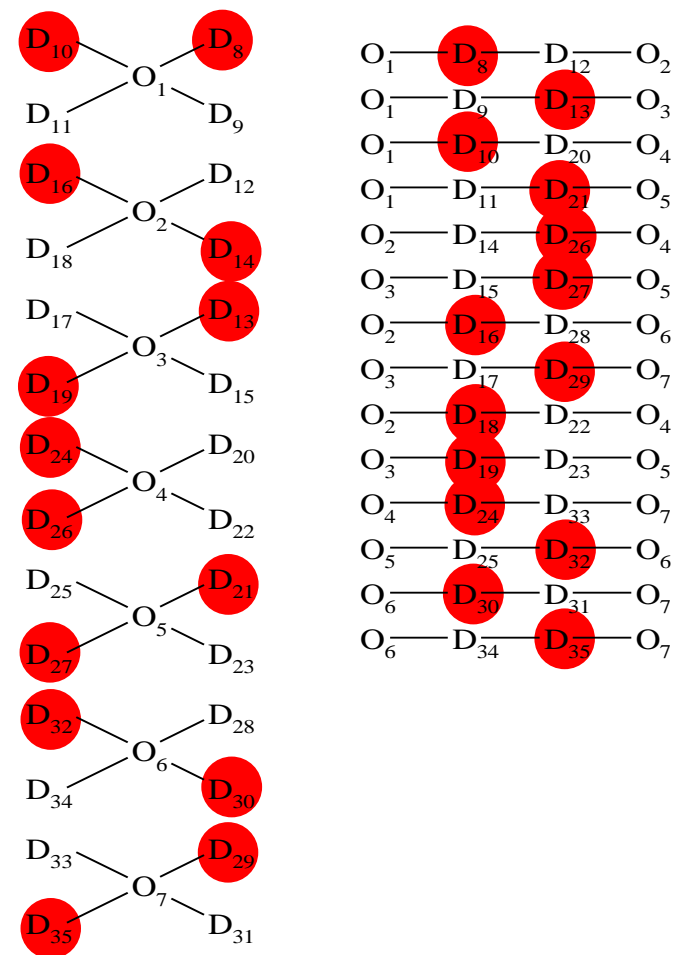
Most complicated structure of all phases of ice
(7 water molecules in the asymmetric unit)

Structure of ice XIII

Table 1. Fractional coordinates and isotropic atomic-displacement parameters (U_{iso}) for ice XIII (80 K and ambient pressure). Numbers in parentheses are statistical errors of the last significant digit. Deuterium positions with refined fractional occupancies <0.1 are omitted from the table. The spacegroup is $P2_1/a$ and the unit cell parameters are as follows: $a = 9.2417(1) \text{ \AA}$, $b = 7.4724(1) \text{ \AA}$, $c = 10.2970(1) \text{ \AA}$, $\beta = 109.6873(9)^\circ$. Data were collected after cooling the sample at $\sim 0.2 \text{ K min}^{-1}$ from 130 to 80 K at ambient pressure. All atoms lie on general positions (multiplicity = 4).

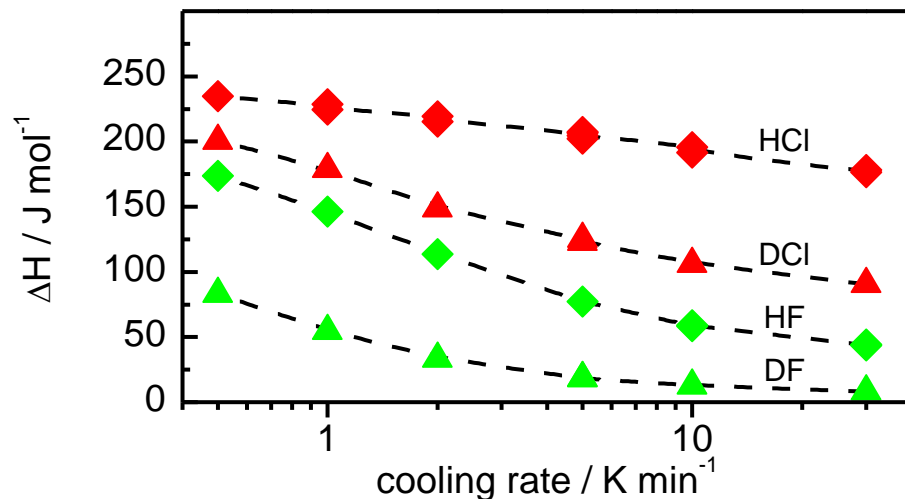
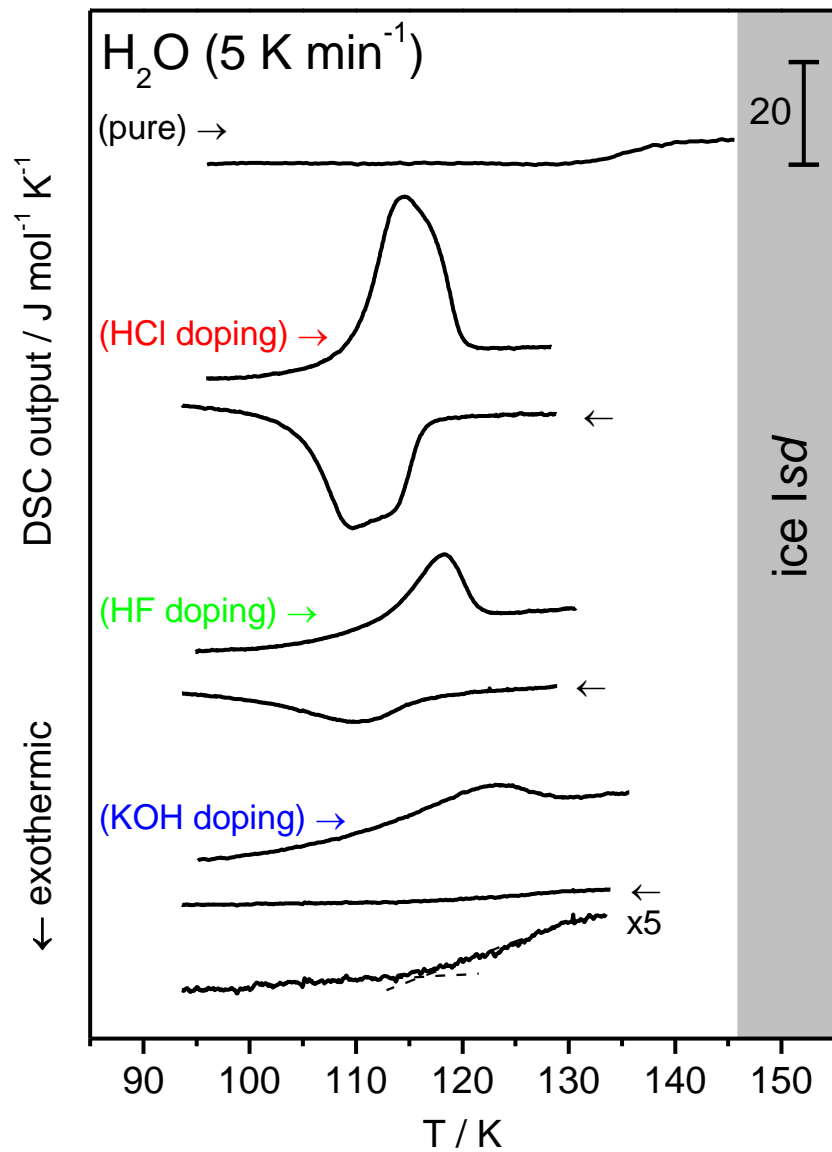
	<i>x</i>	<i>y</i>	<i>z</i>	$U_{iso} * 100$	Occupancies
O1	0.2541(6)	0.5629(5)	0.2517(5)	0.41(3)	1.0000
O2	0.4771(6)	0.7992(5)	0.4089(5)	0.41(3)	1.0000
O3	0.0503(6)	0.8082(6)	0.0941(5)	0.41(3)	1.0000
O4	0.2613(5)	0.4045(6)	0.4992(5)	0.41(3)	1.0000
O5	0.2113(4)	0.4029(5)	0.0034(5)	0.41(3)	1.0000
O6	0.4147(5)	0.1103(7)	0.2336(4)	0.41(3)	1.0000
O7	0.1245(5)	0.1142(6)	0.2643(4)	0.41(3)	1.0000
D8	0.3444(4)	0.6427(5)	0.3008(3)	1.01(3)	0.991(6)
D10	0.2458(5)	0.4942(5)	0.3299(5)	1.01(3)	0.943(5)
D13	0.1074(4)	0.7187(5)	0.1563(4)	1.01(3)	0.952(6)
D16	0.4820(4)	0.9075(5)	0.3558(4)	1.01(3)	0.968(6)
D18	0.5763(5)	0.7499(5)	0.4437(4)	1.01(3)	0.974(7)
D19	0.9486(5)	0.7508(5)	0.0478(4)	1.01(3)	1.037(5)
D21	0.2372(3)	0.4543(5)	0.0989(4)	1.01(3)	1.015(6)
D24	0.3043(4)	0.4904(6)	0.5777(4)	1.01(3)	0.896(5)
D26	0.1708(4)	0.3555(6)	0.5137(4)	1.01(3)	1.015(5)
D27	0.3072(4)	0.3737(6)	0.9904(3)	1.01(3)	1.014(5)
D29	0.0781(4)	0.0194(6)	0.1989(4)	1.01(3)	0.938(5)
D30	0.3250(5)	0.1374(5)	0.2554(5)	1.01(3)	0.916(6)
D32	0.3823(5)	0.0496(6)	0.1467(5)	1.01(3)	0.920(6)
D35	0.0509(4)	0.2082(6)	0.2548(5)	1.01(3)	0.911(7)

ice XIII ($P2_1/a$)



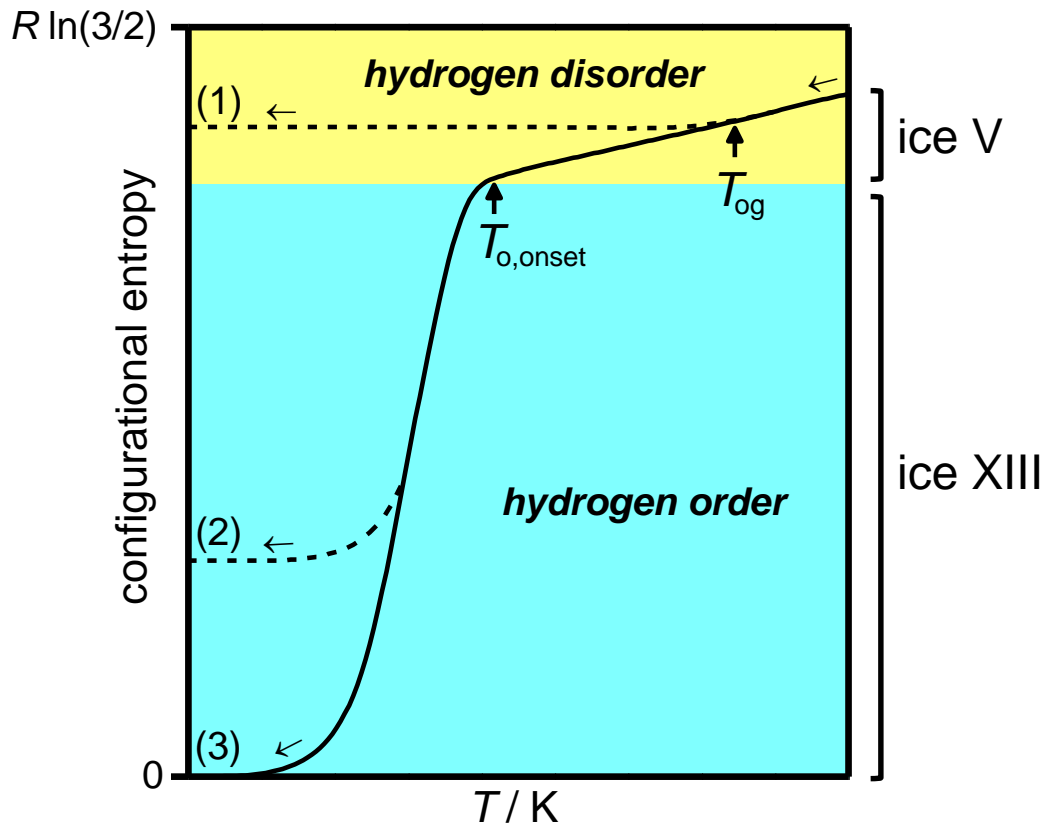
One structure out of 35 possible ones in $P2_1/a$.
Confirmed by DFT to be the lowest energy structure.

Kinetics of hydrogen ordering



Glass-transition features for pure and KOH-doped ice V.
 First-order like transitions for HCl- and HF-doped samples.
 Ordering transition can be quenched.
 HCl is better than HF at facilitating the phase transition to ice XIII.
 H₂O samples are easier to hydrogen order than D₂O.
 Maximal ΔH value around 250 J mol⁻¹.
 Loss of 66% of Pauling entropy.

Kinetics of hydrogen ordering



Depending on dopant, cooling rate and pressure different states are obtained:

- (1) orientational glass
- (2) partially disorder in the ordered phase
- (3) fully hydrogen-ordered phase

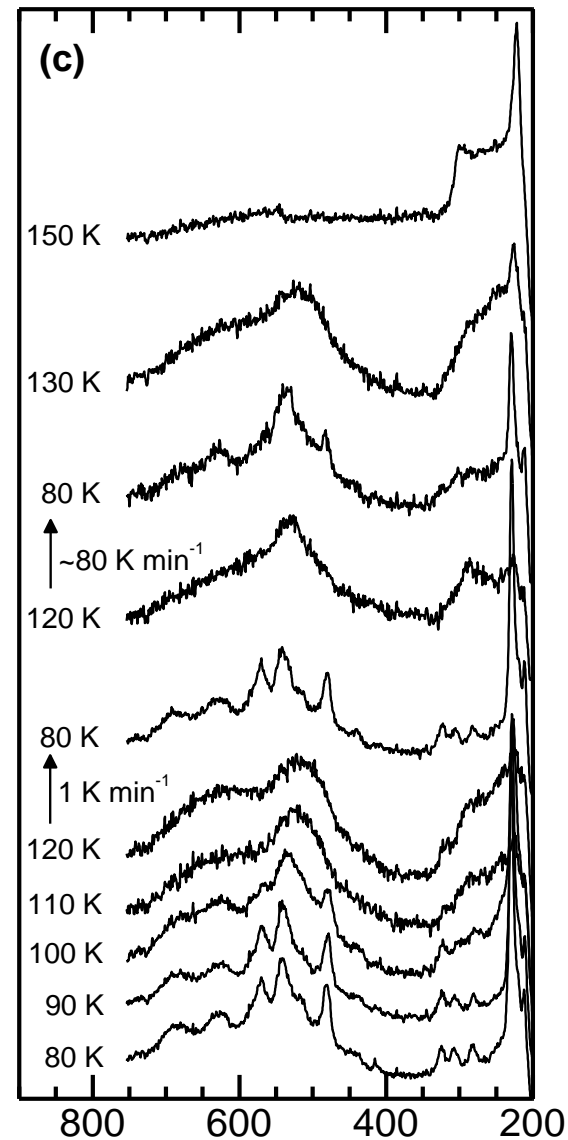
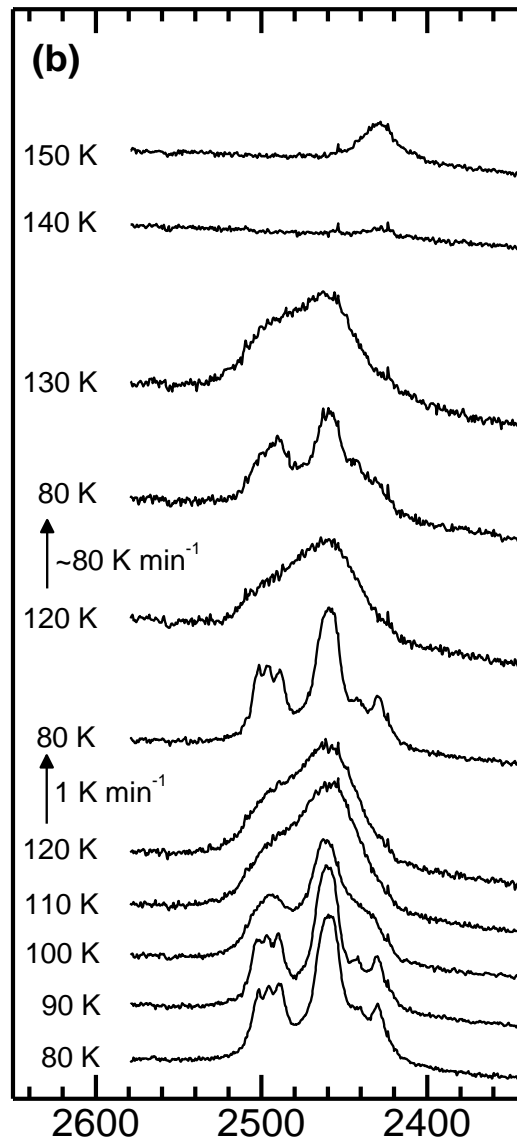
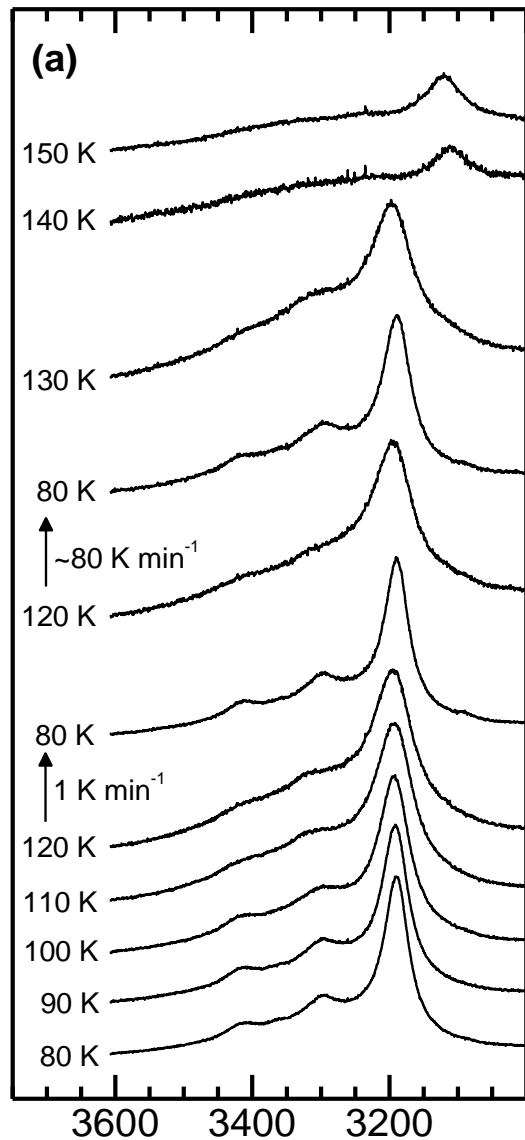
Complete hydrogen order is difficult to achieve due to the cooperative mechanism of molecular reorientation.

Raman spectroscopy of ice XIII/V

coupled O-H stretching

decoupled O-D stretching

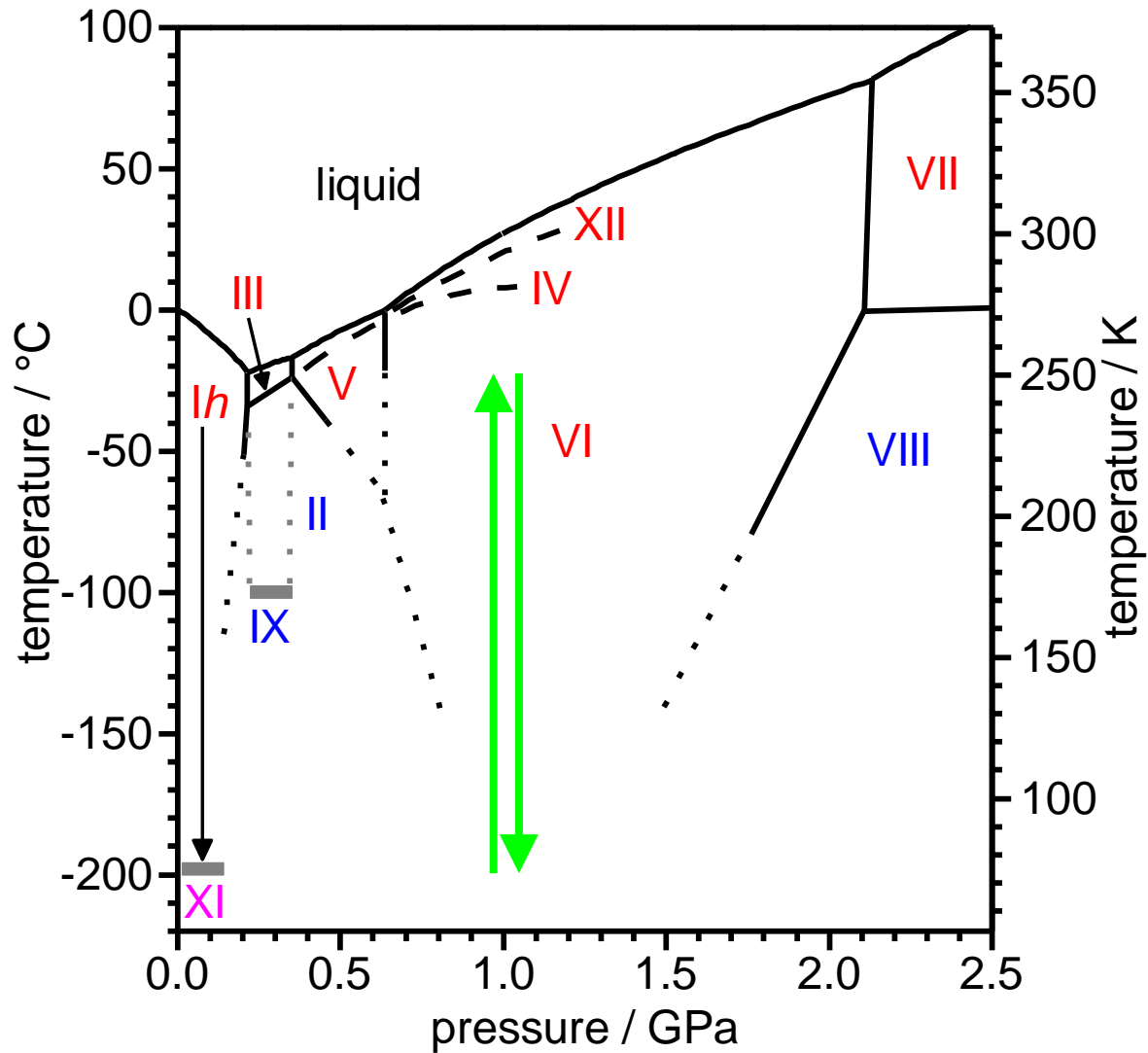
lattice modes



ice XIII

Raman Shift / cm⁻¹

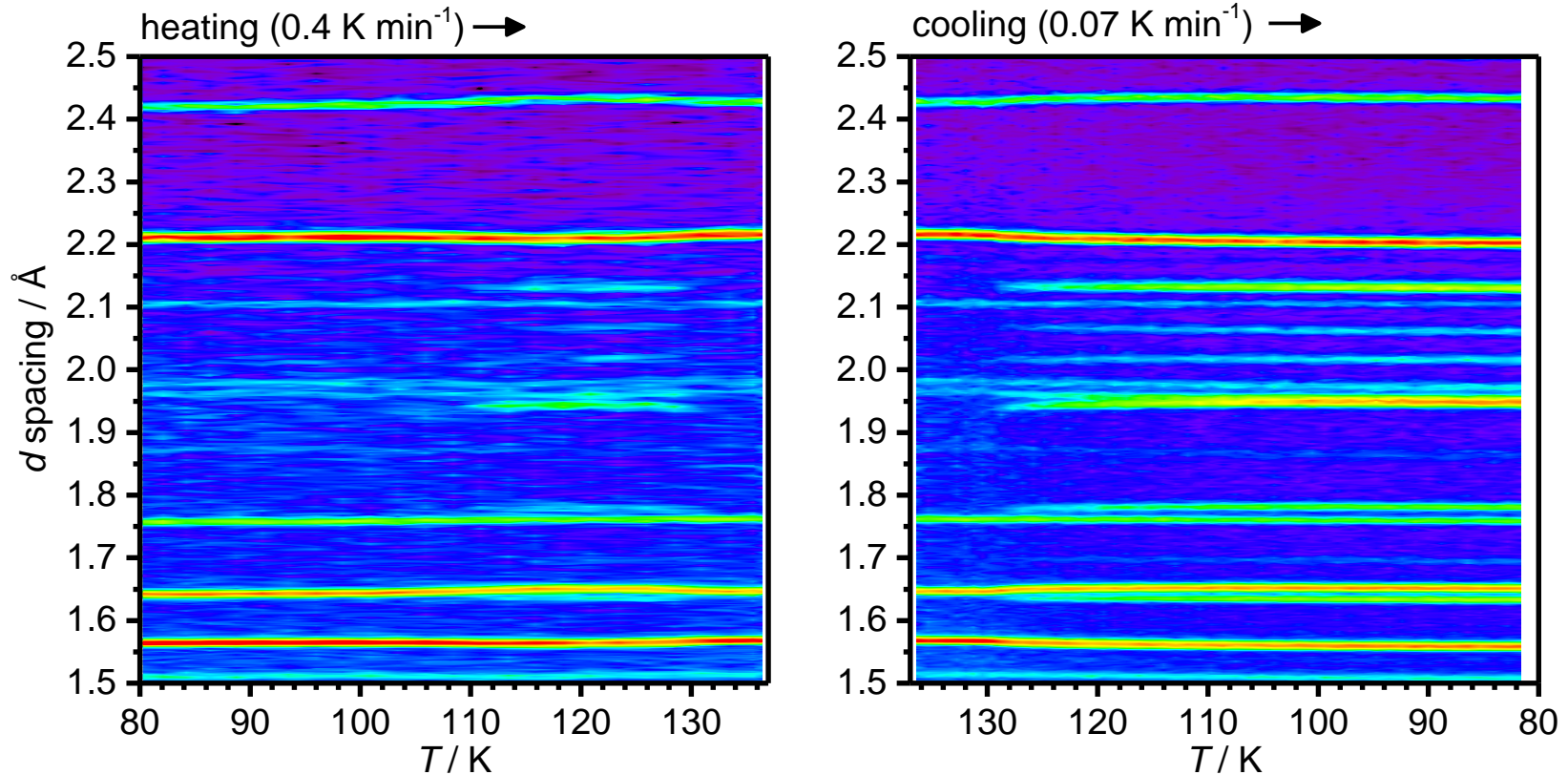
The ice VI to ice XV phase transition



Isobaric heating of DCl-doped ice Ih at 1.0 GPa followed by cooling back to 77 K.

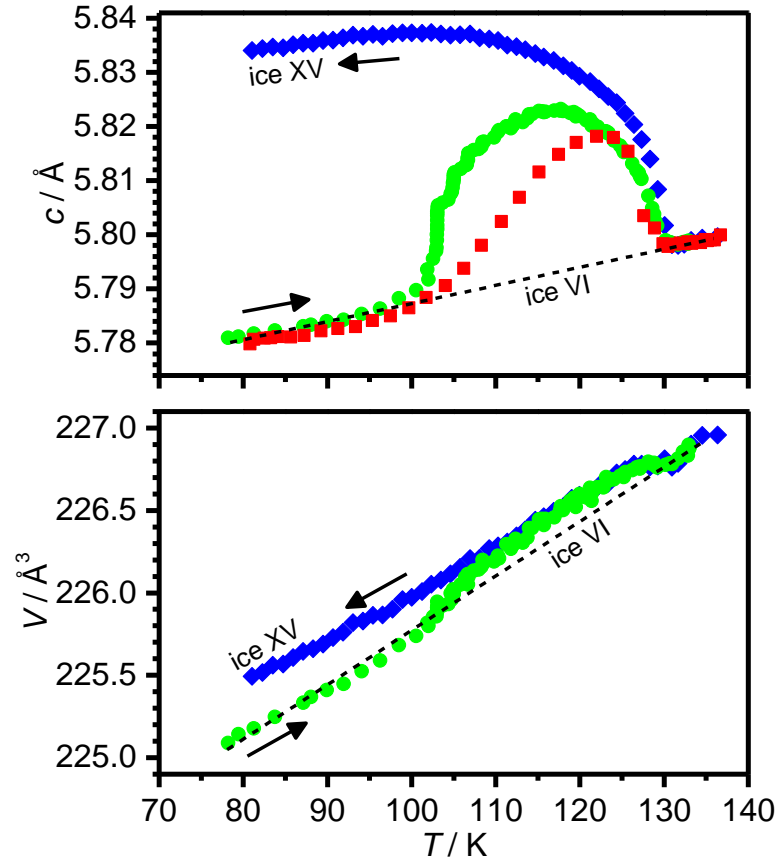
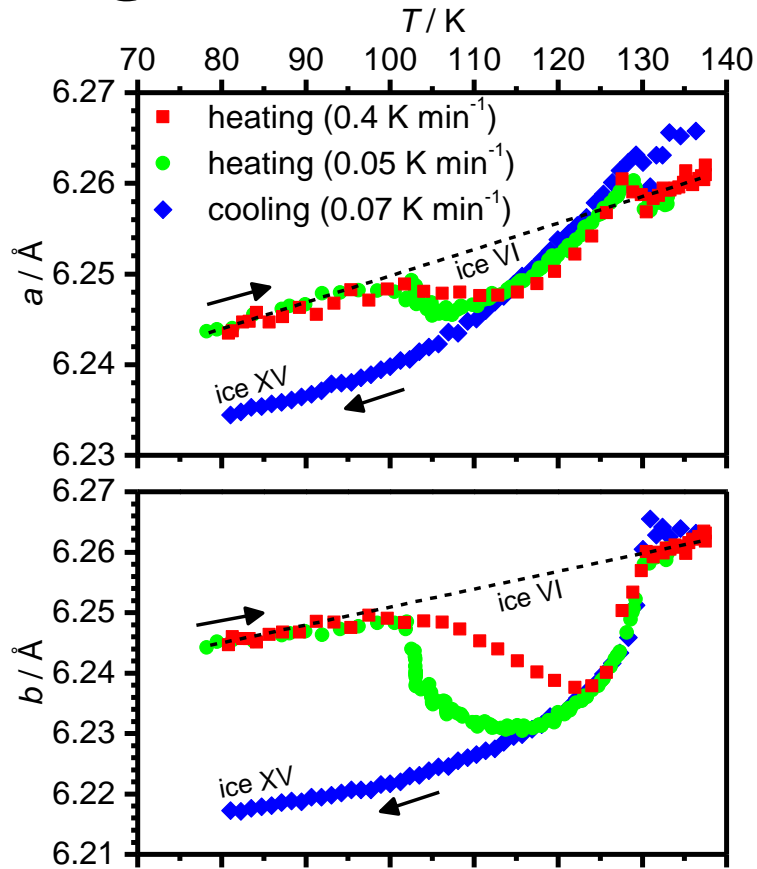
Neutron diffraction

0.01 M DCI-doped pressure-quenched D₂O sample



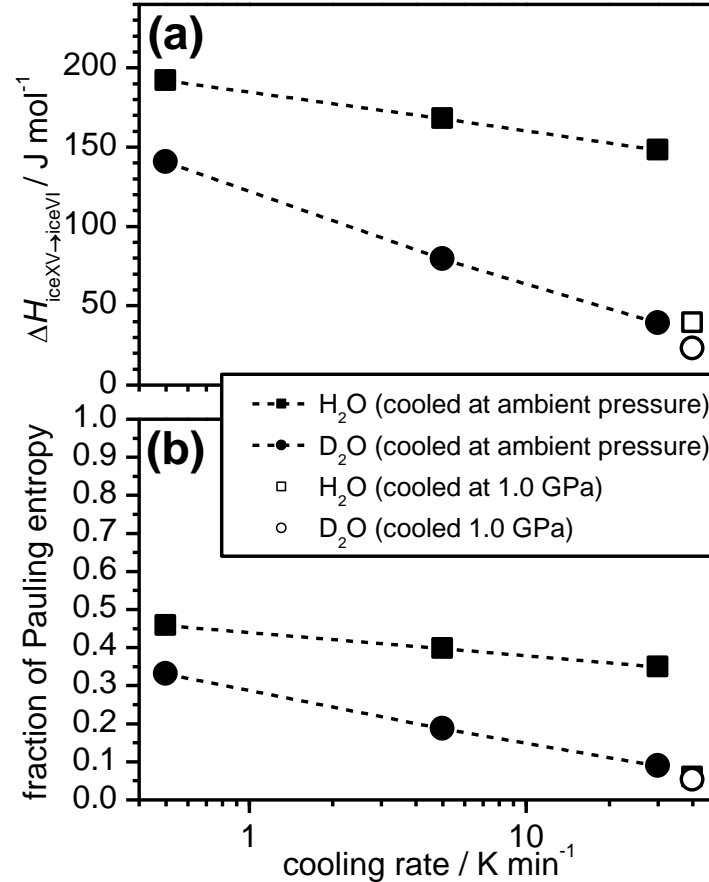
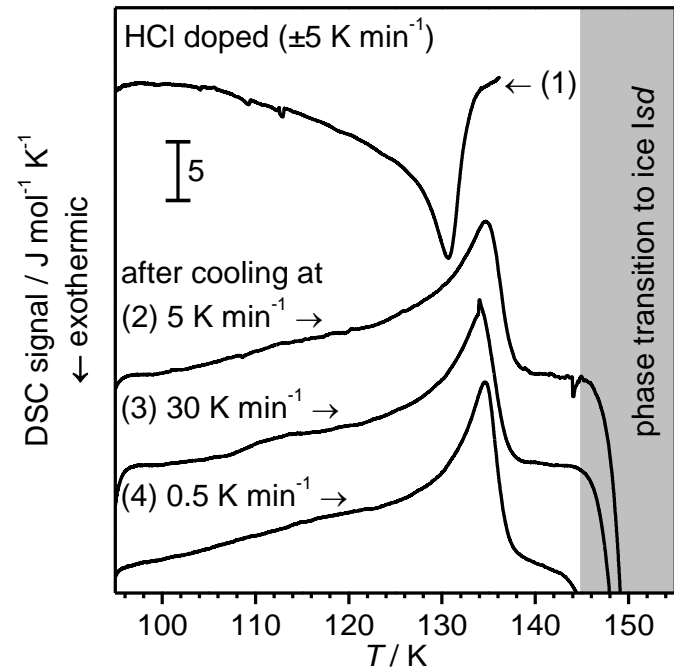
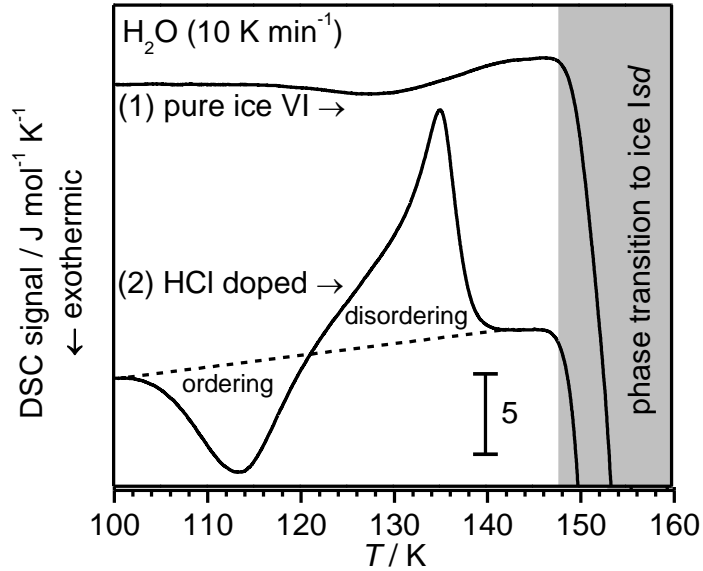
'Transient' hydrogen ordering upon heating pressure-quenched sample.
More ordered ice XV after slow-cooling.

Changes in lattice constants



Contractions in a and b , and expansion in c upon hydrogen-ordering.
Ice XV is 0.14% less dense than ice VI.
Hydrogen ordering upon cooling fast initially but slows down.
No metastable stages upon heating.

Calorimetry

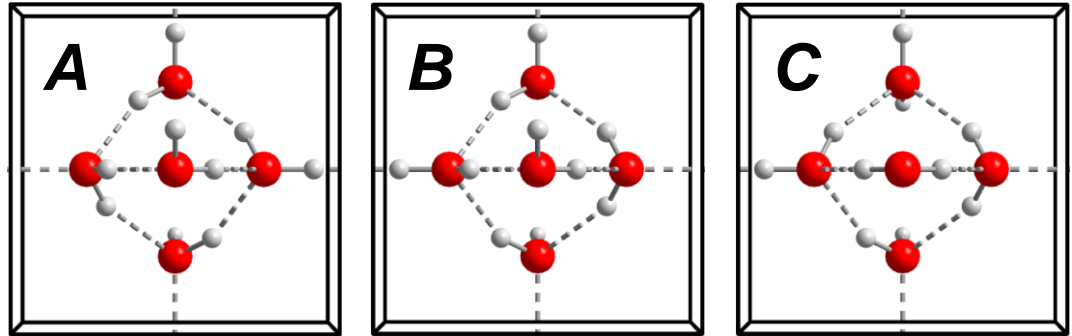


$$\Delta S = \int_{T_1}^{T_2} \frac{C_p}{T} dT$$

Consistent with changes in lattice constants.
 Independent ordering of the two networks initially?
 H₂O is easier to order than D₂O.
 Difficult to lose more than 50% of Pauling entropy.

The structure of ice XV

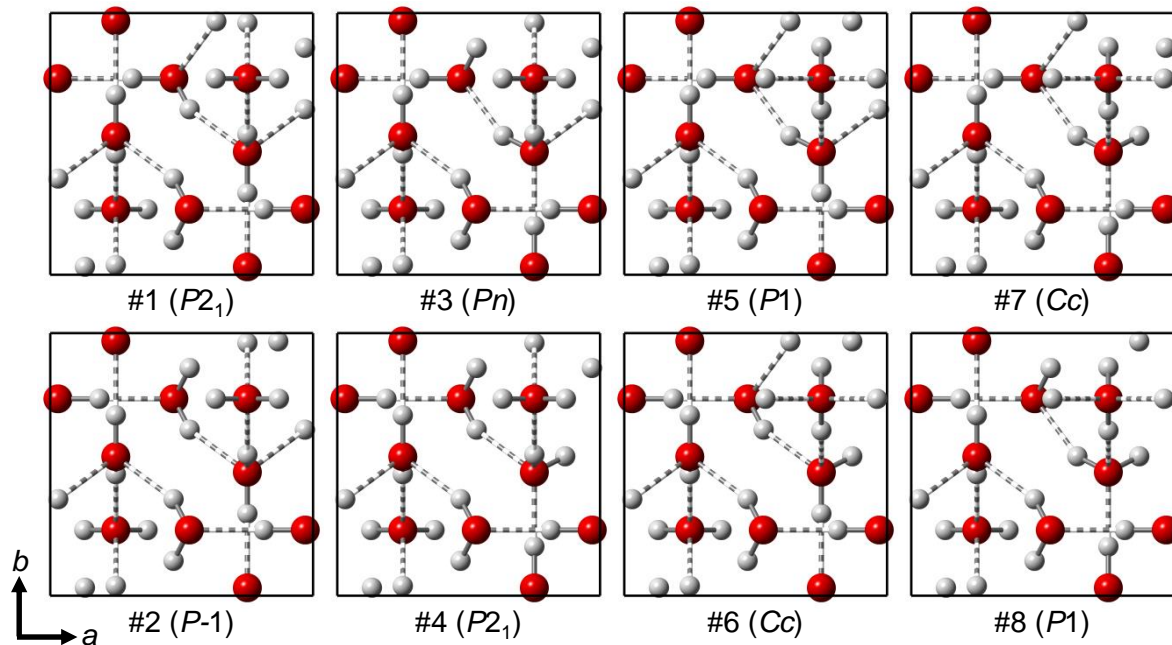
Hydrogen-ordered structures
of single networks:



most polar

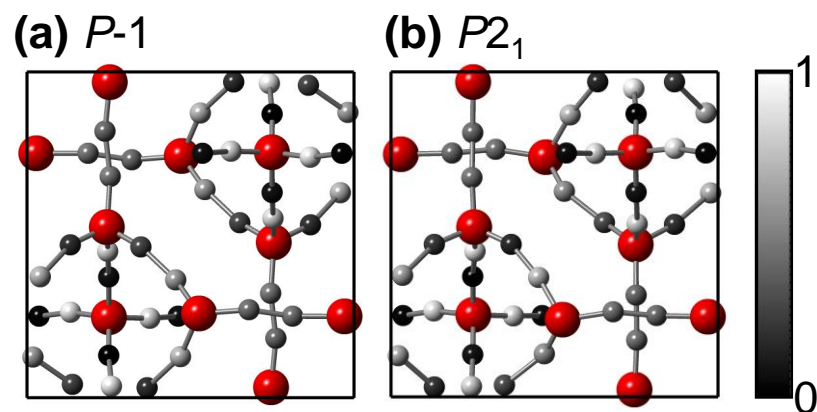
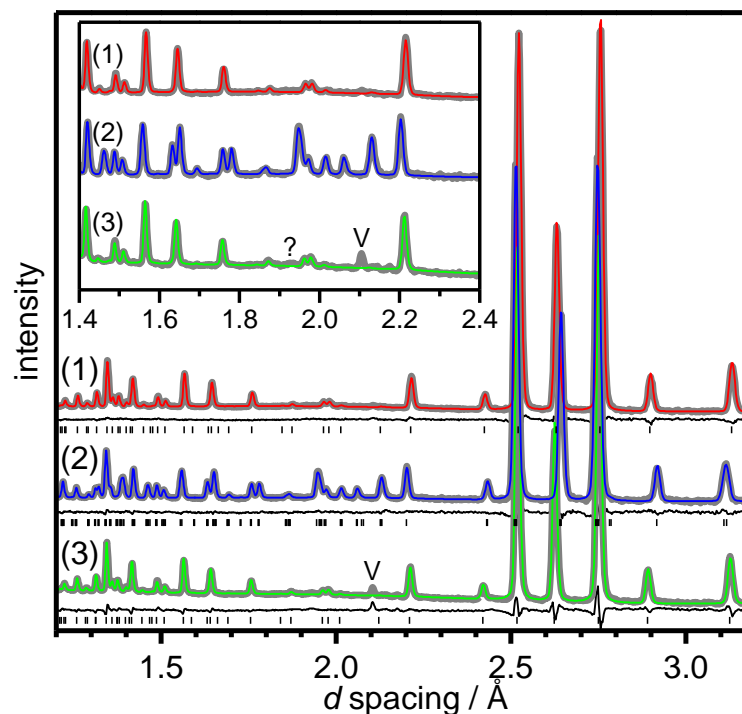
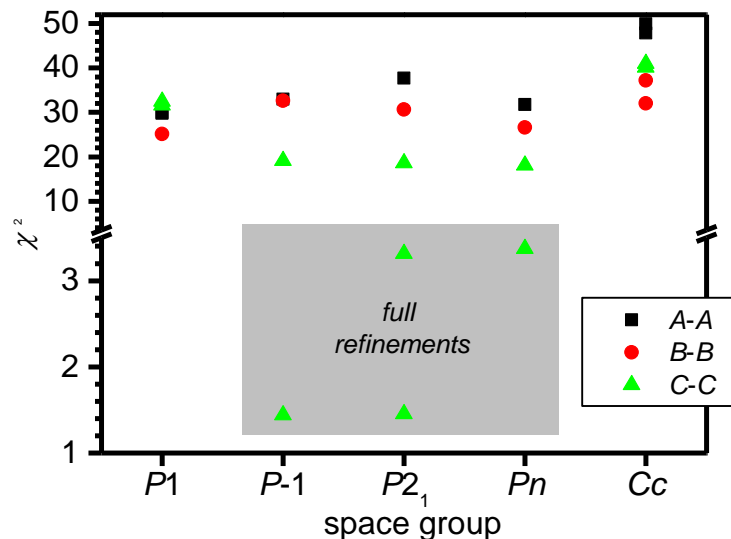
Combination results in *A-A*, *B-B*, *C-C*, *A-B*, *B-C* and *C-A* overall structures.

C-C structures:



In total: 3×7 *homo*-network structure + 3×8 *hetero*-network structures = 45

Testing the various structures

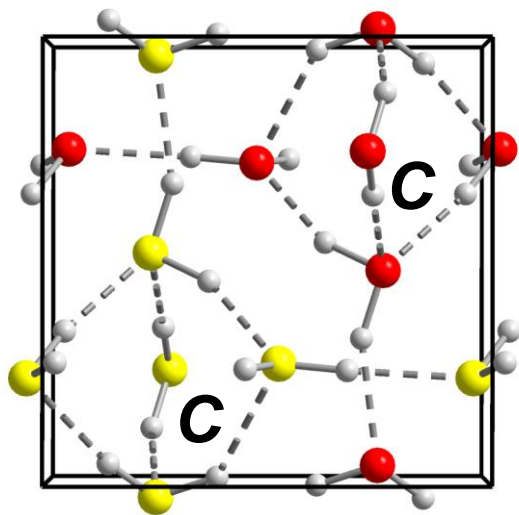


- (1) ice VI at 135 K
- (2) ice XV at 80 K after slow-cooling at ambient pressure
- (3) ice VI at 80 K after slow-cooling at 1.4 GPa

The $P-1$ and $P2_1$ models describe essentially the same partially disordered structure. Difficult to tell the difference between internal and external racemate by diffraction. $P2_1$ violates ice rules and is non-polar.

The most stable structure?

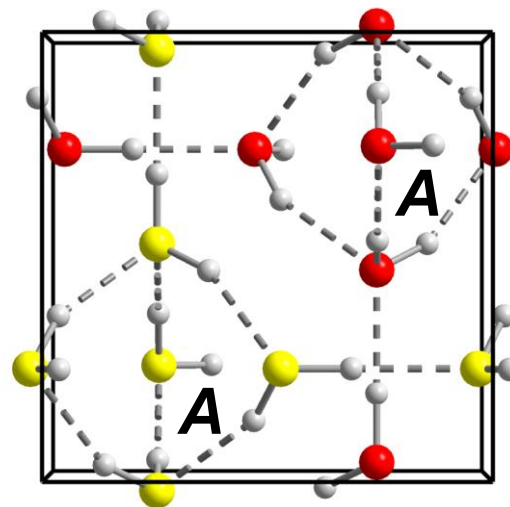
P-1



experimental

K.D. Nanda, G.J.O. Beran, *J. Phys. Chem. Lett.*, 4 (2013) 3165

Cc



VS.

C. Knight, S. J. Singer, *J. Phys. Chem. B*, 109 (2005) 21040

J.-L. Kuo, W. F. Kuhs, *J. Phys. Chem. B*, 110 (2006) 3697

M. Del Ben, J. VandeVondele, B. Slater, *J. Phys. Chem. Lett.* 5, (2014)

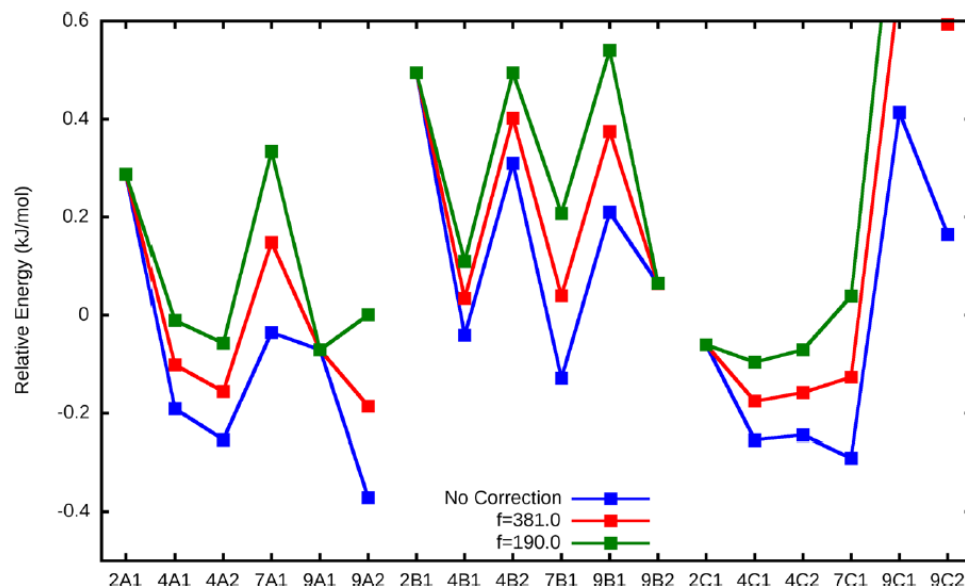
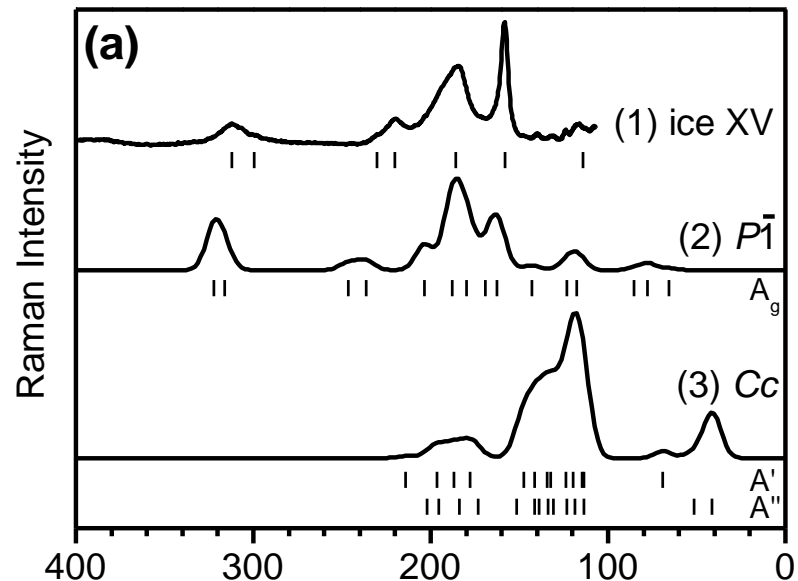


Figure 5. Relative energies in kilojoules per mole per molecule, with respect to the average, at the RI-RPA level of theory for the 18 symmetry inequivalent structures in the ice XV unit cell, including corrections for different dielectric boundary conditions.

Raman spectroscopy of ice XV

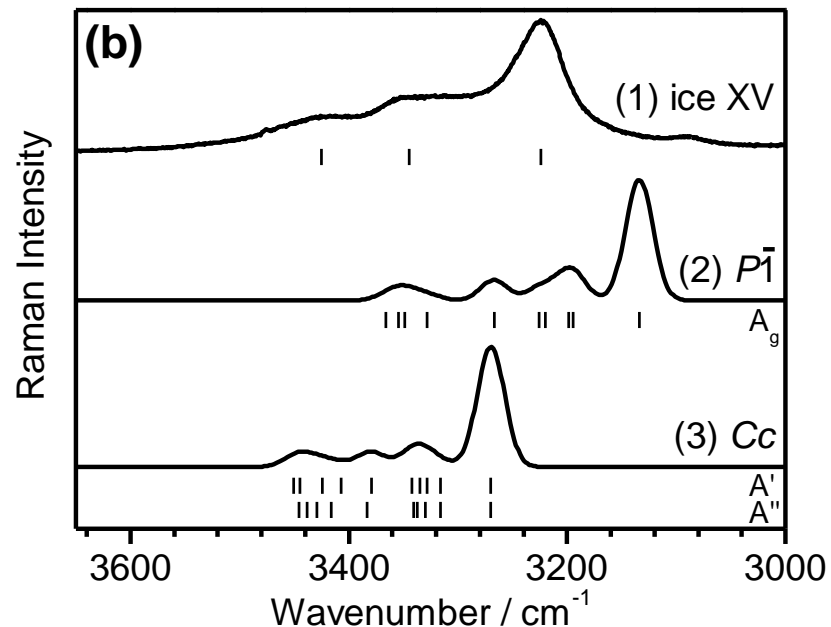
Lattice modes

Vibrations of rigid water molecules
(Translations or rotations)



O-H stretching modes

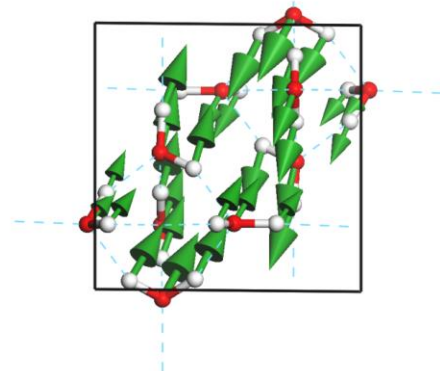
Coupling of symmetric and asymmetric stretching vibrations



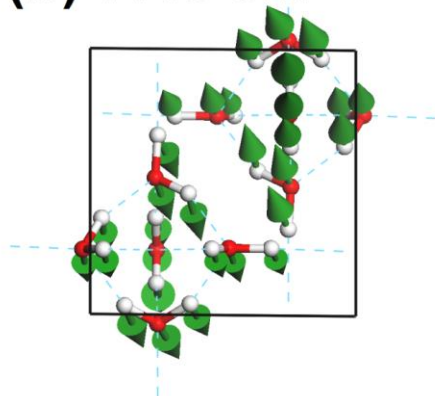
Raman spectroscopy of ice XV

Rigid network modes

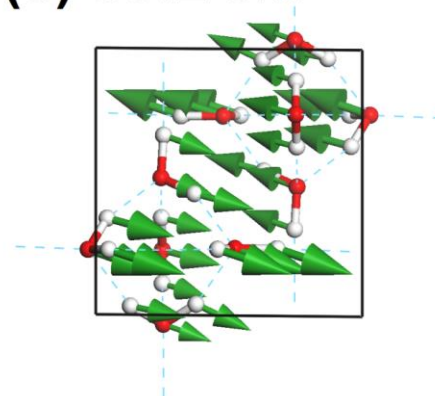
(a) 65.8 cm⁻¹



(b) 77.8 cm⁻¹

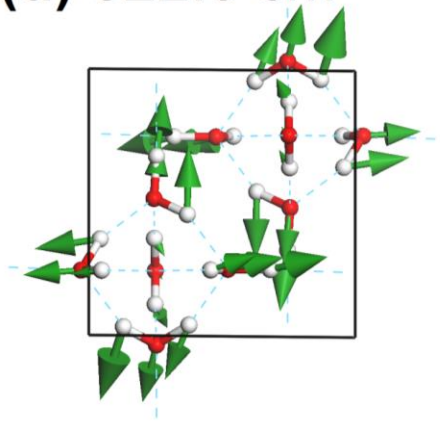


(c) 85.2 cm⁻¹



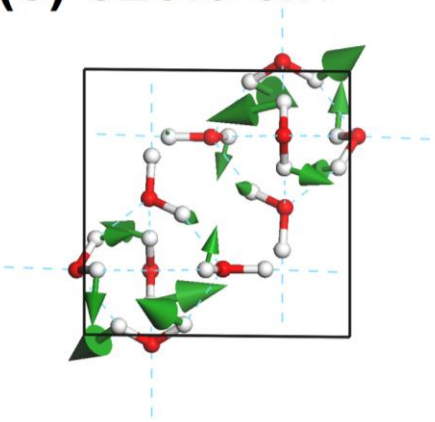
Breathing mode

(d) 322.0 cm⁻¹



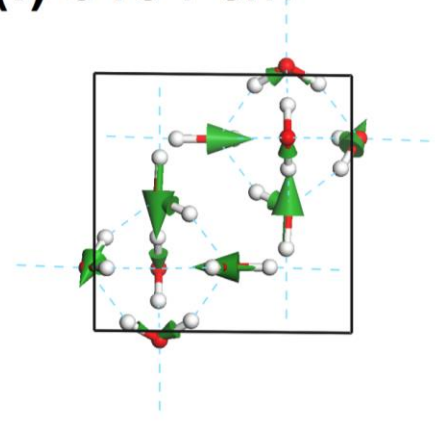
Rotations

(e) 520.6 cm⁻¹

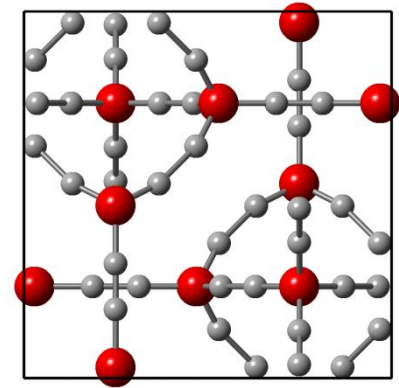
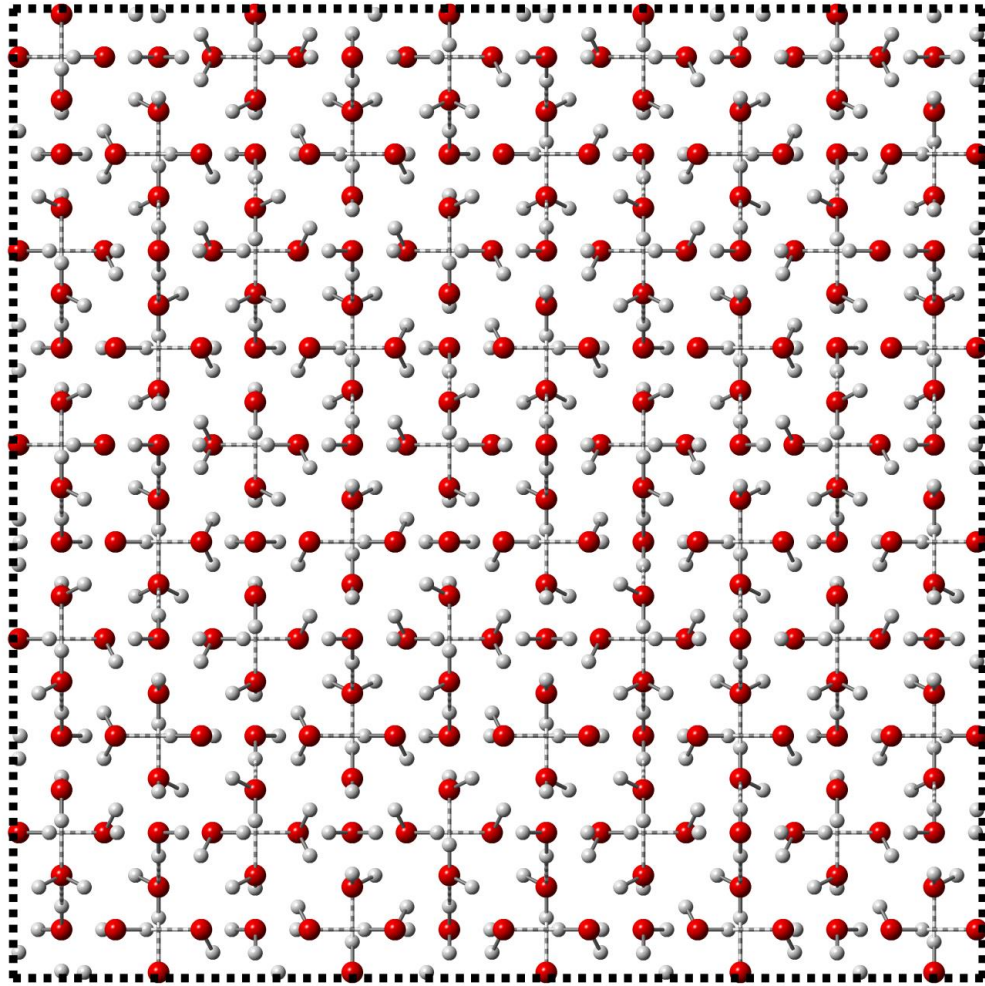


Isolated O-H stretch

(f) 3134 cm⁻¹



Supercell representing ice VI



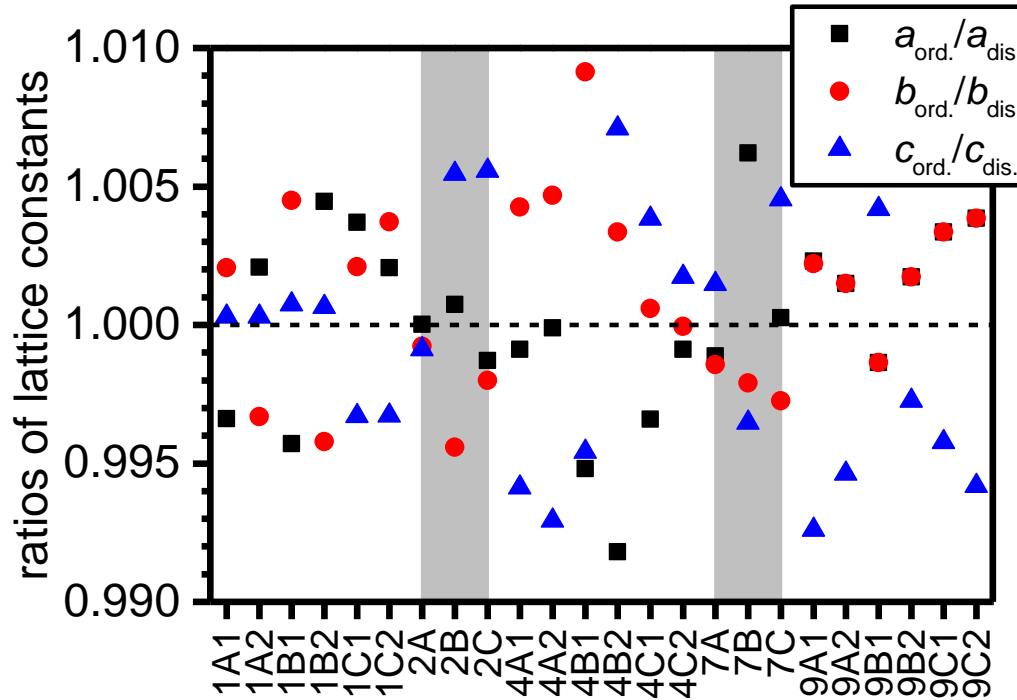
Our *RandomIce* program creates supercell structures consistent with the fractional occupancies of the small unit cell describing the average structure.

Algorithm works on the basis of migrating H_3O^+ defect.

Several hundred million defect loops are performed in an overnight run.

High-symmetry of average structure does not reflect the local symmetry.

Changes in lattice constants from DFT



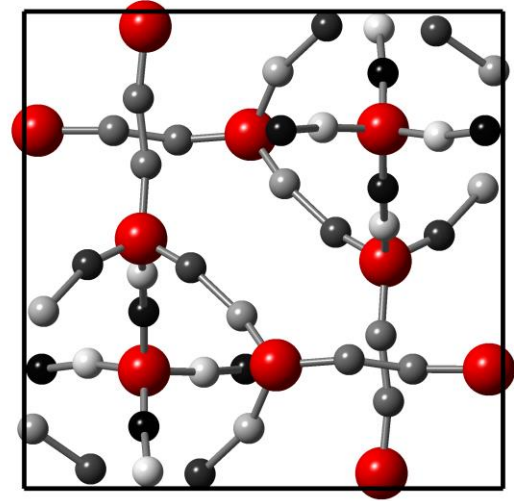
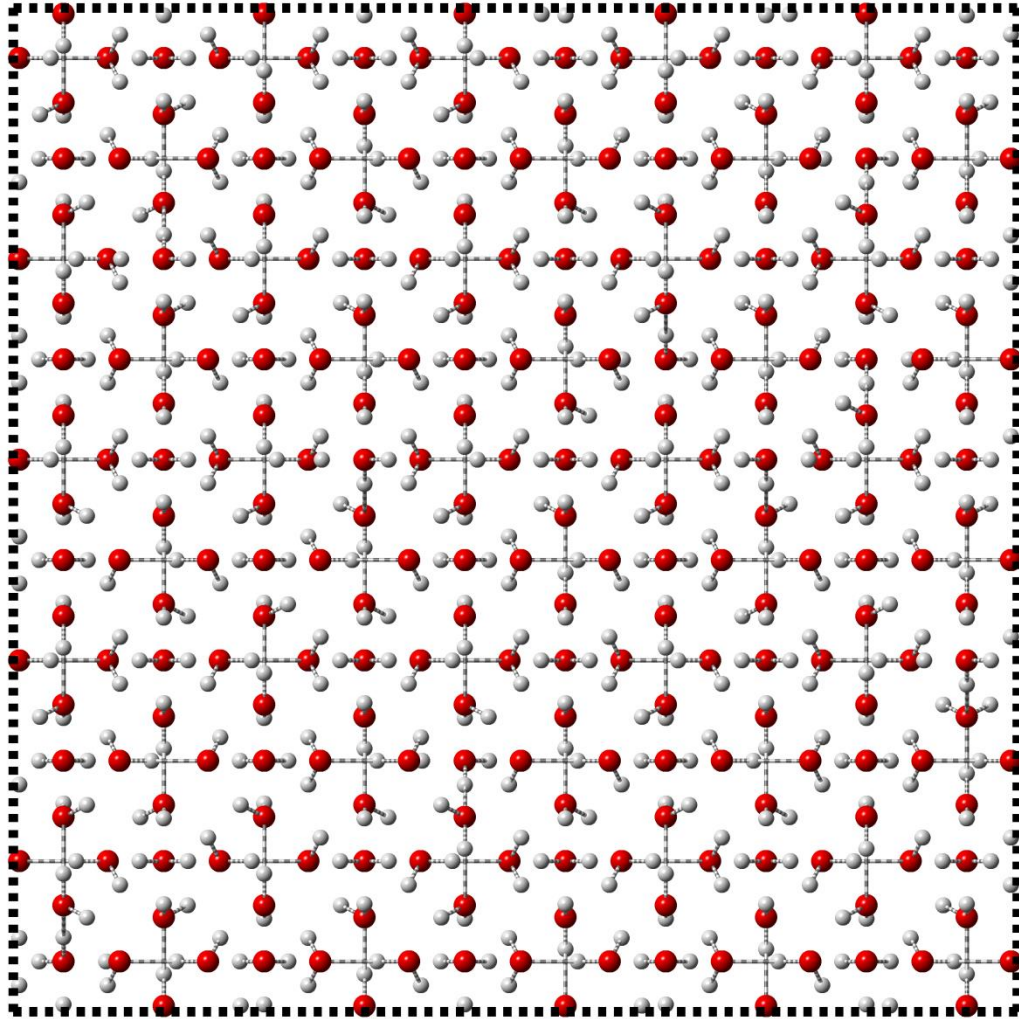
Experimental findings for the ice VI to XV phase transition:

- (1) a and b contract
- (2) c expands
- (3) b changes more than a
- (4) C-type motifs

The $P-1$ model is the only one that fulfils all conditions.

Ice VIII is also antiferroelectric but contains the most polar ice Ic networks.

Ice XV supercell based on P-1 model

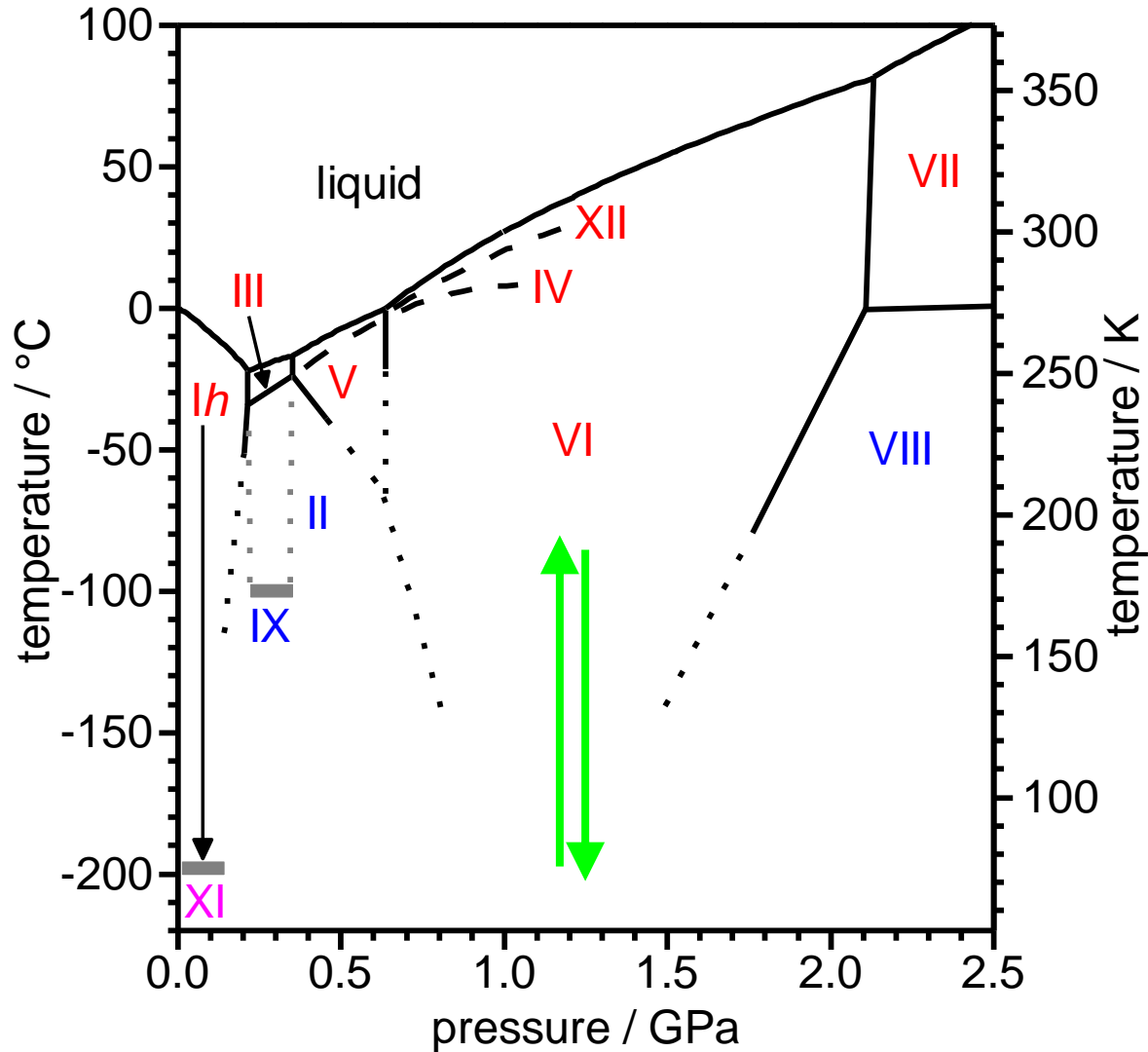


82.0 % 'straight' apex molecules
45.3 % C-type motifs

Most accurate structural
description of ice XV?

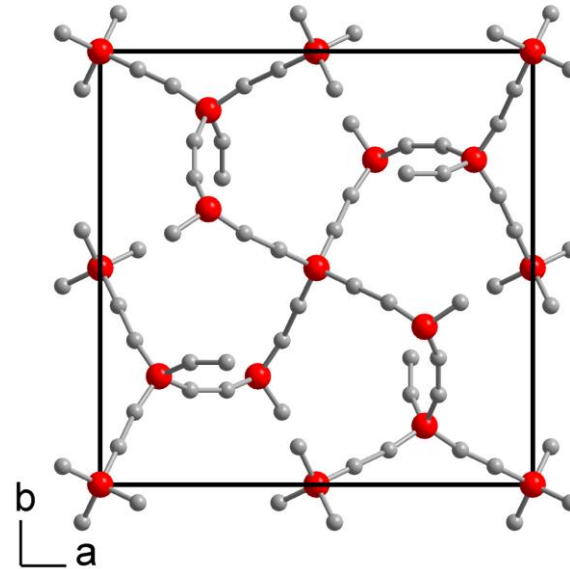
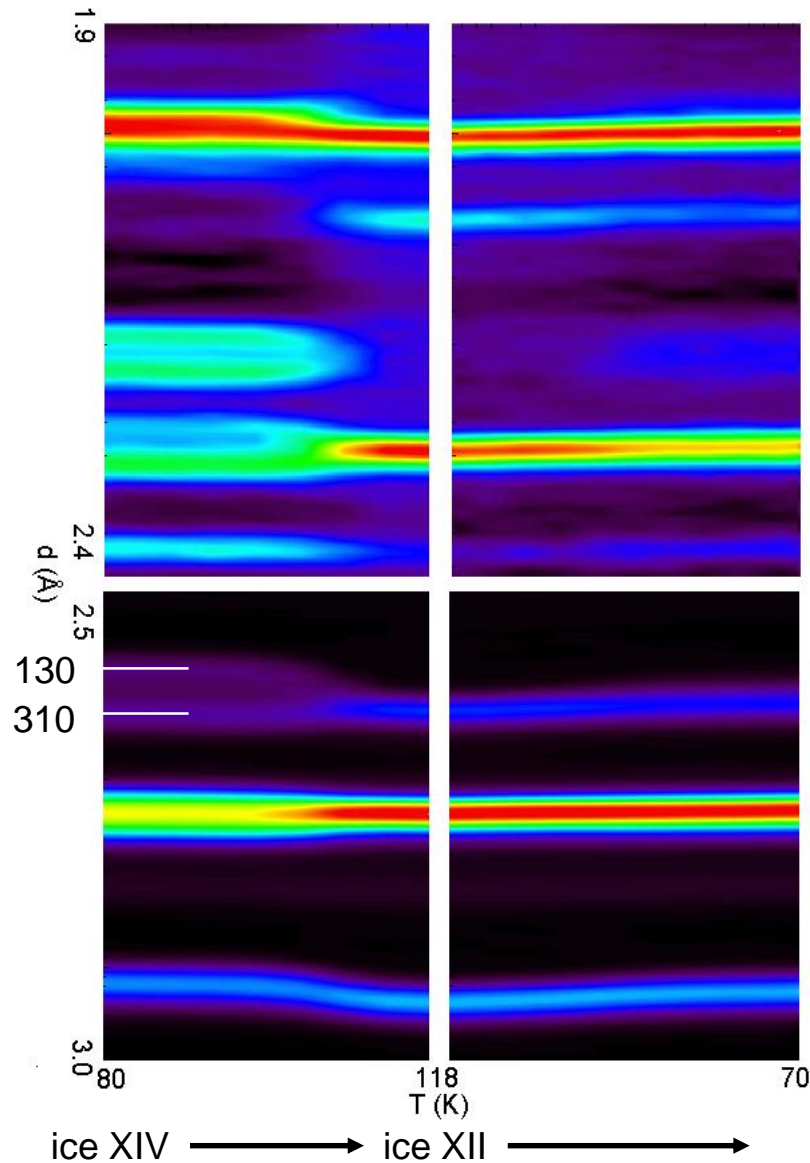
Future effort must be to make
more ordered ice XV.

The ice XII to ice XIV phase transition

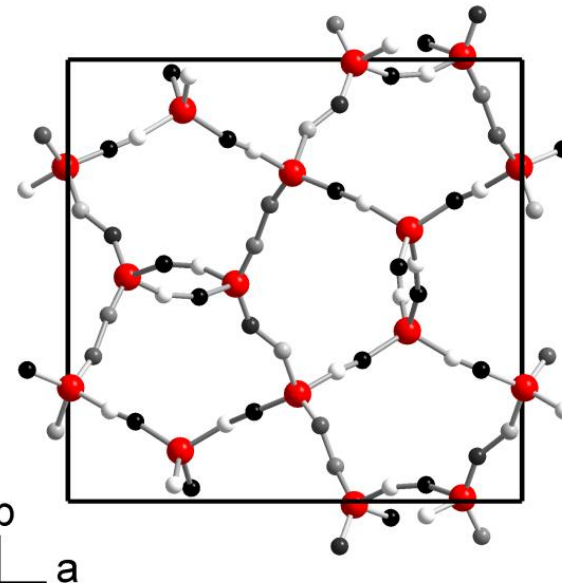


Isobaric heating of doped high-density amorphous ice at 1.2 GPa followed by cooling back to 77 K at 0.8 K min⁻¹.

Neutron diffraction and crystal structure



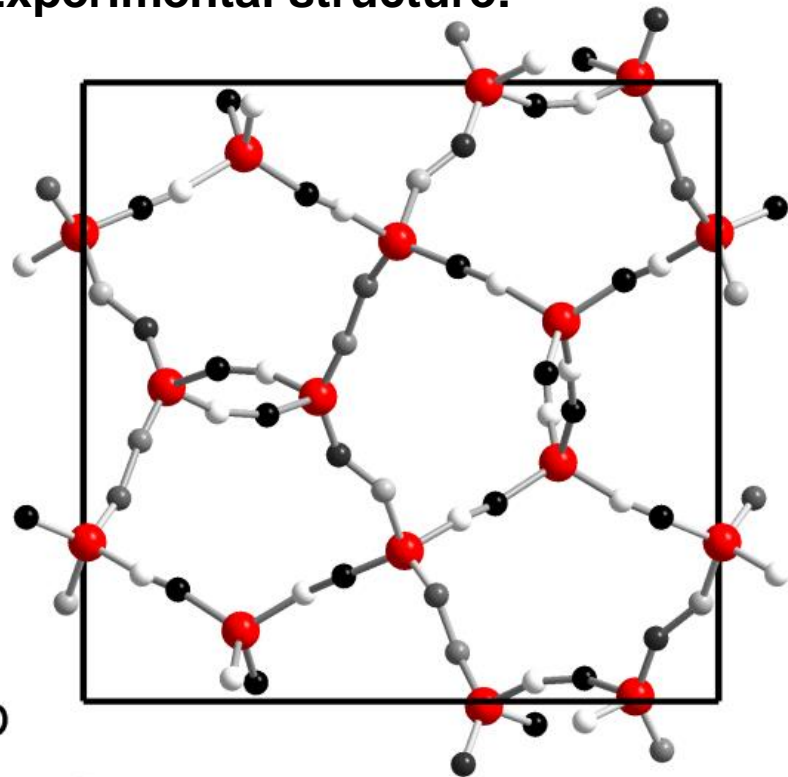
ice XII
($I4(\bar{2})2d$)



ice XIV
($P2_12_12_1$)

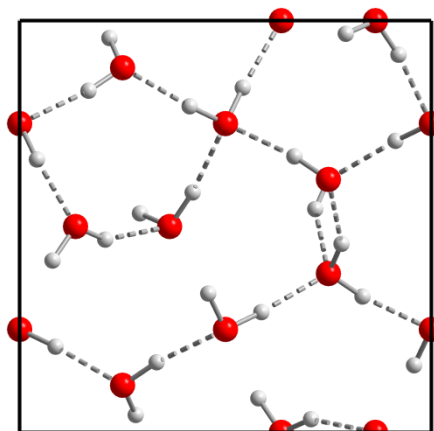
Ice XIV – DFT predicts the right structure

Experimental structure:

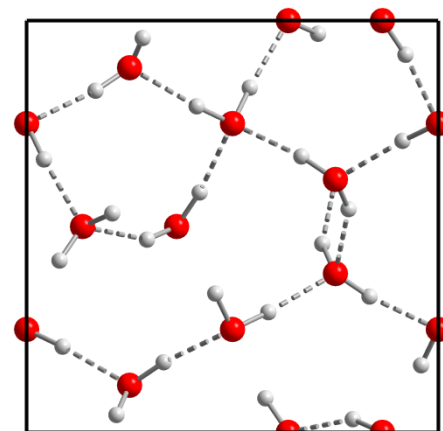


ice XIV
($P2_12_12_1$)

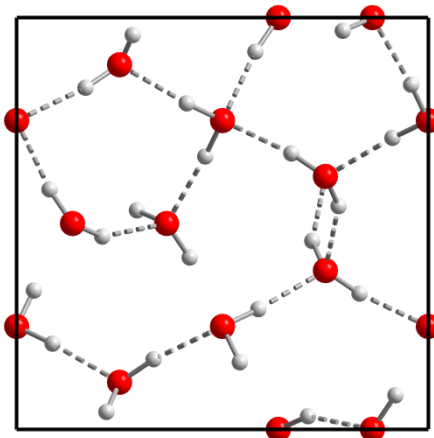
DFT structures:



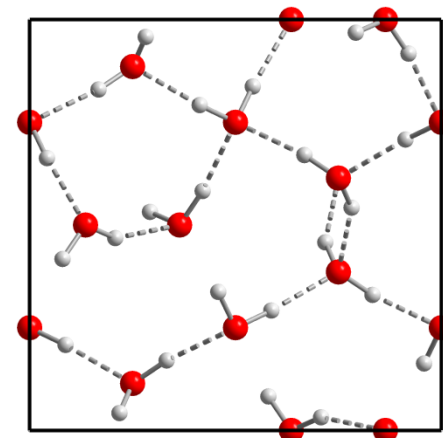
-10865.948 kcal mol⁻¹



-10865.987 kcal mol⁻¹

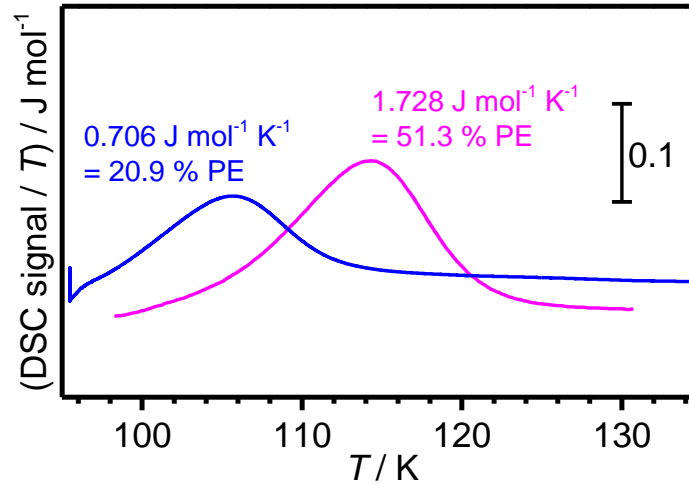
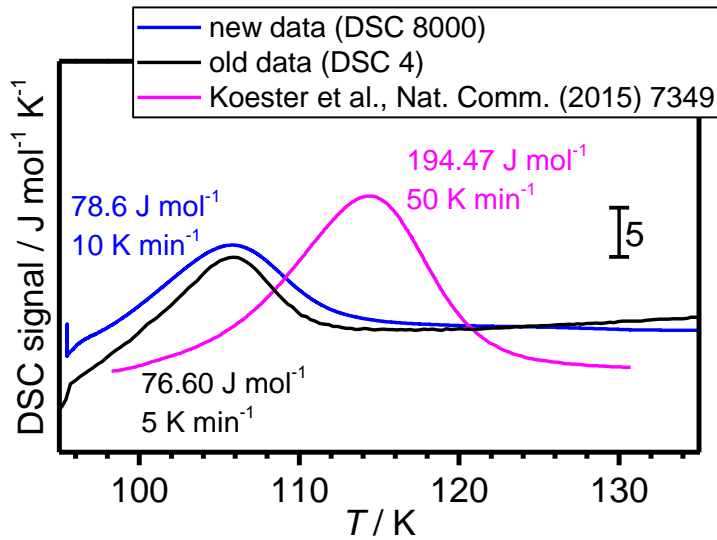


-10866.094 kcal mol⁻¹



-10866.137 kcal mol⁻¹

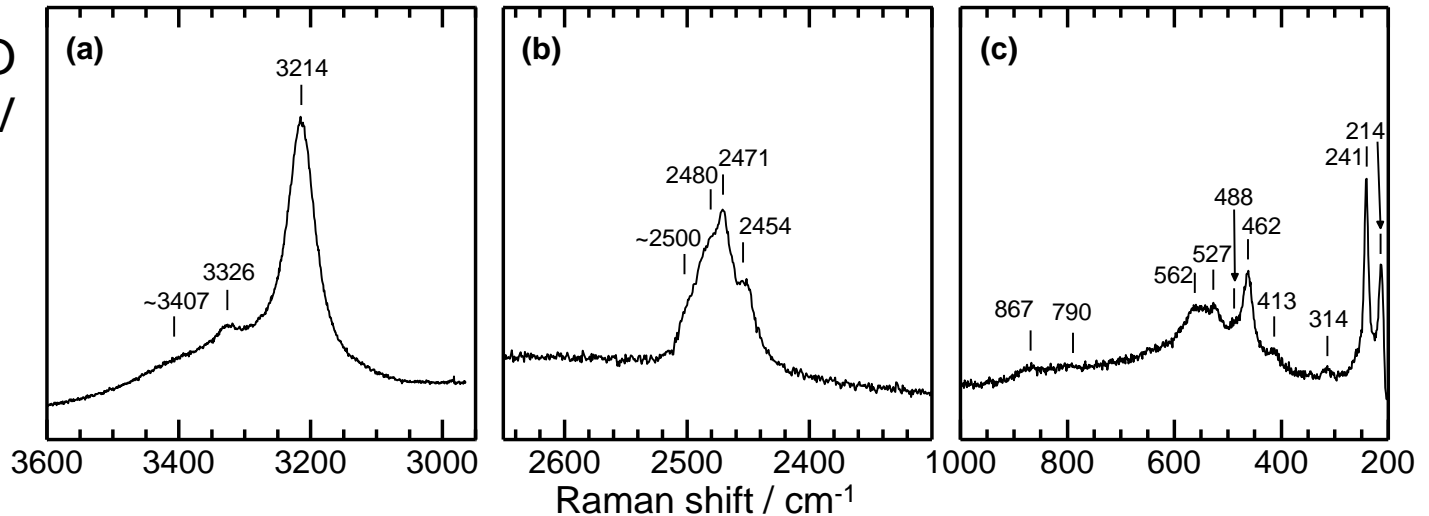
Calorimetry and spectroscopy of ice XIV



$$\Delta S = \int_{T_1}^{T_2} \frac{C_p}{T} dT$$

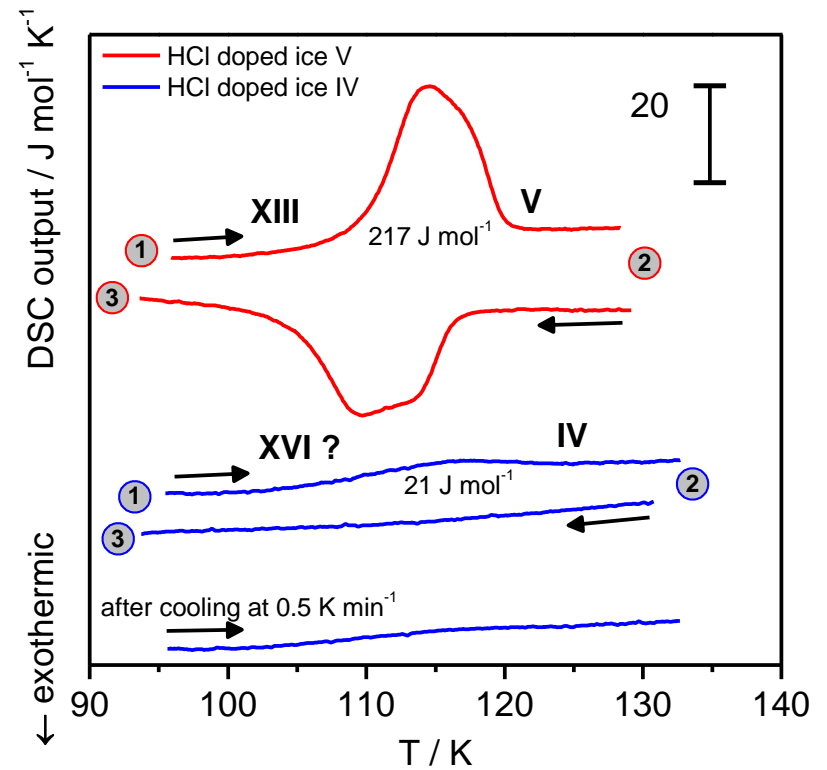
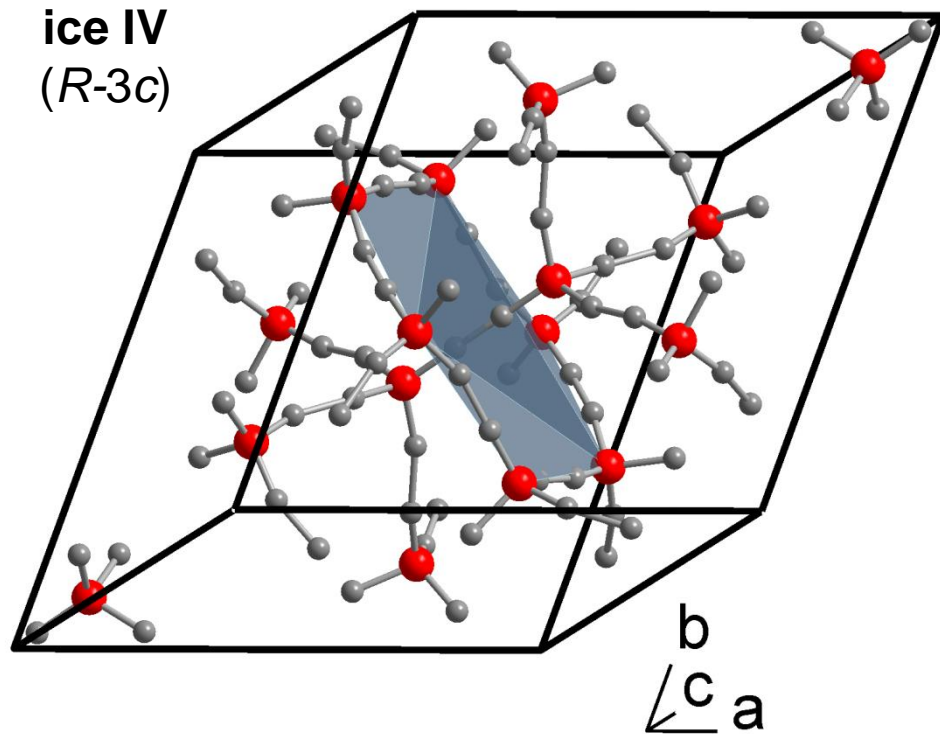
Question mark over "full loss of Pauling entropy" claimed by Koester *et al.*

H₂O
+5% D₂O ice XIV



Raman spectroscopy suggests that ice XIV is not fully hydrogen-ordered.

Hydrogen ordering of ice IV

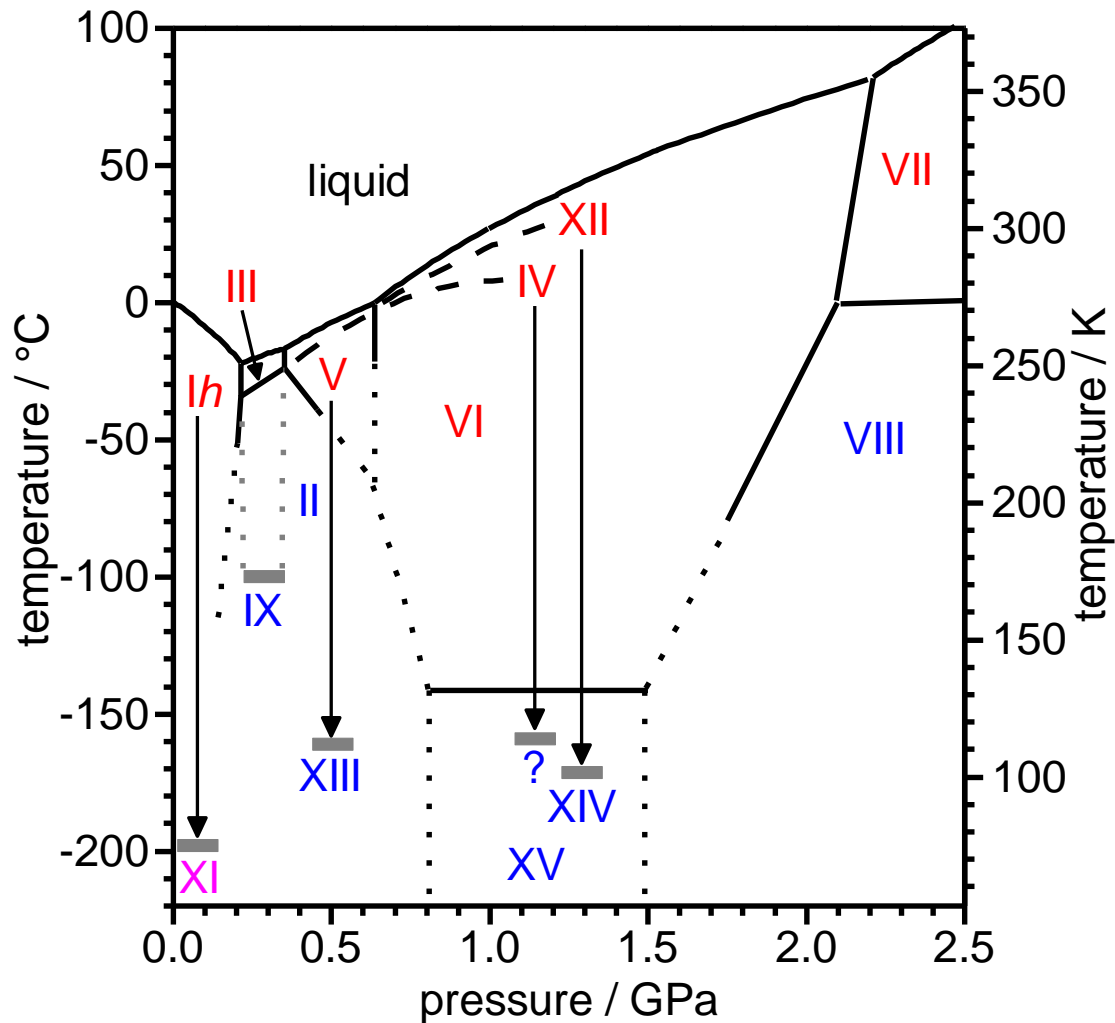


Entropy change of 5.4 % of the Pauling entropy.

Slow-cooling at ambient pressure does not increase the amount of order in ice IV.

However, the ice IV ordering temperature can be read off.

Final phase diagram



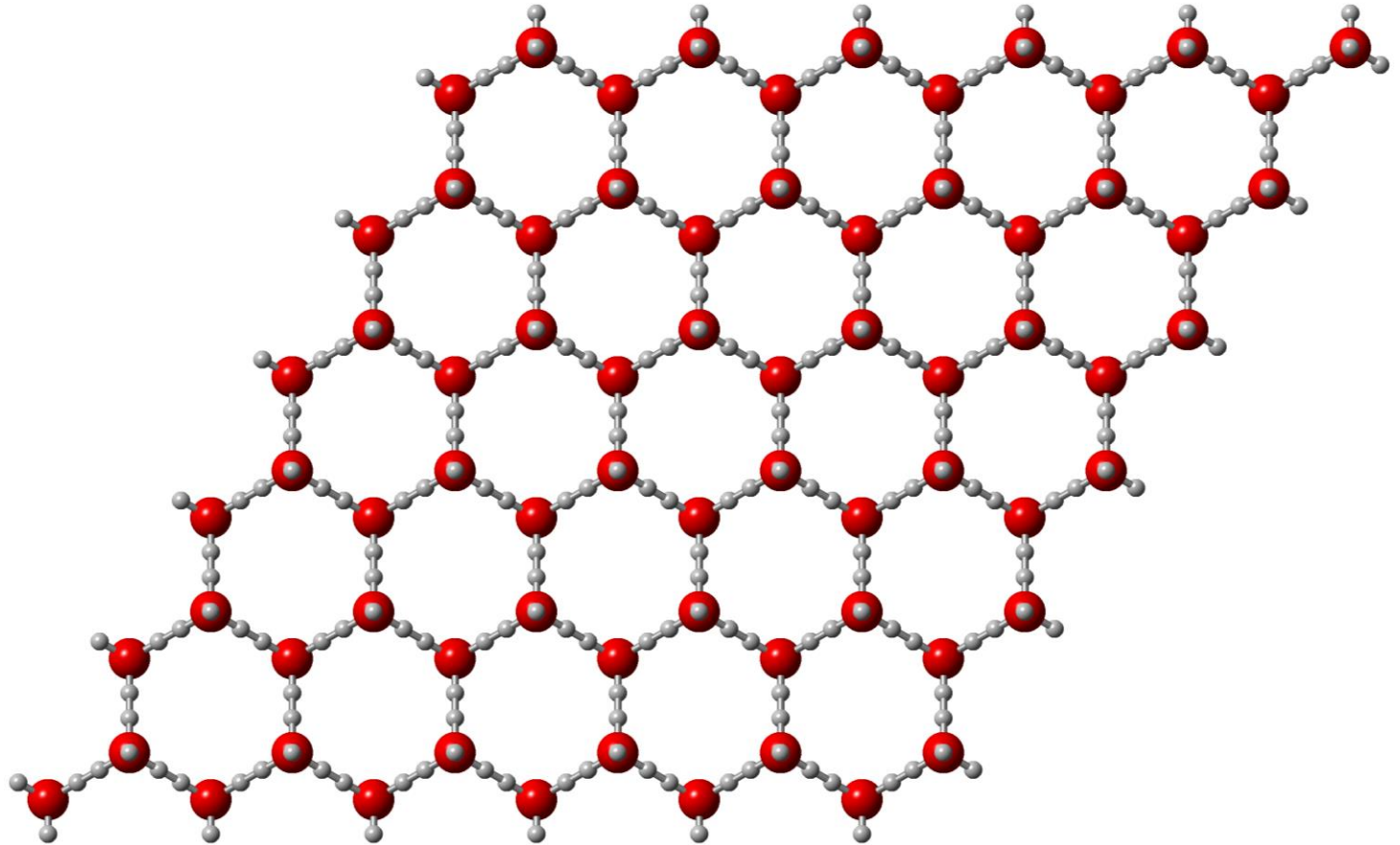
- hydrogen-disordered ice
- hydrogen-ordered ice (anti-ferroelectric)
- hydrogen-ordered ice (ferroelectric)

2. Stacking disordered ice

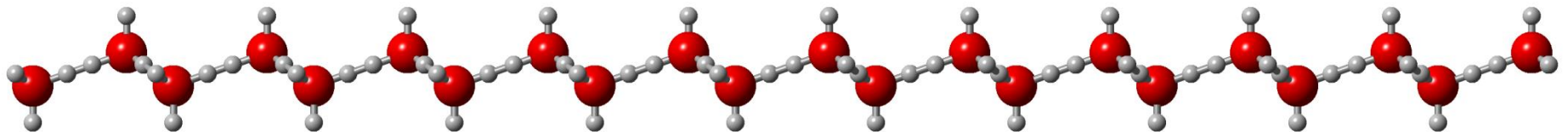


A single layer of ice I

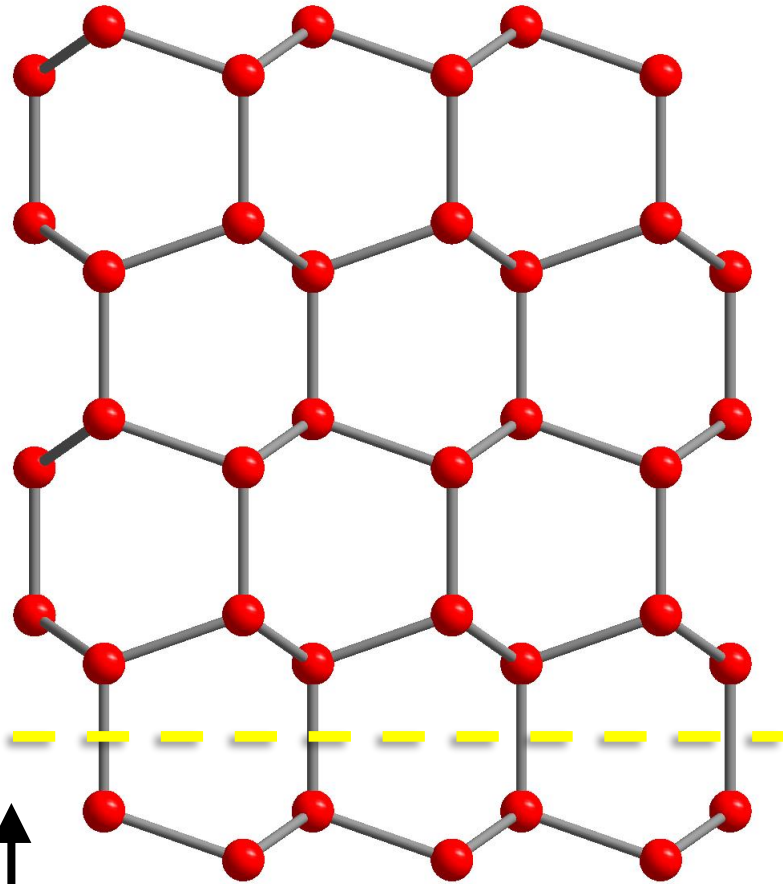
Top view



Side view



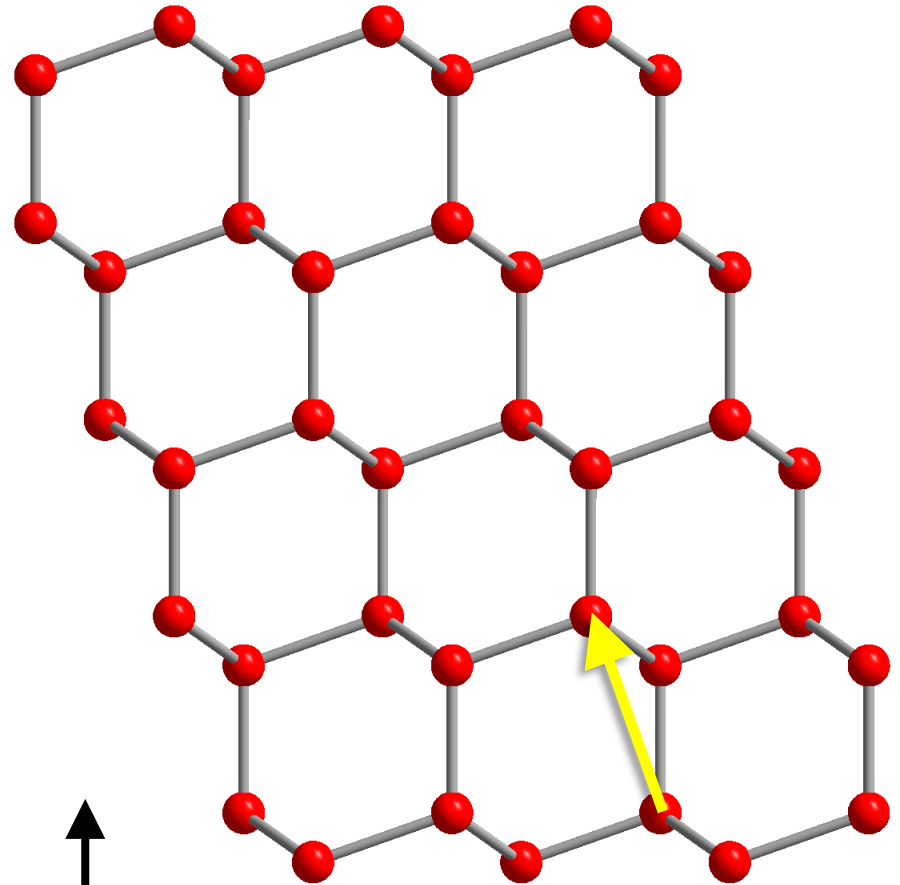
Stacking of layers



[0001]

ice Ih

hexagonal ($P6_3/mmc$)

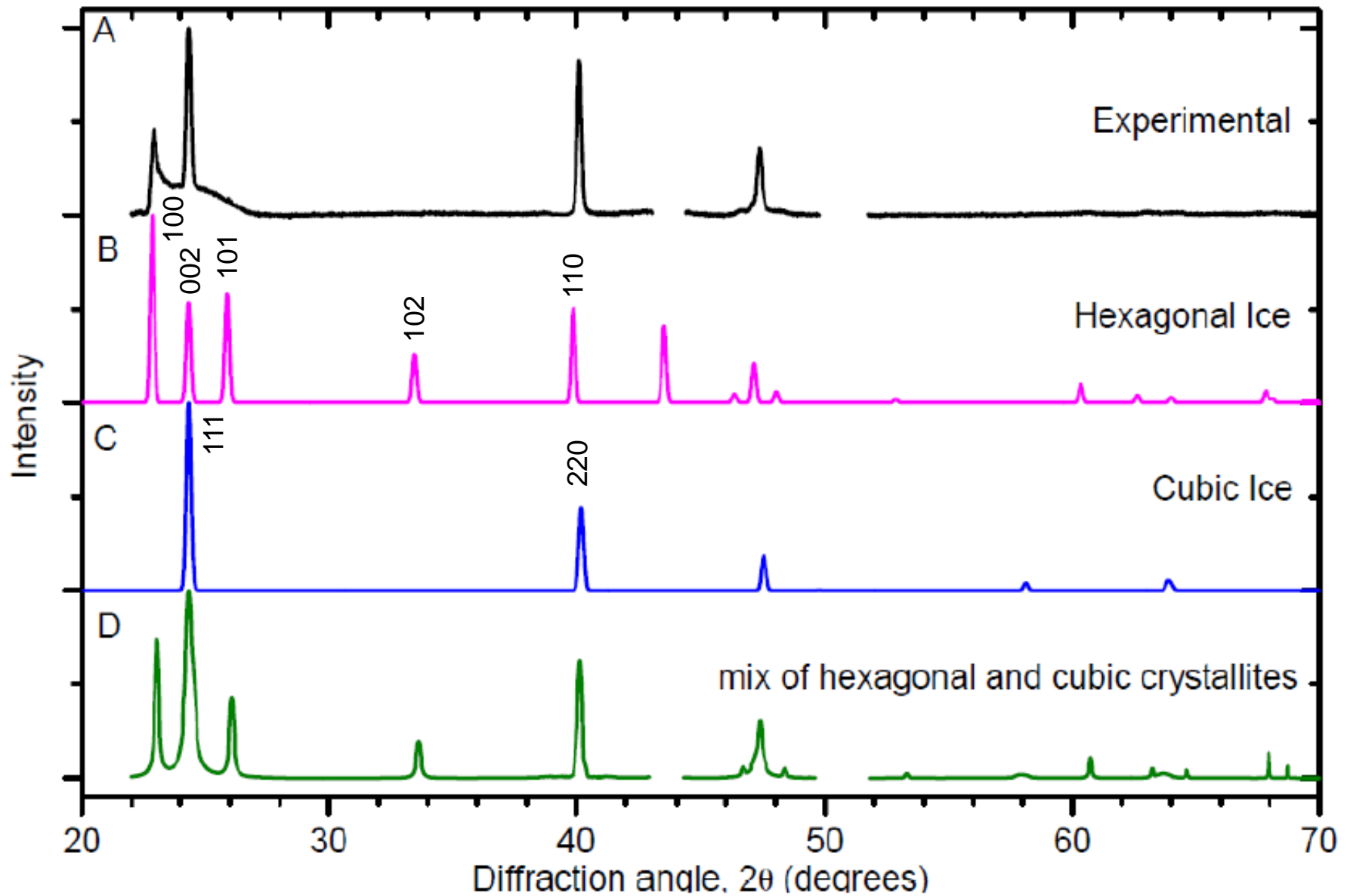


[111]

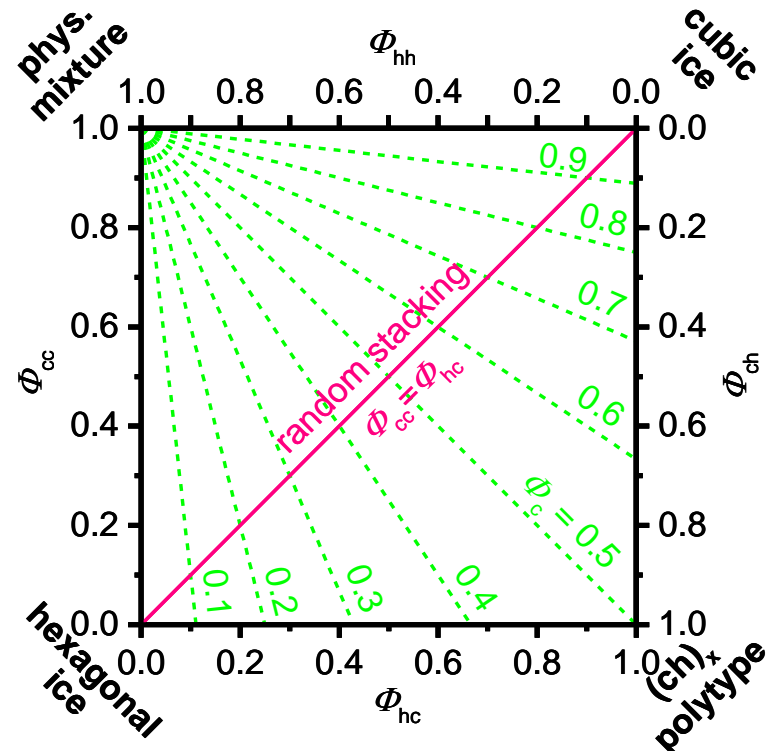
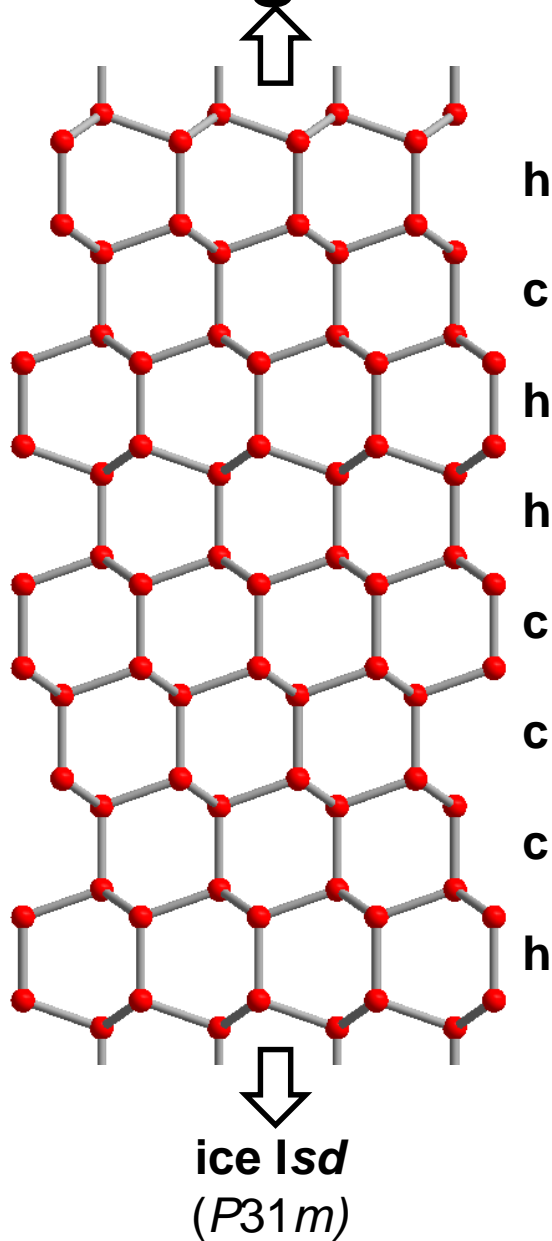
ice Ic

cubic ($Fd-3m$)

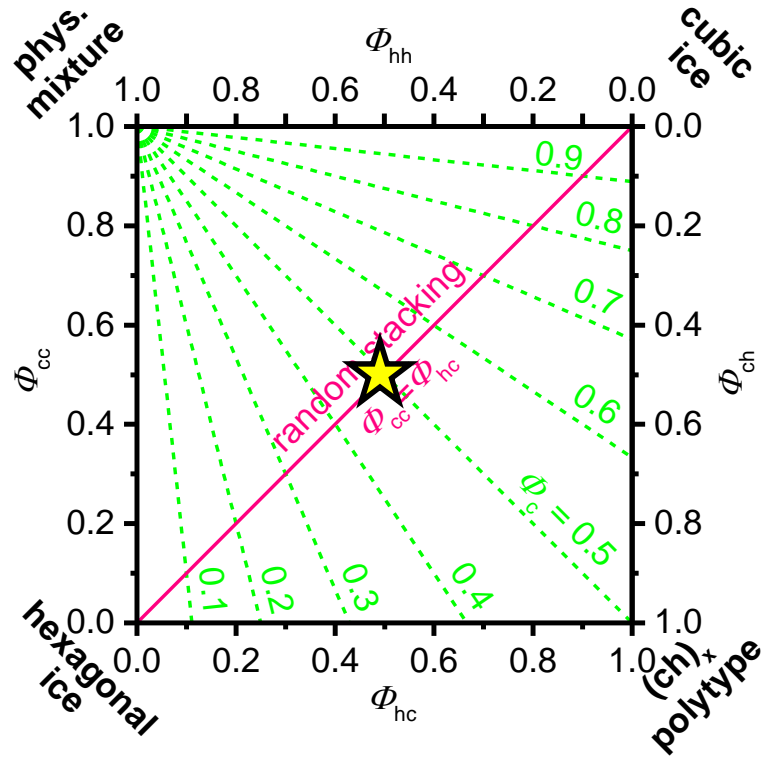
Ice from supercooled water droplets (~232 K)



Stacking disordered ice (ice I_{sd})



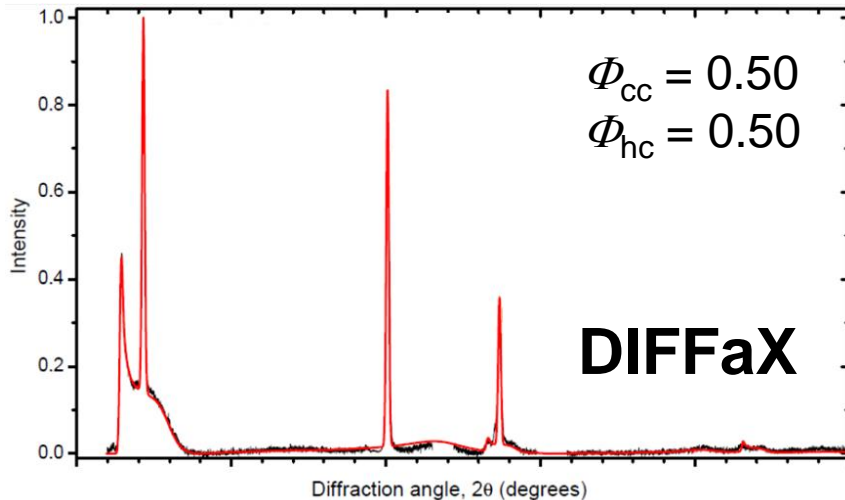
Ice from supercooled water droplets (~232 K)



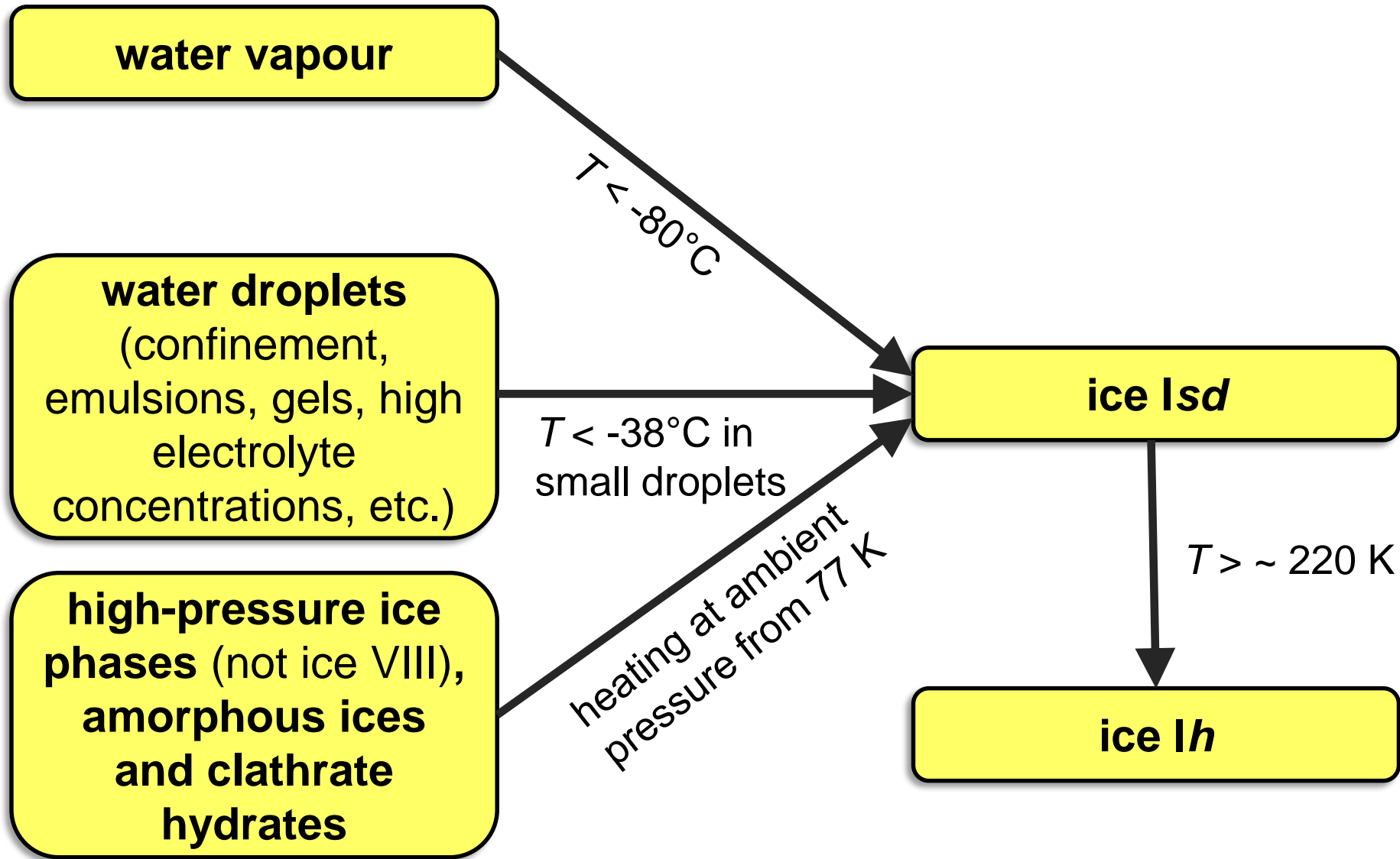
Supercooled water freezes to give ice *Isd* with 50% cubicity and random stacking.

"Cubic ice" does not describe this structure accurately. It describes one corner of the stackogram.

Suggestion by Kuhs *et al.* to call this material ice *Ich* or ice *Ihc* depending on the dominating type of stacking.



Preparation of stacking disordered ice



Memory effects

zero order (no memory)	first order	second order
probabilities defined for: c, h	cc, ch, hc, hh	ccc, cch, hcc, hch, chc, chh, hhc, hhh
$\Phi_c = \frac{\Phi_{hc}}{\Phi_{hc} + (1 - \Phi_{cc})}$	$\Phi_{cc} = \frac{\Phi_{ccc}}{\Phi_{ccc} + (1 - \Phi_{hcc})}$	Φ_{ccc}
		Φ_{hcc}
	$\Phi_{hc} = \frac{\Phi_{hhc}}{\Phi_{hhc} + (1 - \Phi_{chc})}$	Φ_{chc}
		Φ_{hhc}

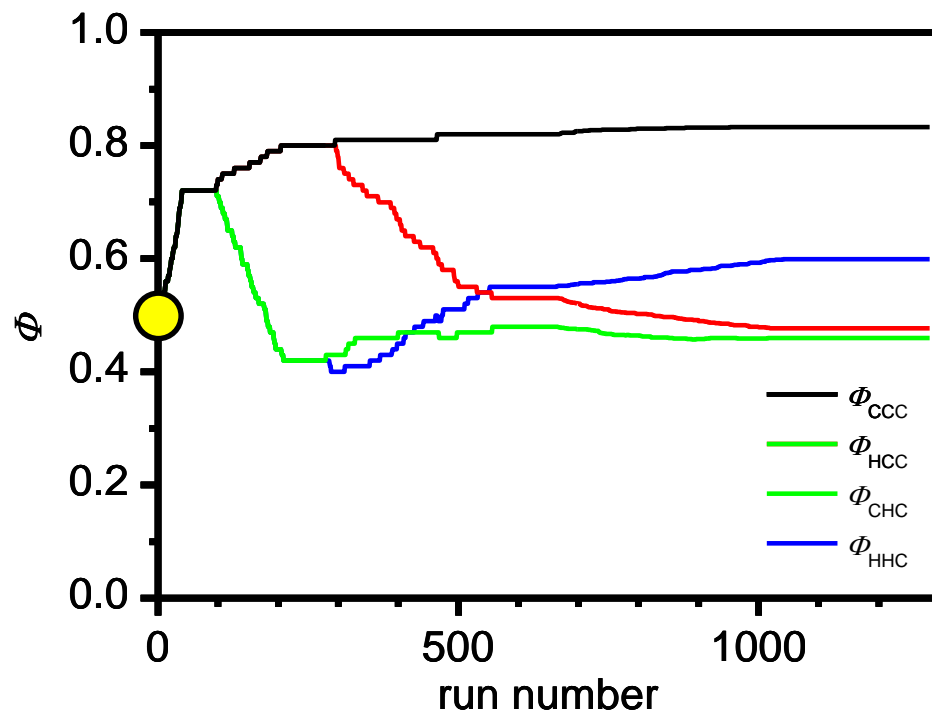
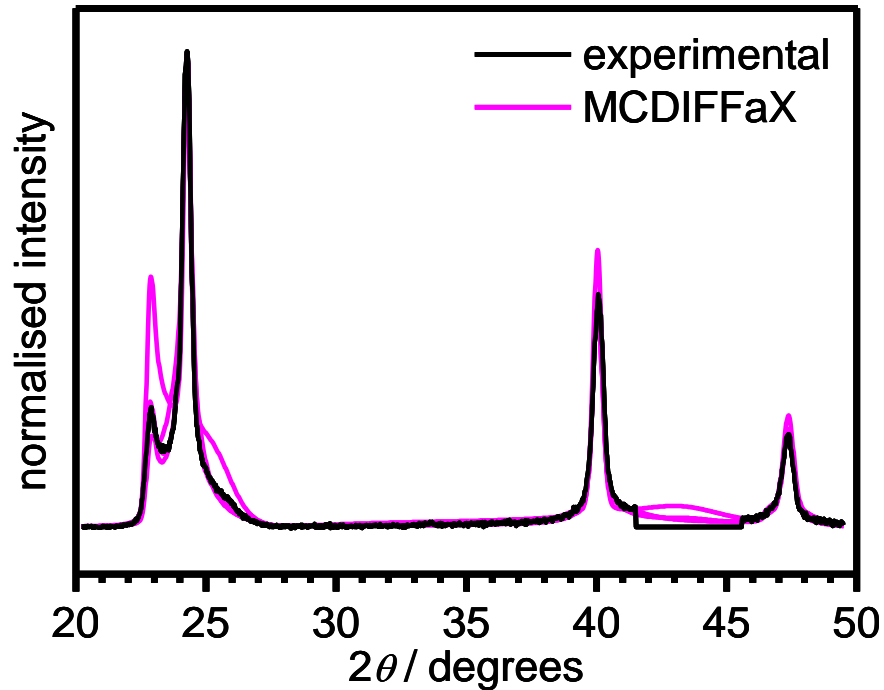


Φ_c = cubicity

$1 - \Phi_c = \Phi_h$ (hexagonality)

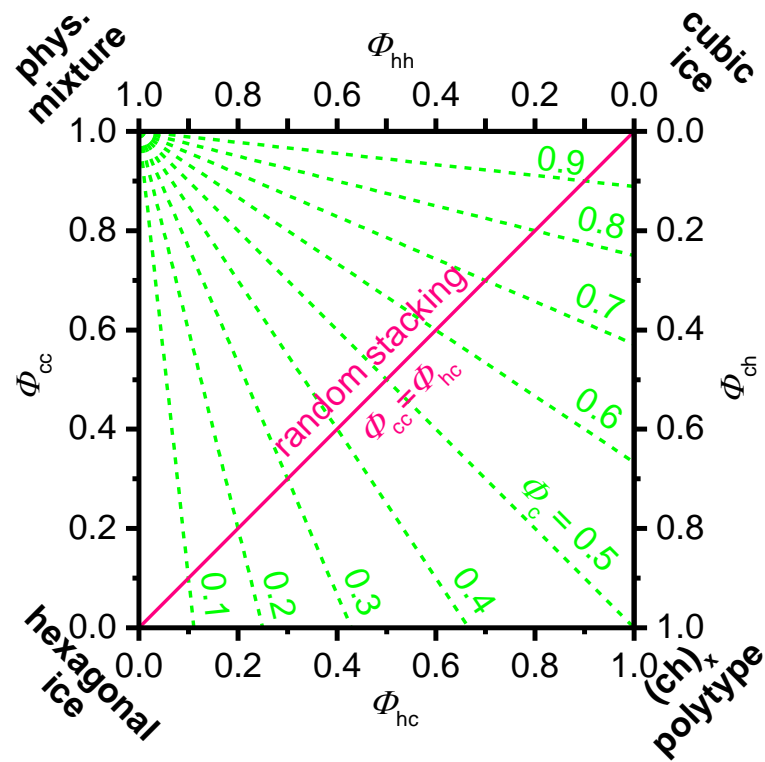
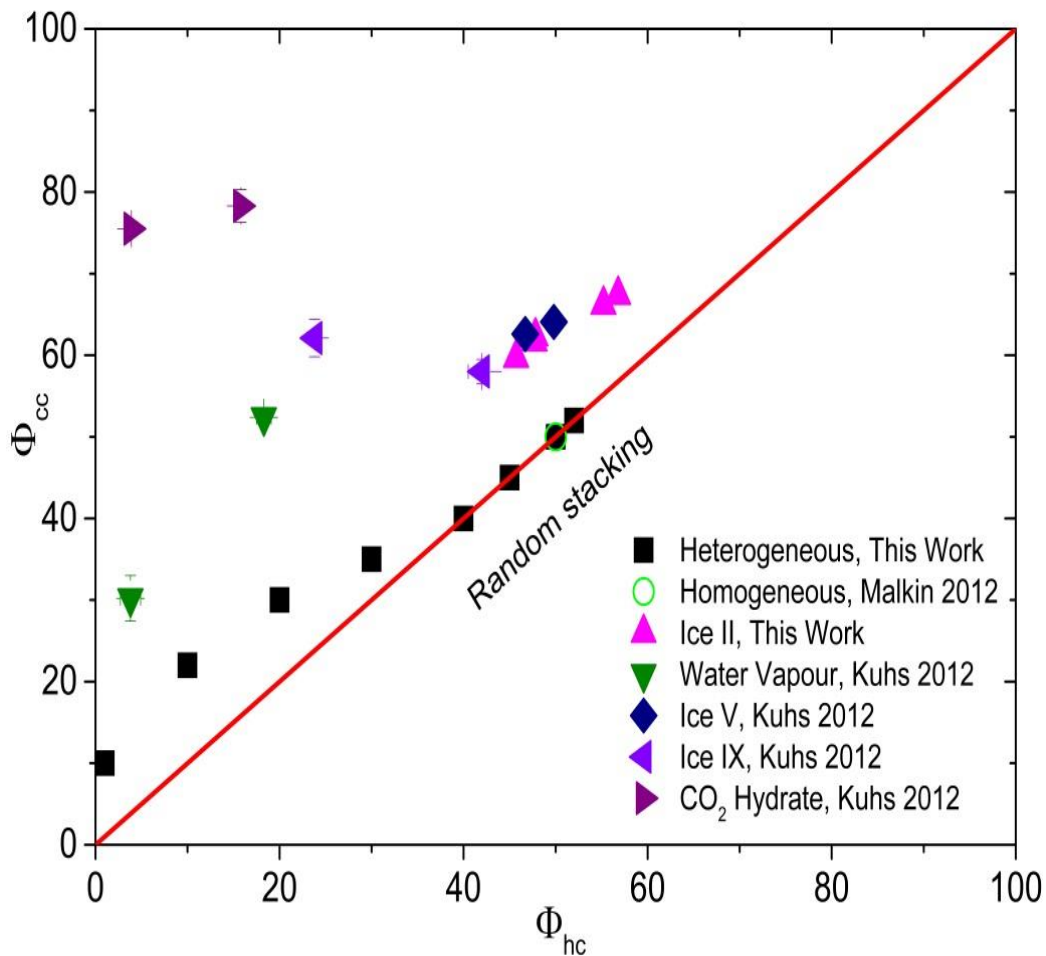
DIFFaX (Treacy *et al.*) in a least-square environment

Refines stacking probabilities (up to 2nd order memory effects), lattice constants, zero shift and peak-profile parameters (u, v, w, GL)



$\Phi_C(\text{zero order})=0.72, \Phi_C(\text{1st order})=0.677, \Phi_C(\text{2nd order})=0.670$

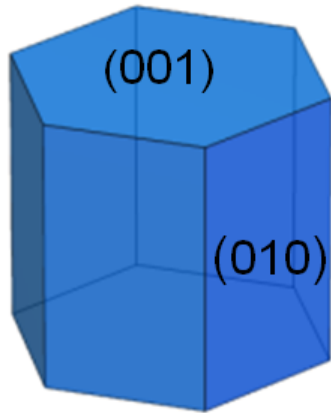
Stacking disordered ice (ice I_{sd})



Tendency to stay in cubic or hexagonal sequences
Still a long way to perfect ice I_c!

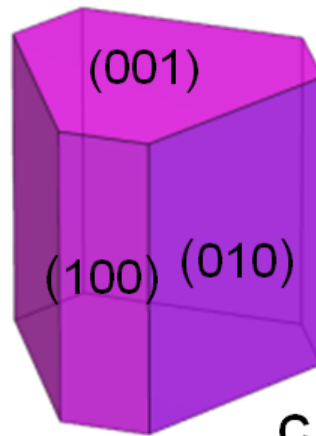
Crystal morphology predictions

(a)



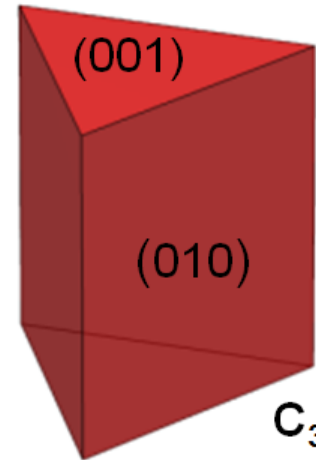
D_{6h}

(b)



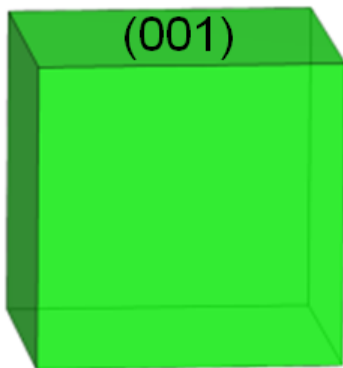
C_{3v}

(c)



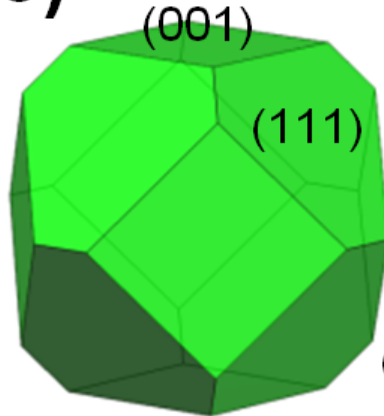
C_{3v}

(d)



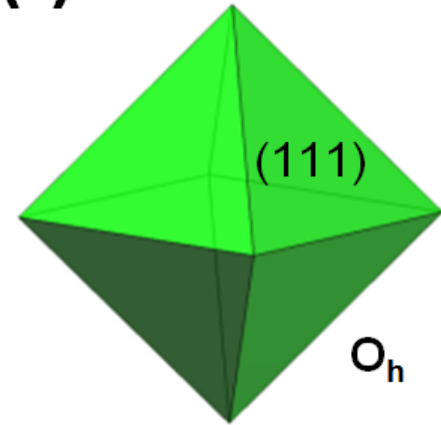
O_h

(e)



O_h

(f)



O_h

Stacking disorder becomes relevant below -15°C .

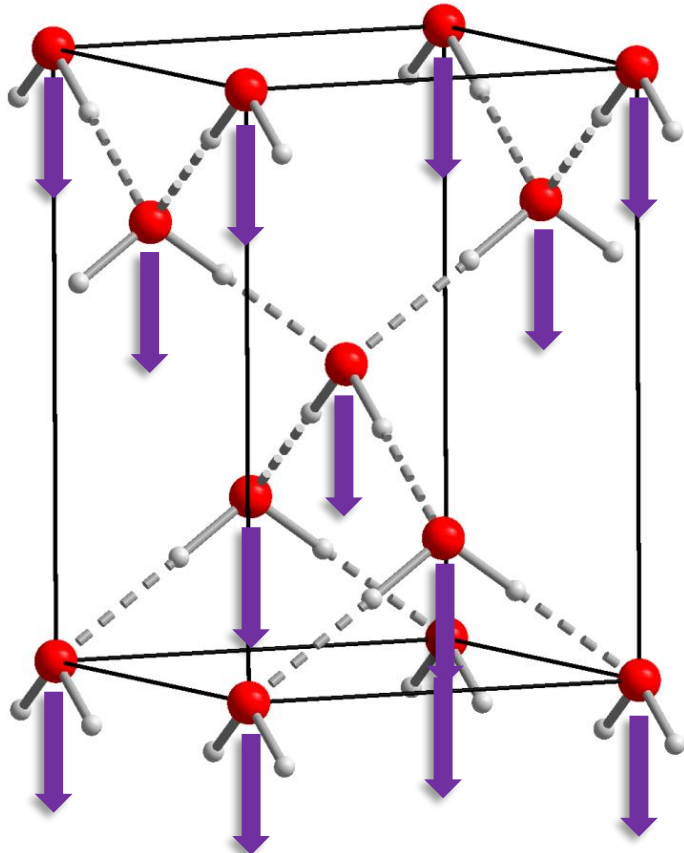
Perfect cubic ice

Scheiner's halo:

A rare halo at 28 degrees from the sun or the moon.

First observation: 20th of March 1629

Hydrogen ordered counterpart:



Snow flakes with three-fold symmetry

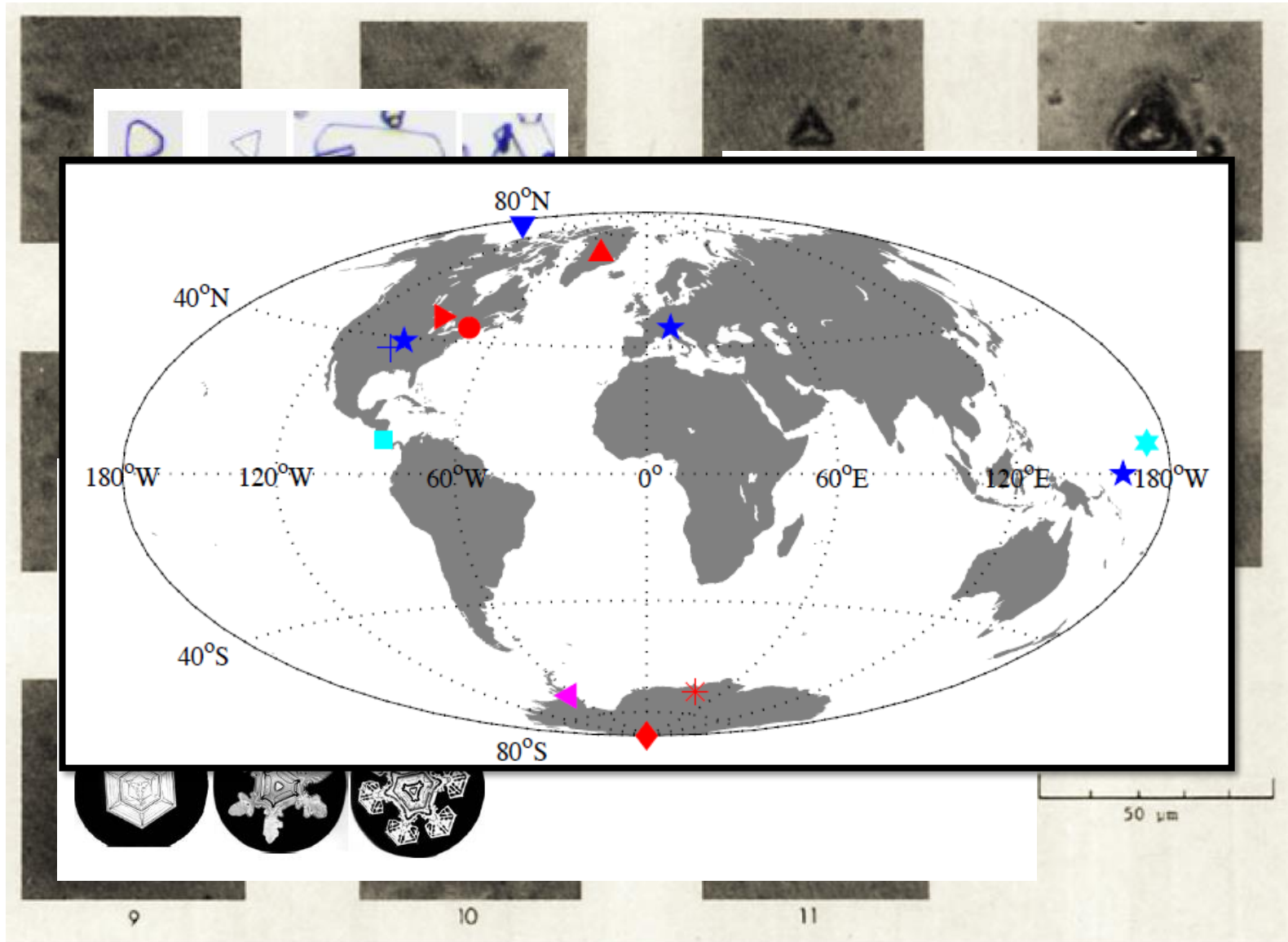
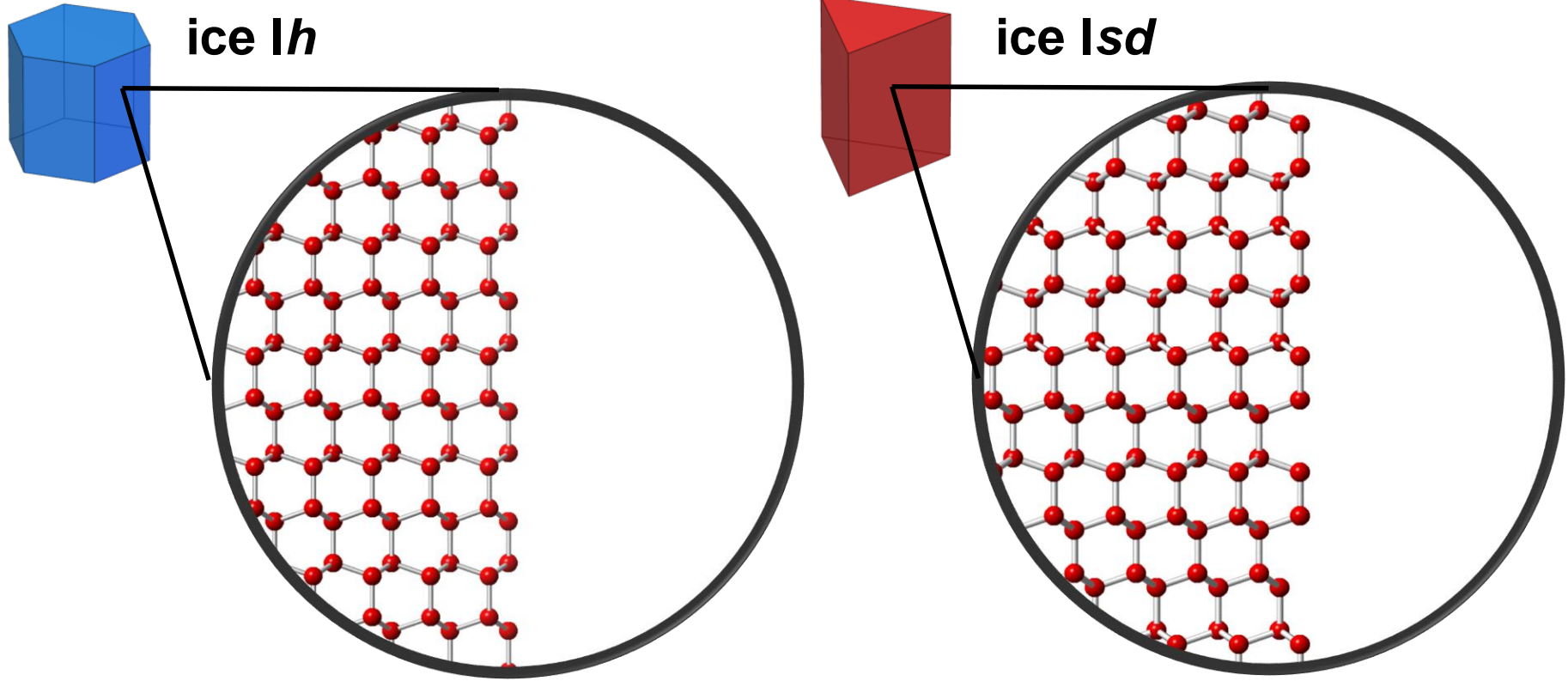


FIG. 3. Examples of trigonal ice crystal shapes observed in the cirrus layer.

Differences between ice *Ih* and *Isd*



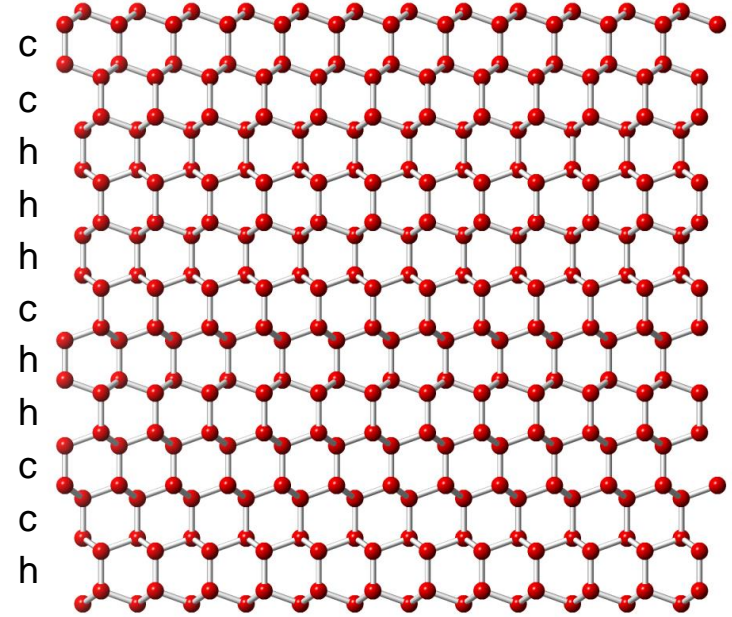
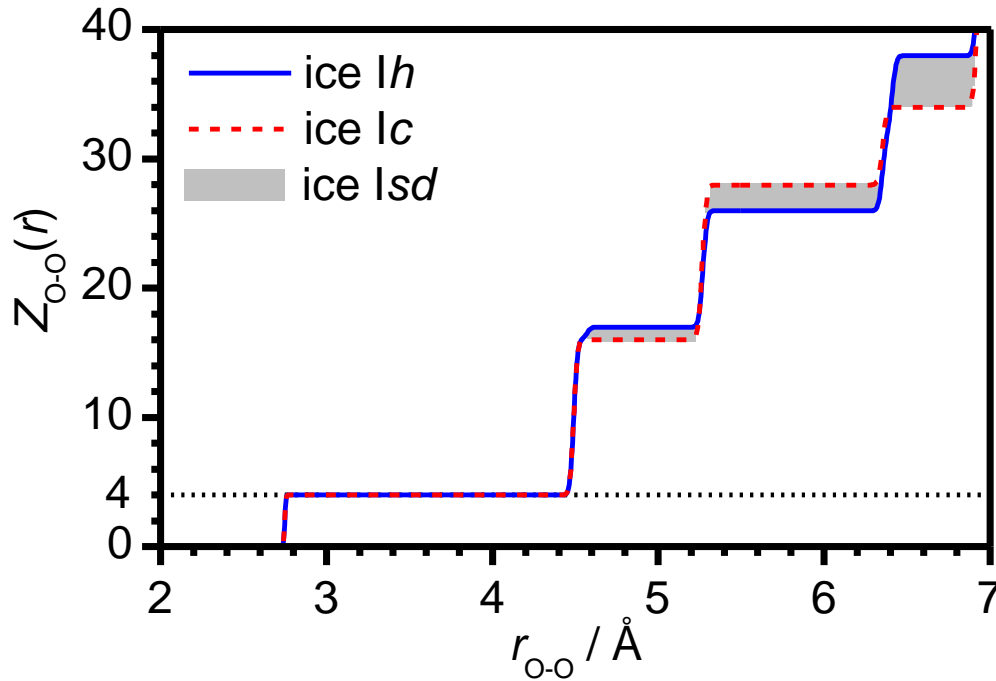
Different crystal morphologies and light scattering properties.

Prismatic faces of ice *Isd* are 'rougher' (→ surface chemistry).

Ice *Isd* has a higher vapour pressure than *Ih*.

Growing realisation that stacking disorder in ice has profound consequences on its chemical and physical properties.

Spectroscopy of stacking disordered ice

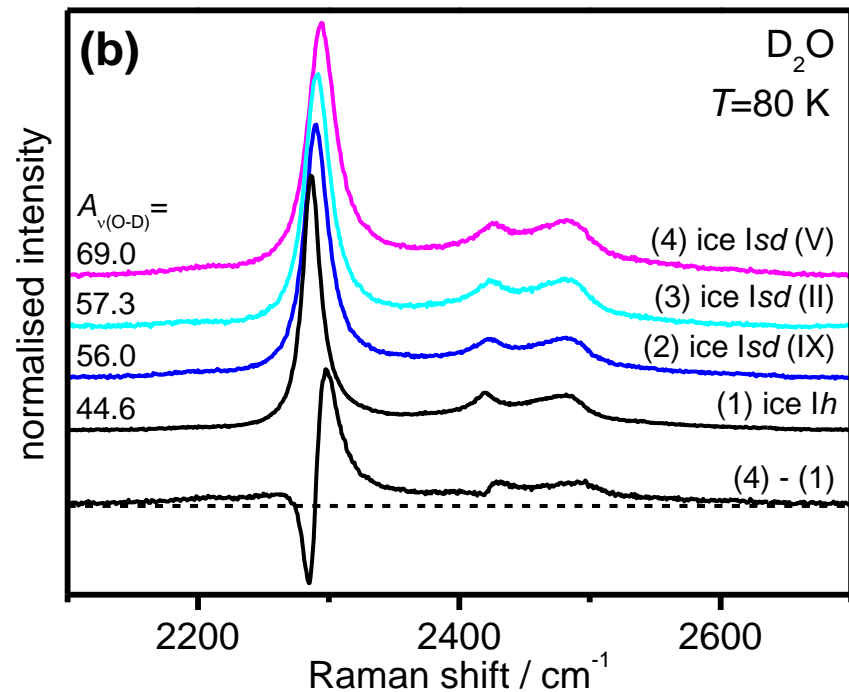
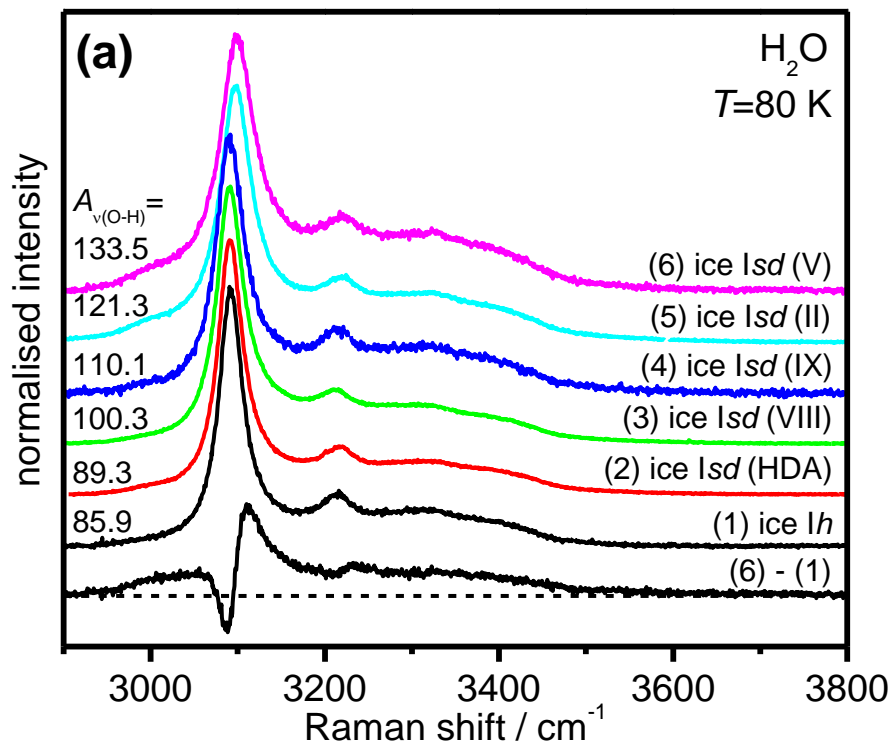


Subtle structural differences and local density fluctuations in the ice I family beyond the first coordination shell.

Can we detect stacking disorder in ice spectroscopically?

Urgent demand for lab studies as well as for remote applications.

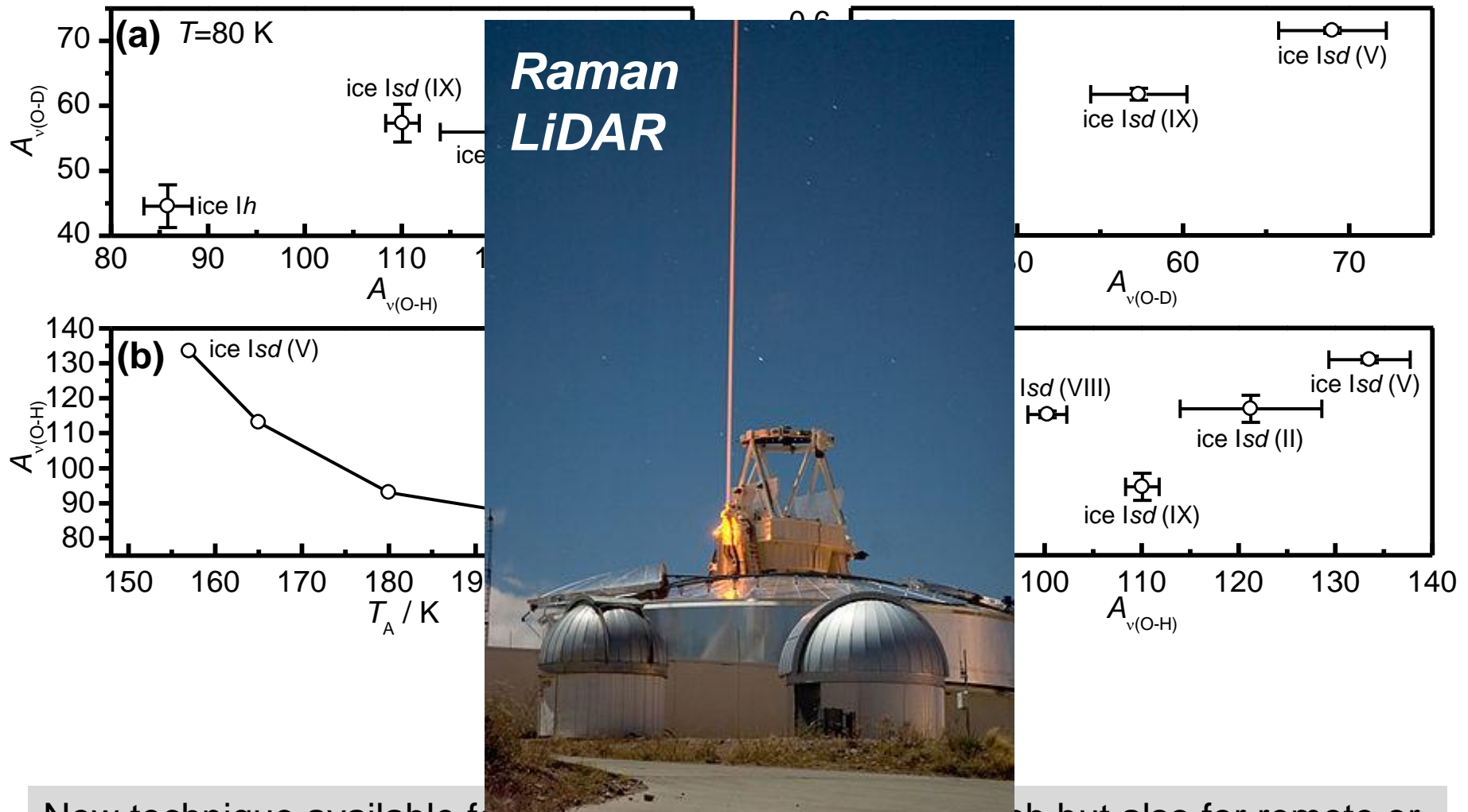
Coupled stretching modes of ice *Isd*



Spectral differences exist between ice *Isd* and ice *Ih*.

The integrated peak areas are a measure for the extent of stacking disorder in ice.

Correlations with other techniques



New technique available for characterizing ice Isd in the lab but also for remote or even telescopic applications.

Near-space balloon with Arduino

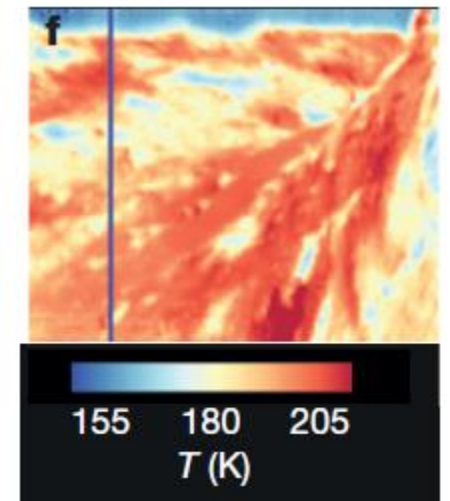
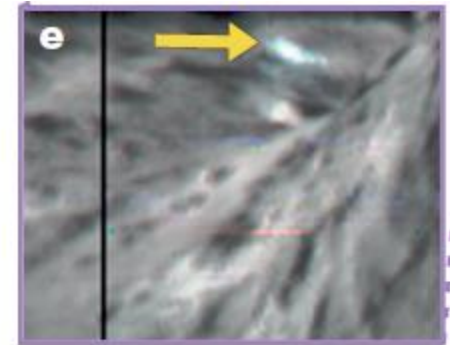
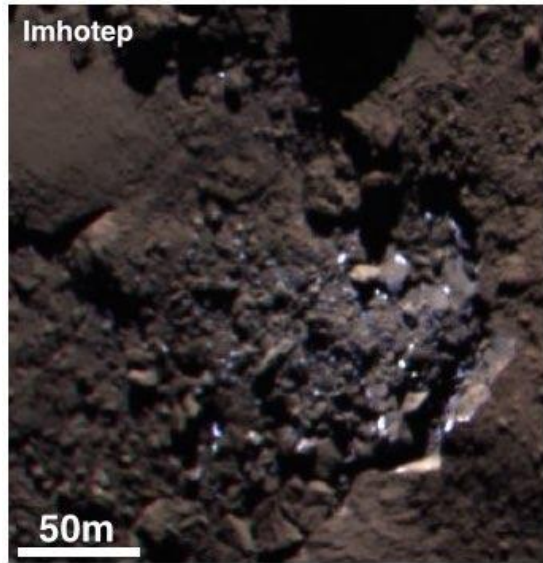
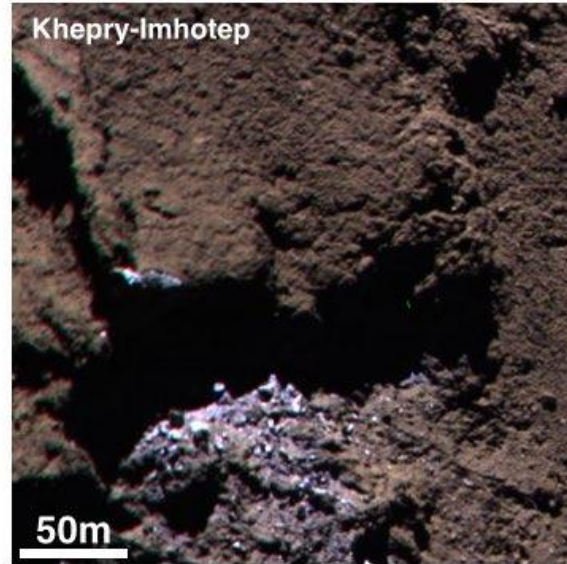
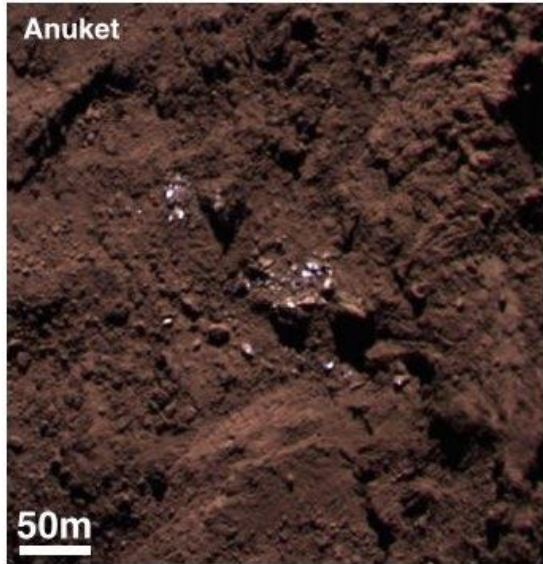


- 1) Weather
- 2) Parachute
- 3) Duct-tape
- 4) Buzzer
- 5) Hand-wired
- 6) GPS antenna
- 7) Lithium
- 8) Canon point-and-shoot camera, hacked with CDHX firmware upgrade
- 9) Arduino Uno microcontroller with Trackuino radio transmitter shield
- 10) External temperature sensor
- 11) Coat-hanger radio antenna

Ice Isd on "Tschuri"

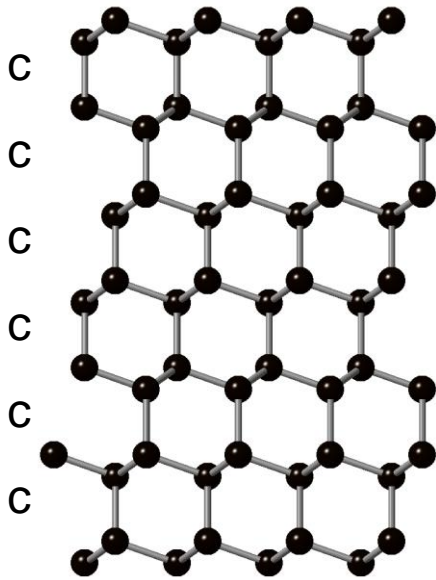


European Space Agency

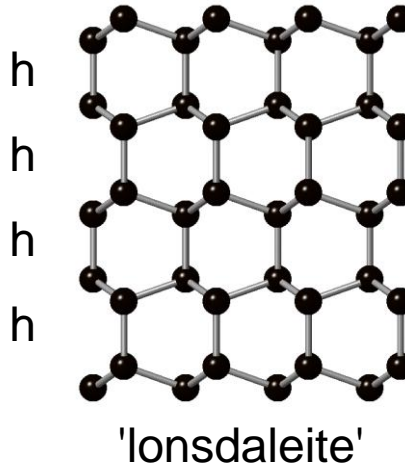


Stacking disorder in diamond

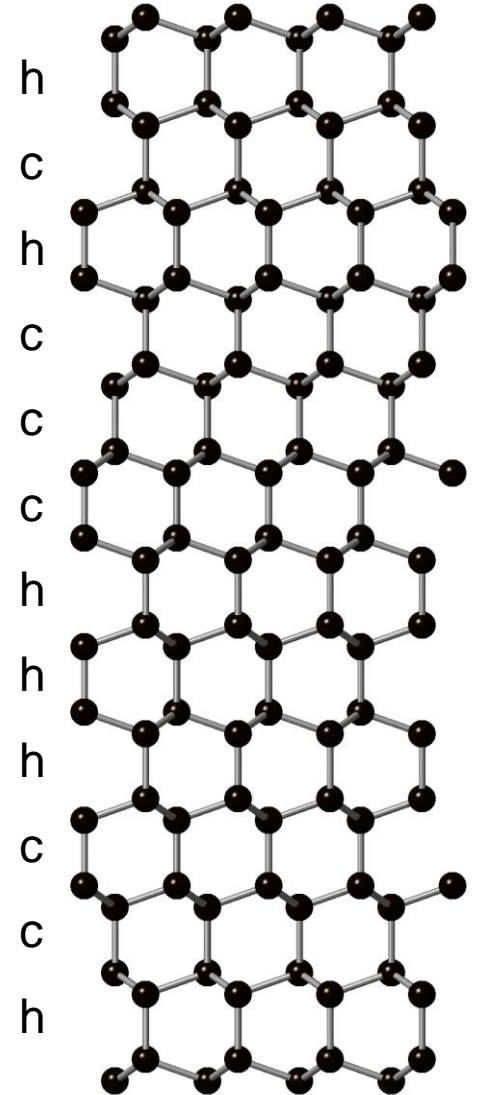
cubic diamond



hexagonal diamond



stacking disordered diamond



Ice I and diamond are isostructural.

Hexagonal diamond?

"Lonsdaleite is harder than diamond"

Z. Pan et al., Phys Rev Lett. 102 (2009) 055503

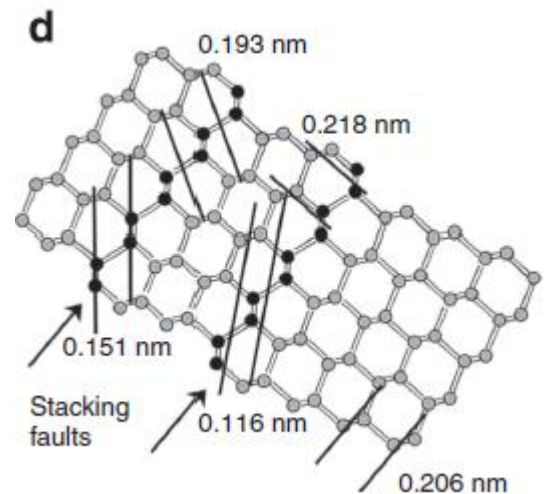
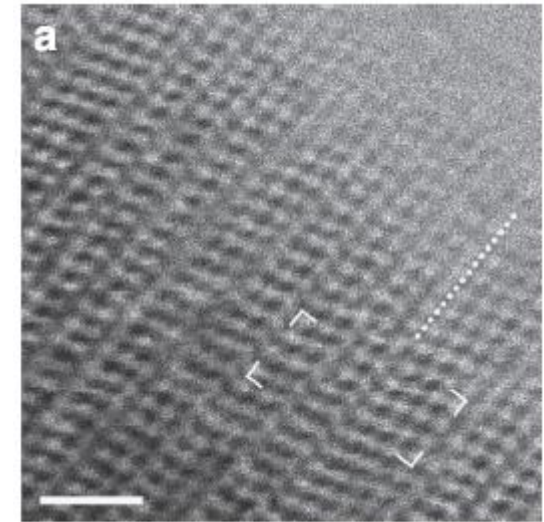
"Lonsdaleite is faulted and twinned cubic diamond"

P. Németh et al., Nat Comm. 5 (2014) 5447

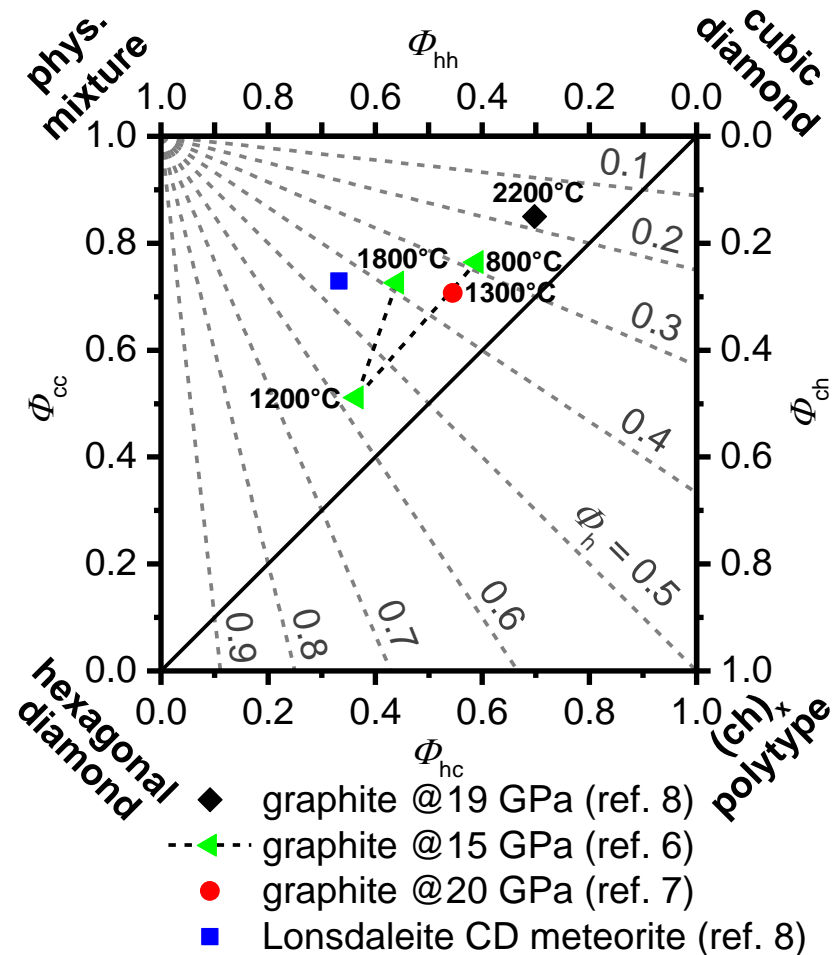
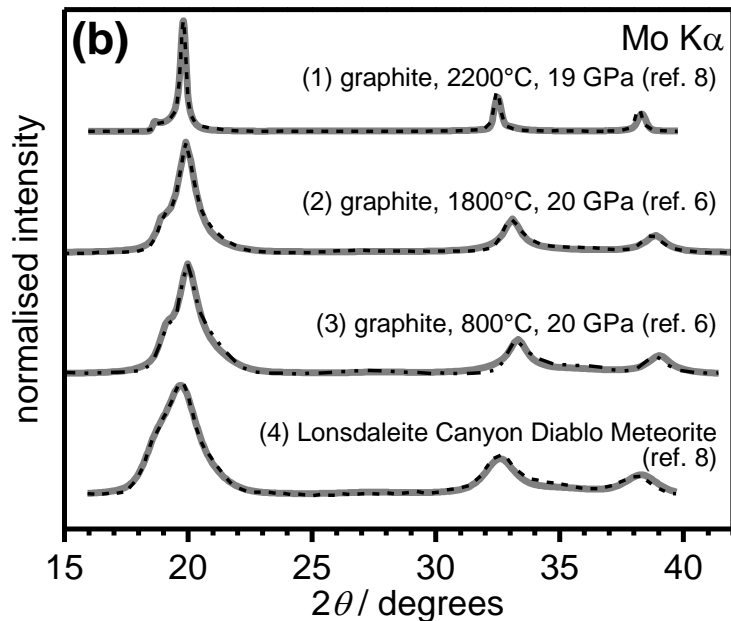
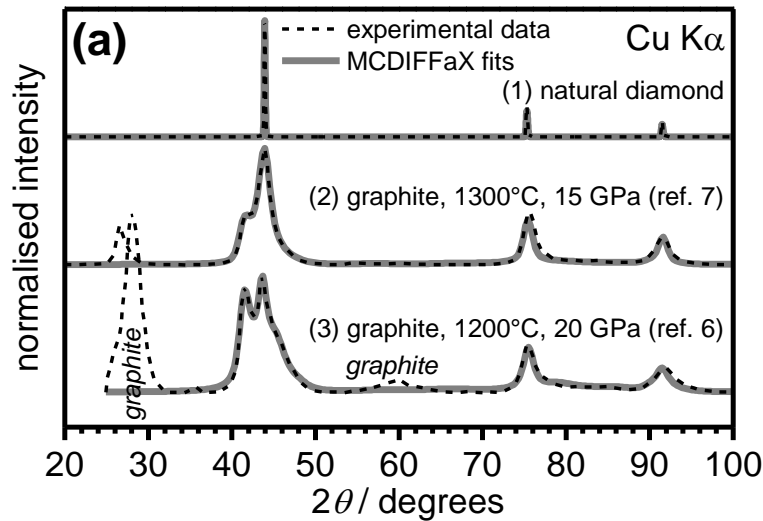


Meteorite Crater (Arizona, USA)

<011> STEM image of Canyon Diablo diamond

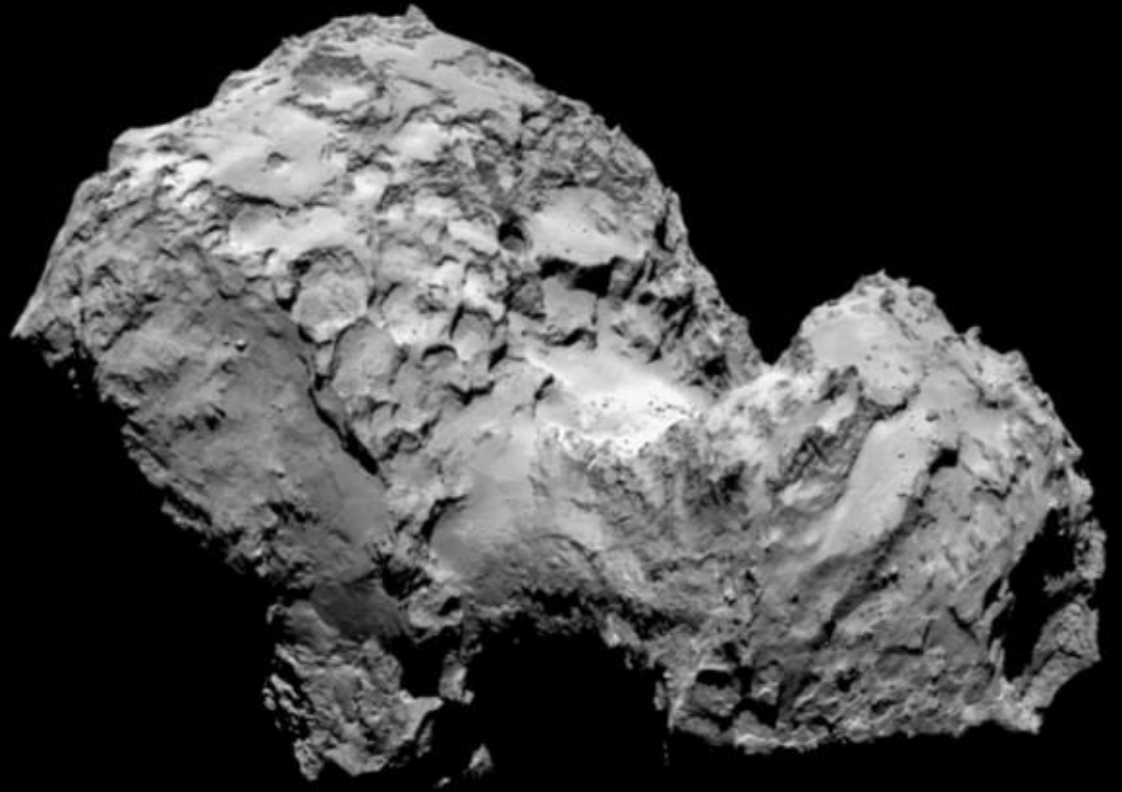


MCDIFFaX analysis of diamond samples

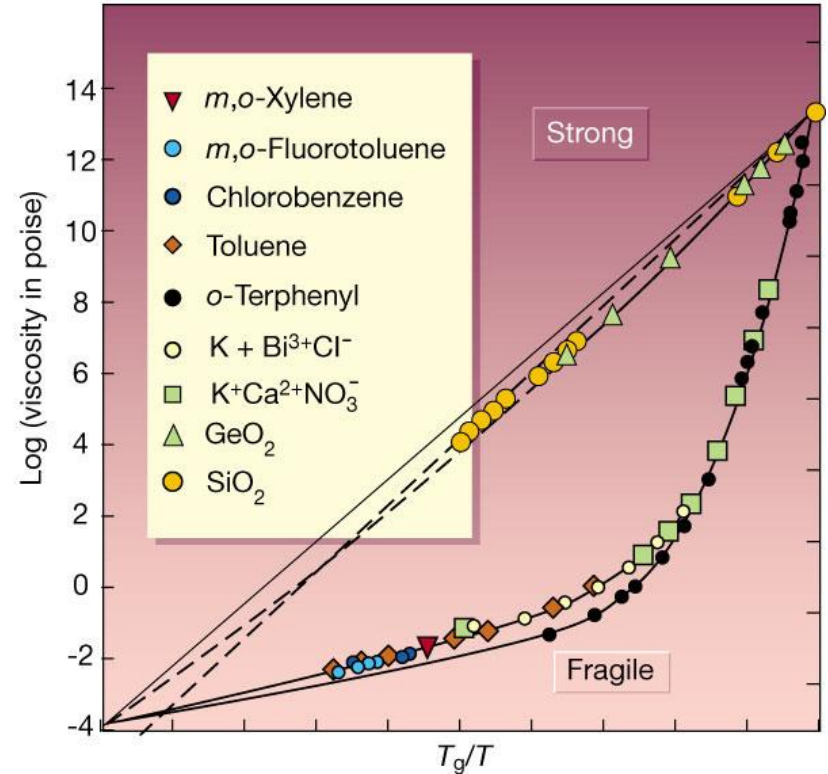
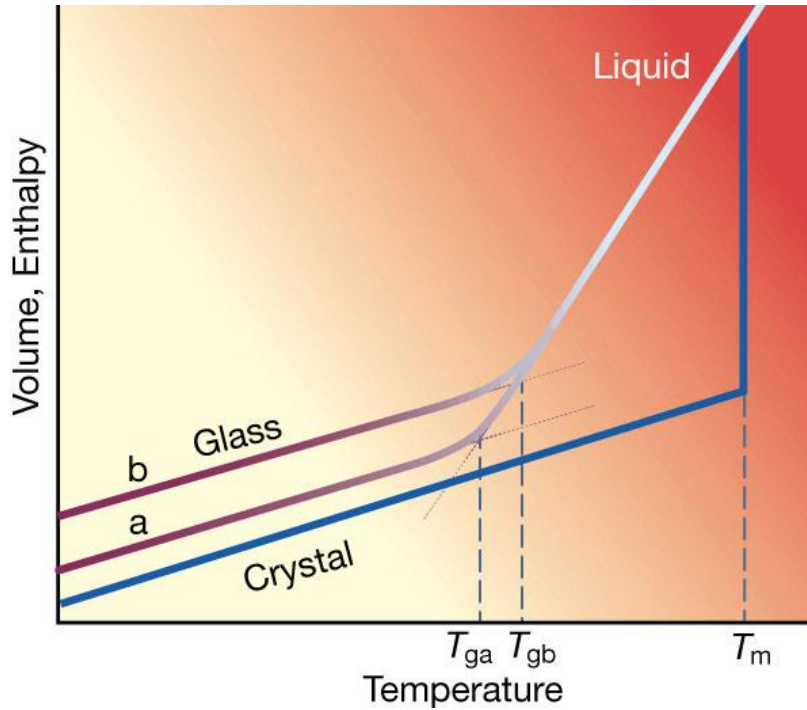


Lonsdaleite is not hexagonal but stacking disordered diamond.

3. Amorphous ice



Typical glass-forming liquids



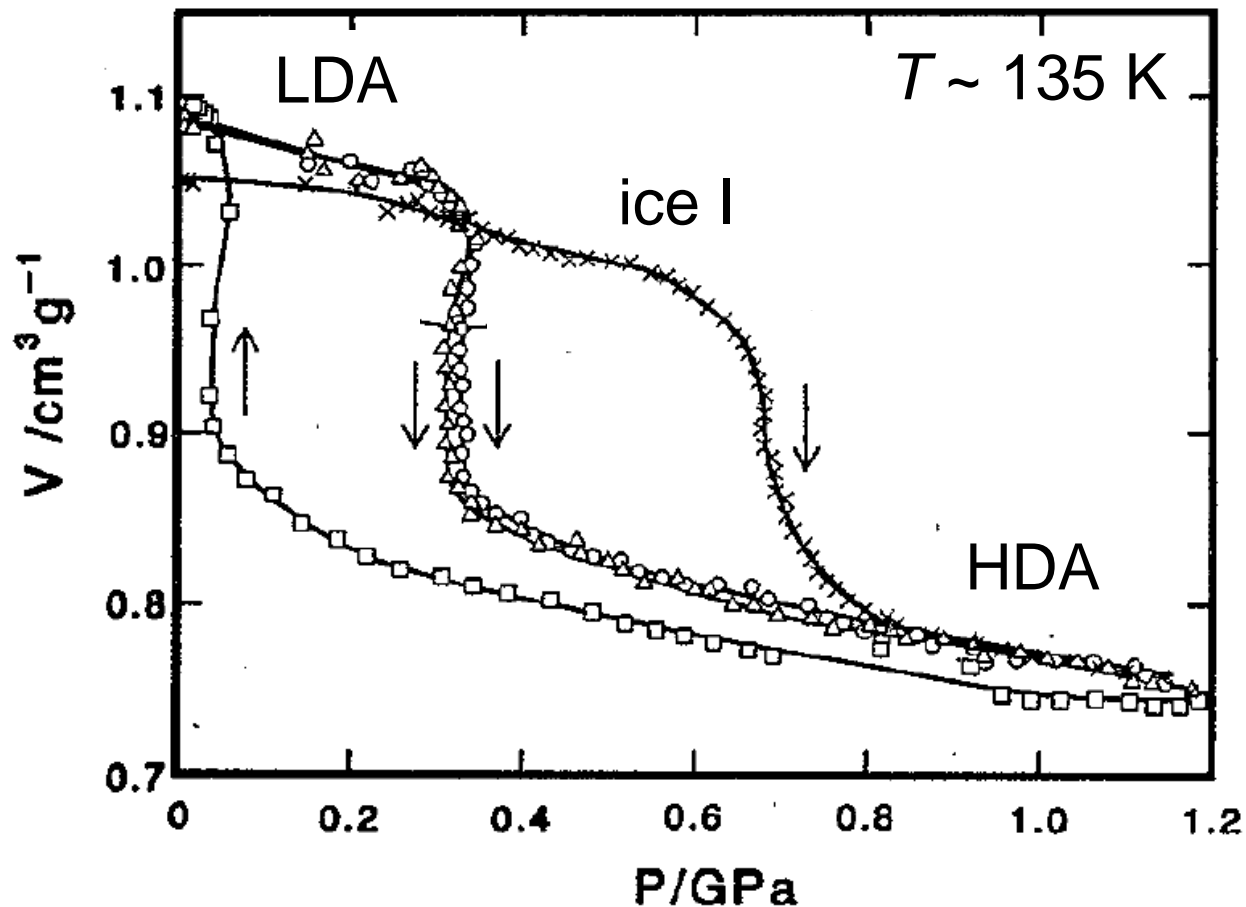
In calorimetry we measure the heat capacity (plus a background function)
 → glass transition: step in heat capacity (ΔC_p)
 → melting of crystal: sharp peak (ΔH)

Classification of glass-forming liquids according to Angell:
 → strong relaxation behaviour (network glasses)
 → fragile relaxation behaviour (molecular glasses)

The polyamorphism of H_2O

LDA = low-density amorphous ice

HDA = high-density amorphous ice



first-order transition
between LDA and HDA
at low temperatures.

LDA and HDA are
amorphous according to
diffraction.

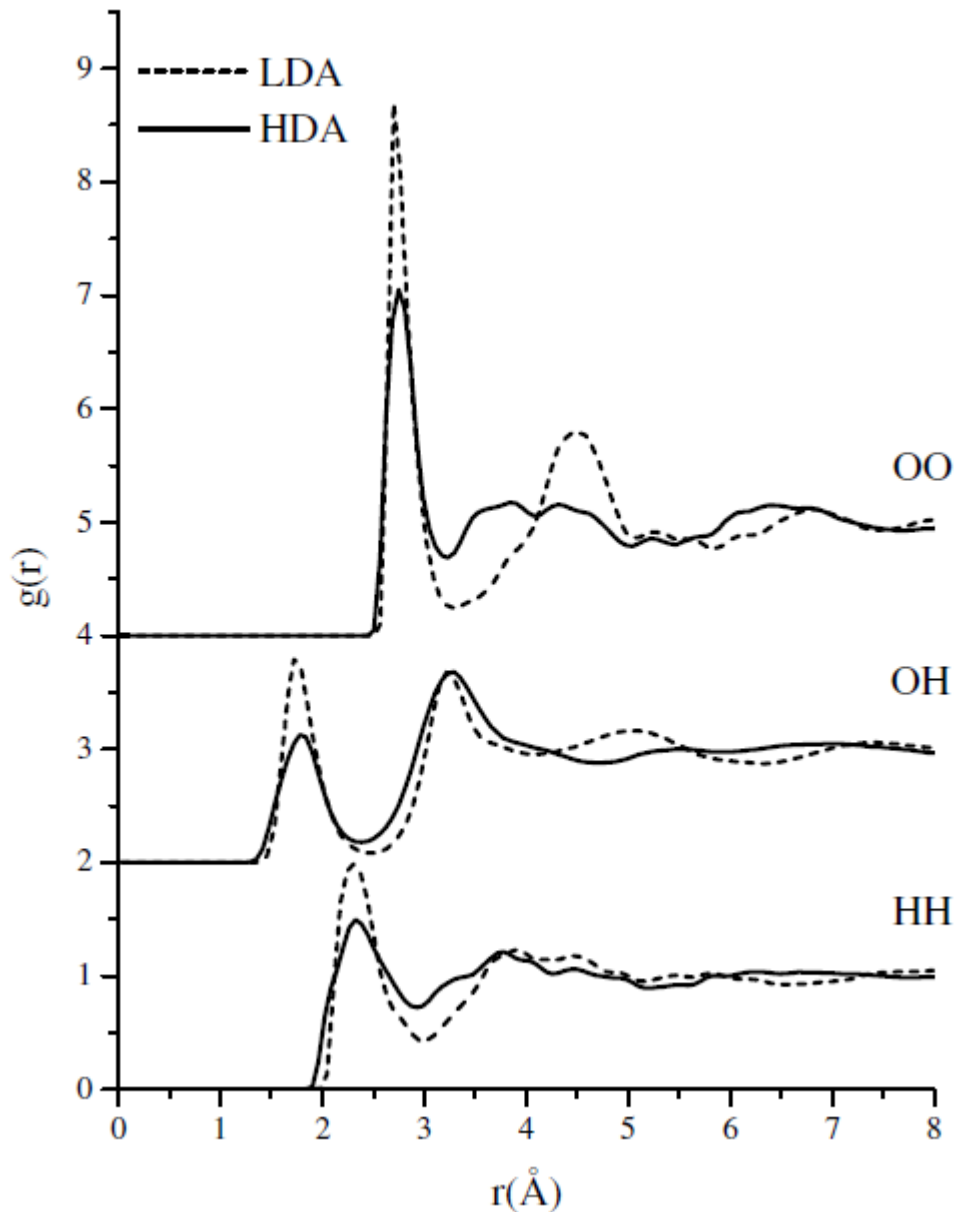
amorphous =
no Bragg peaks

O. Mishima, L. D. Calvert, E. Whalley, Nature 1984, 310, 393.

O. Mishima, L. D. Calvert, E. Whalley, Nature 1985, 314, 76.

O. Mishima, J. Chem. Phys. 1994, 100, 5910.

The structures of LDA and HDA



Water molecules are fully hydrogen bonded in both (tetrahedral networks)

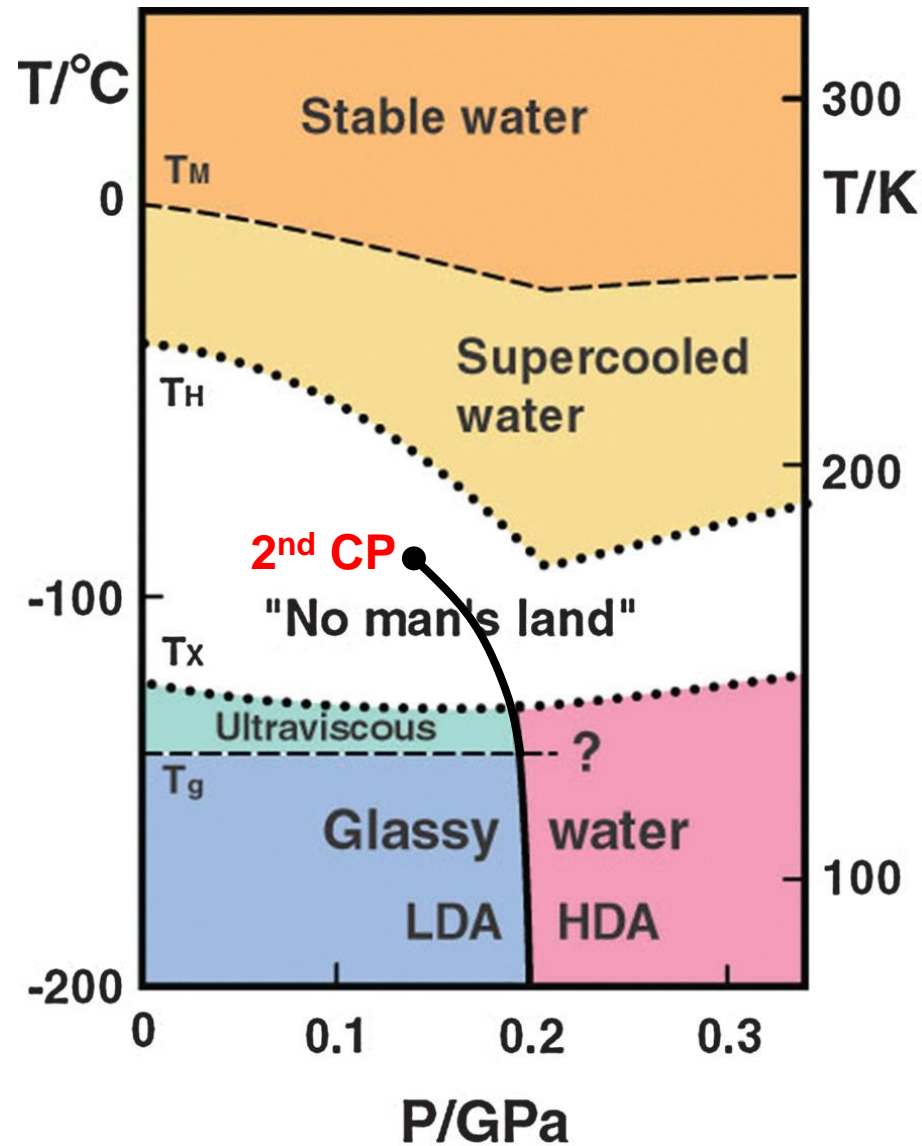
Amorphous ices are 'crystalline' in the first coordination shell.

How much further out does this order persist?

In HDA, a fifth "lynch pin" molecule moves in towards the first coordination shell.

Similar trends as for the crystalline phases of ice.

The 2nd critical point scenario



Only one liquid phase above melting temperature.

LDA and HDA may be glassy materials that have associated liquids (LDL and HDL)

Equilibrium line between LDL and HDL ends in a 2nd critical point.

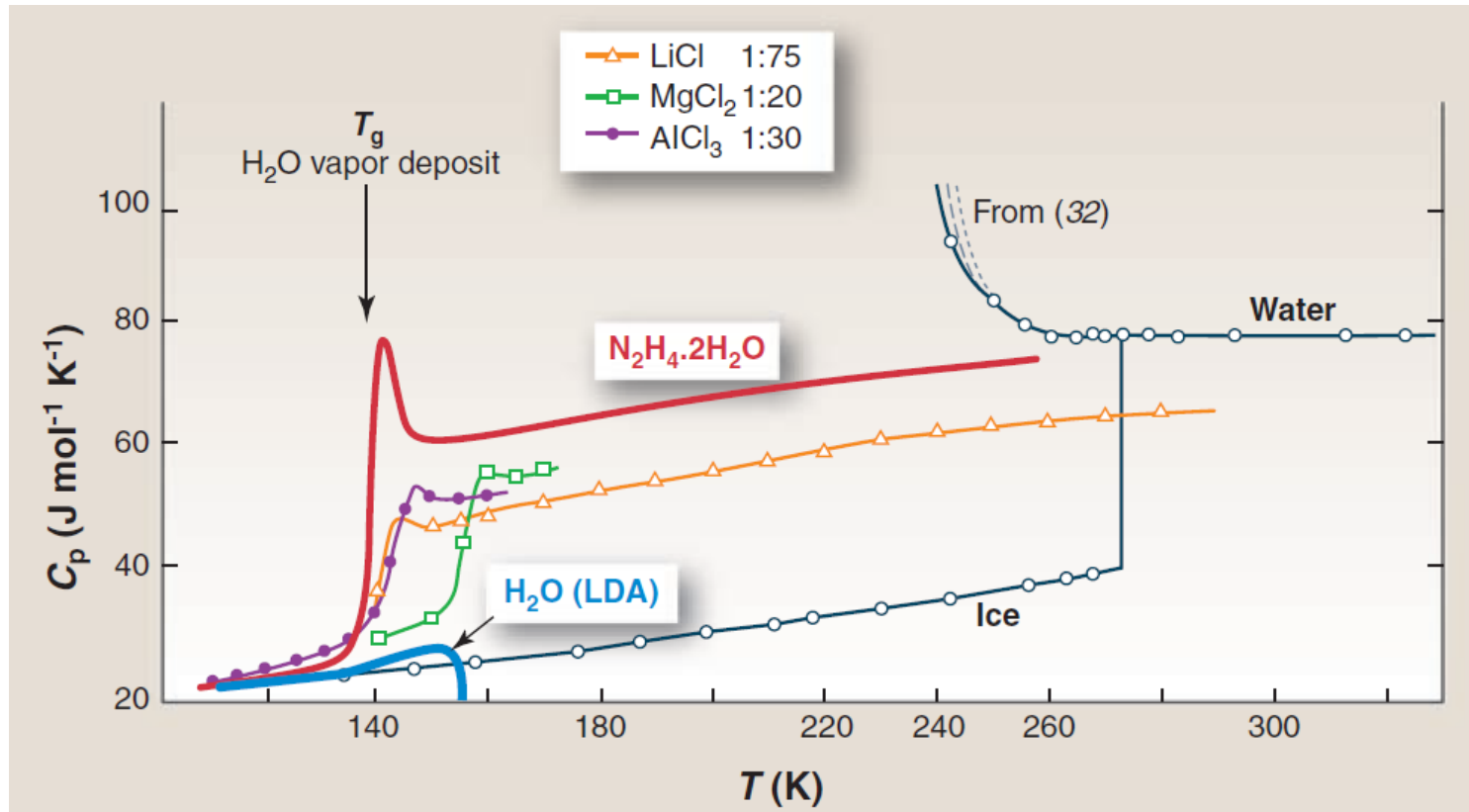
The question of glass transition is critical since this distinguishes glasses from amorphous materials.

P. H. Poole, F. Sciortino, U. Essmann, H. E. Stanley, *Nature*, 360 (1992) 324–328.

H. E. Stanley, C. A. Angell, U. Essmann, M. Hemmati, P. H. Poole, F. Sciortino, *F. Phys. A*, 205 (1994) 122.

F. Sciortino, P. H. Poole, U. Essmann, H. E. Stanley, *Phys. Rev. E*, 55 (1997), 727–737.

Unusual heat capacity behaviour of water



The heat capacity of water *increases* upon cooling.

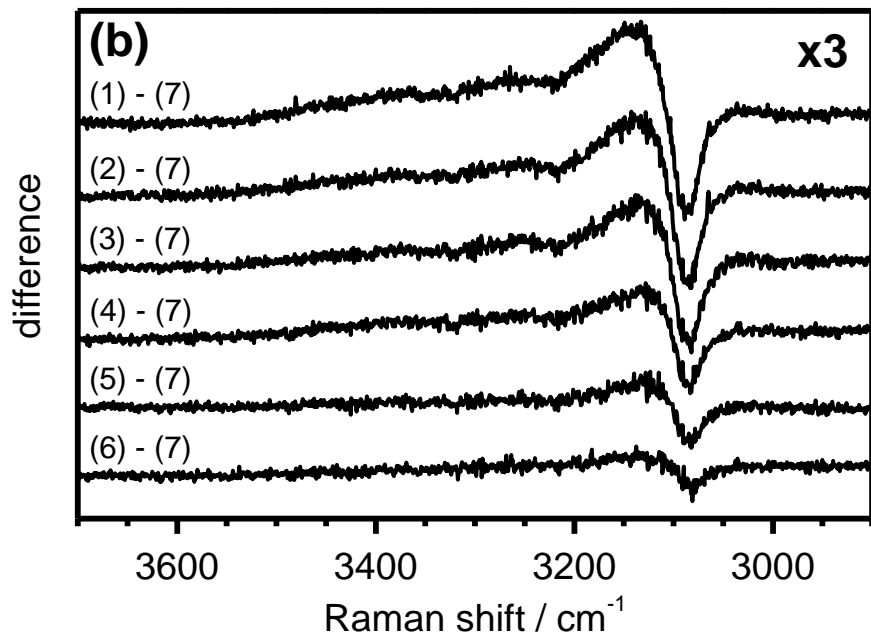
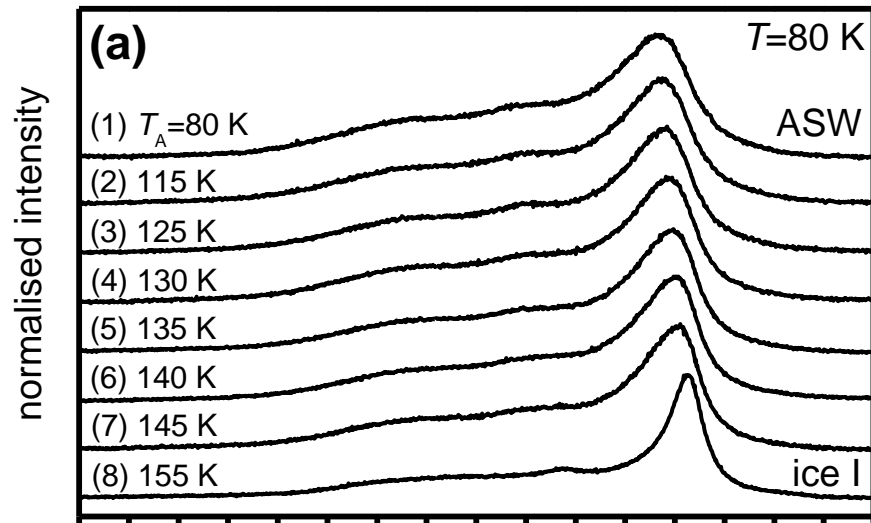
Water is not a simple glass-forming liquid.

Glass-to-liquid transition of LDA at 136 K is highly controversial. Also described as "shadow glass transition" or "order-disorder" transition.

LDA and HDA display *strong* relaxation behaviour.

Liquid water is classified as *fragile*.

Coupled O-H stretching modes of ASW



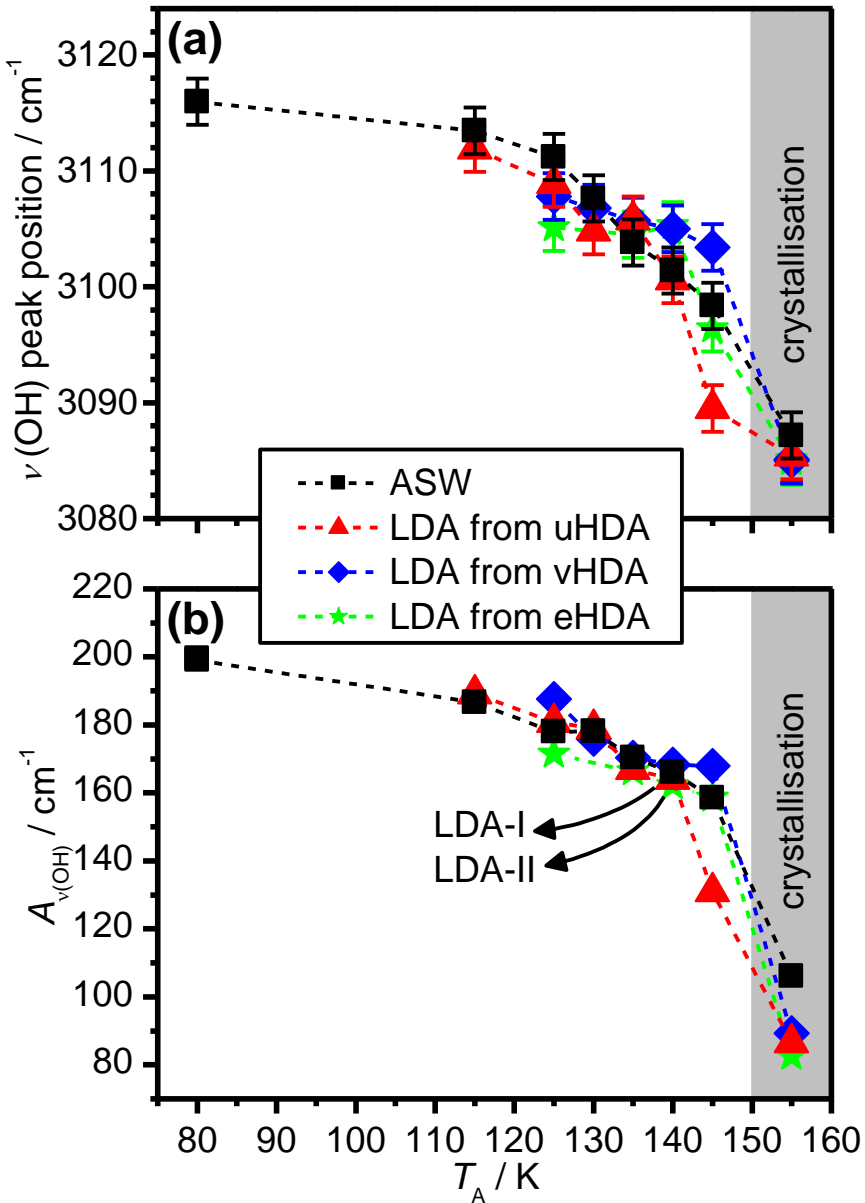
Heating to successively higher annealing temperatures followed by cooling back to 80 K.

Thermal annealing of ASW leads to:

- (1) sharpening of the main peak
- (2) decreases in intensities of the shoulders.
- (3) shift of the main peak

A gradual structural relaxation process takes place upon heating ASW.

LDAs from different origins

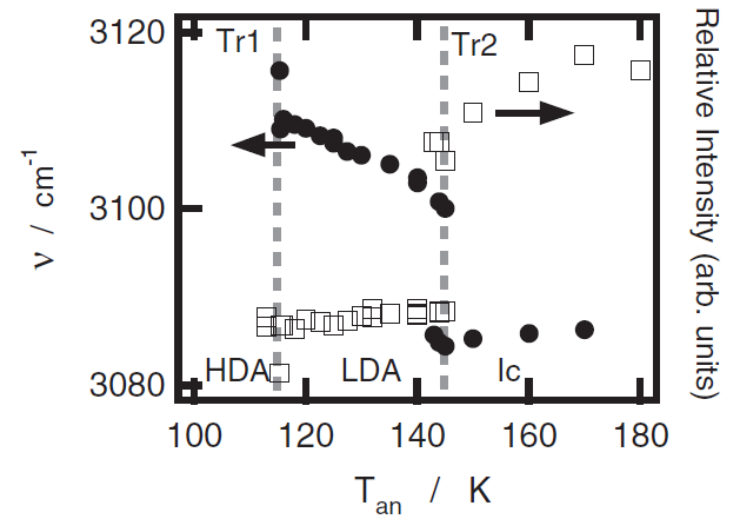


Same structural relaxation process for LDAs from HDAs.

A gradual structural relaxation process takes place upon heating LDA.

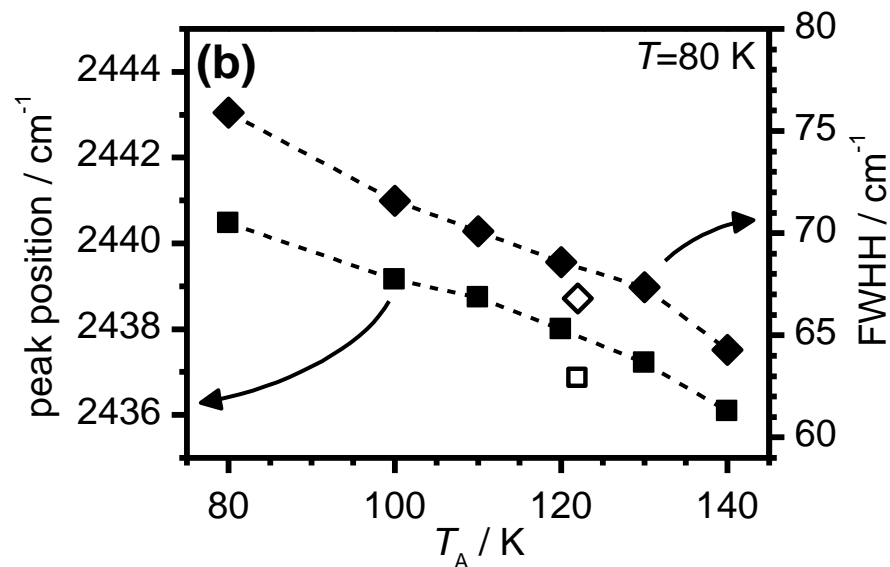
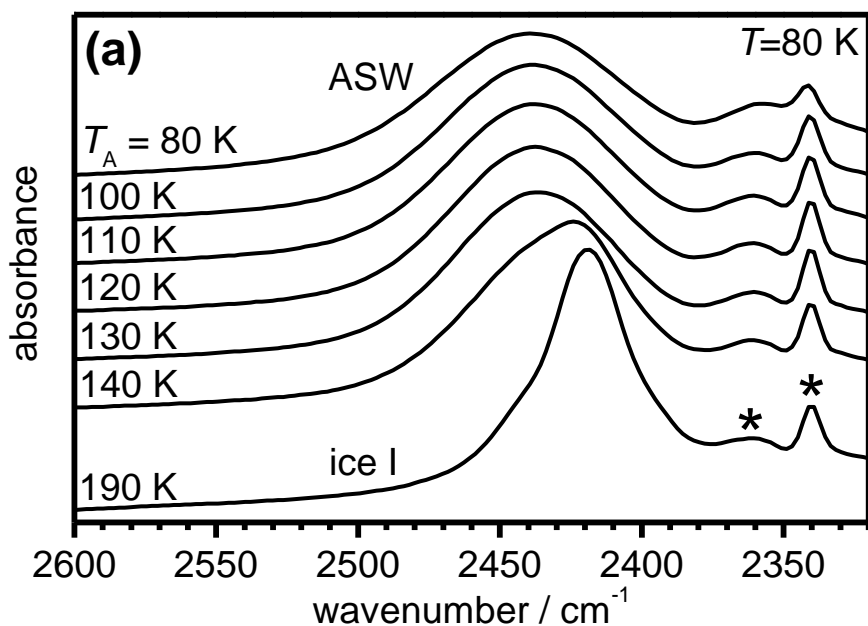
Process is separate from crystallisation and does not seem to reach completion before crystallisation.

Difficult to reconcile with a glass transition to the liquid.



J. J. Shephard, J. S. O. Evans, C. G. Salzmann, J. Phys. Chem. Lett., 4 (2013) 3672-3676
 Y. Suzuki, O. Mishima, J. Phys. Soc. Jpn. 72 (2003) 3128.

Decoupled O-D stretching modes of ASW

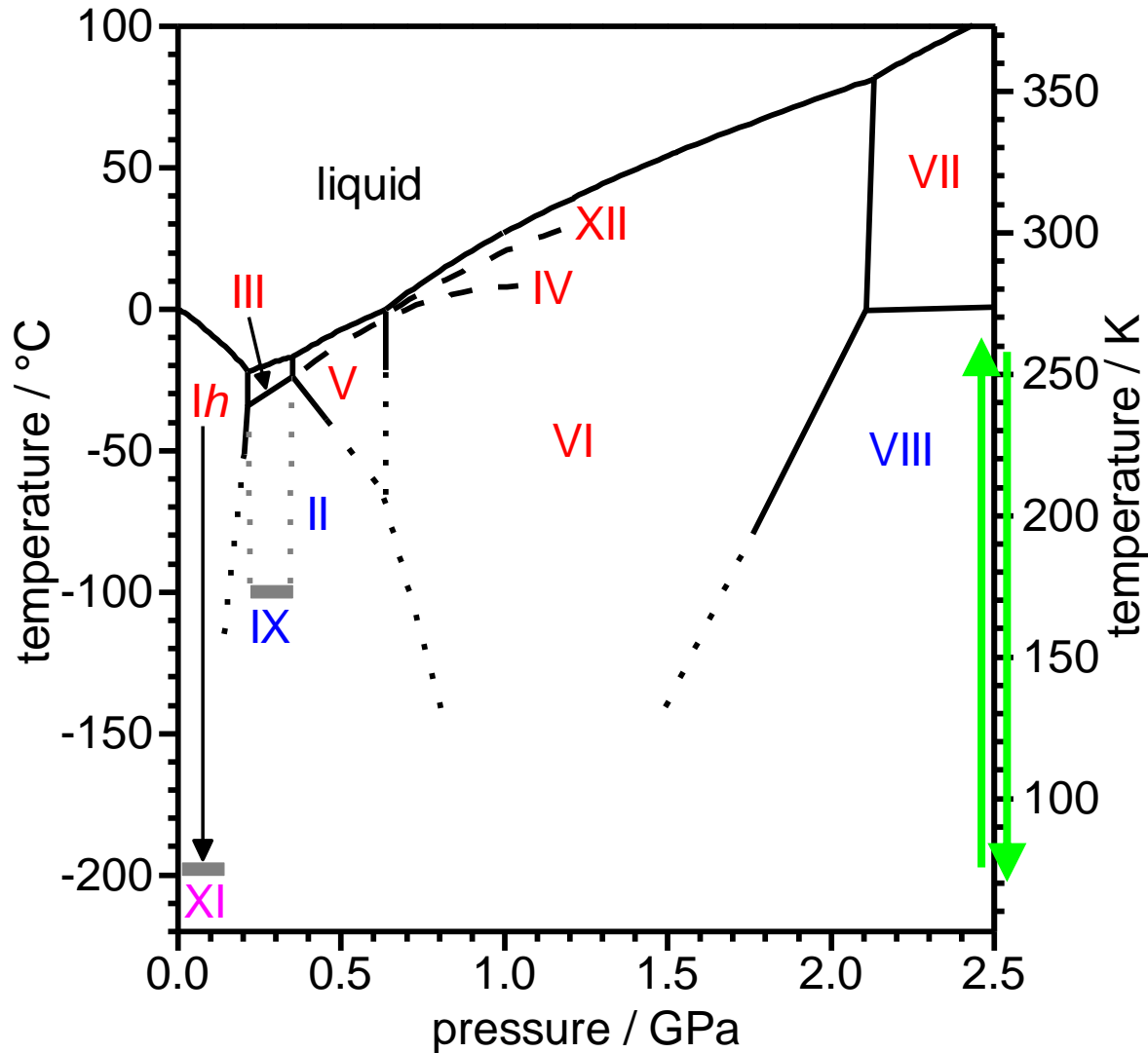


Decoupled O-D modes are sensitive to local structure.

Local structural changes start immediately.

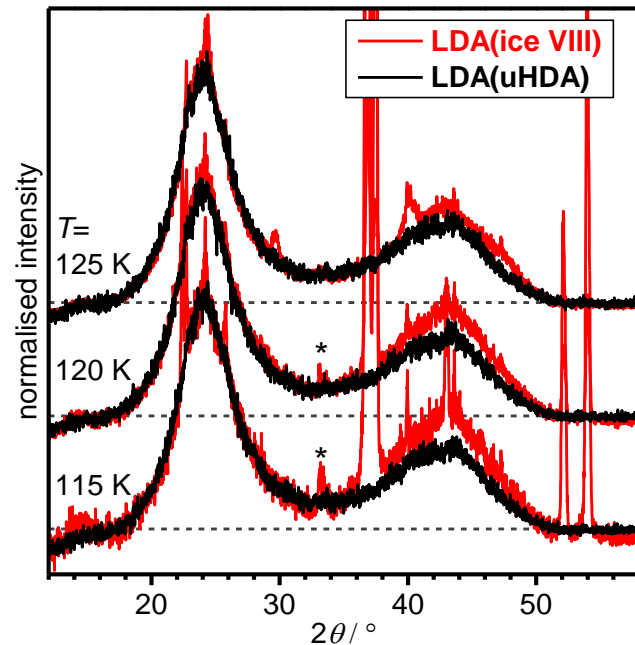
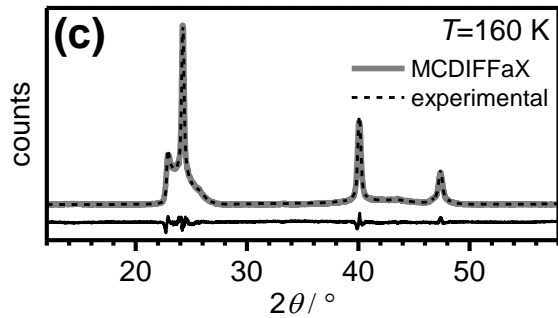
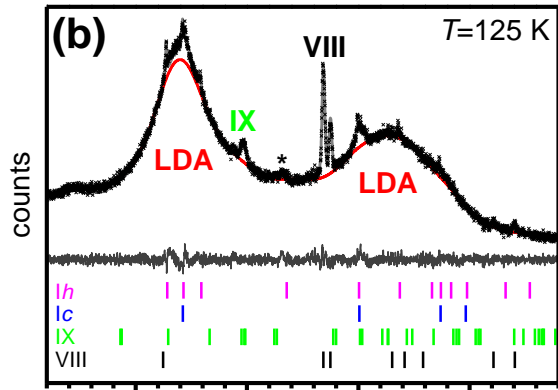
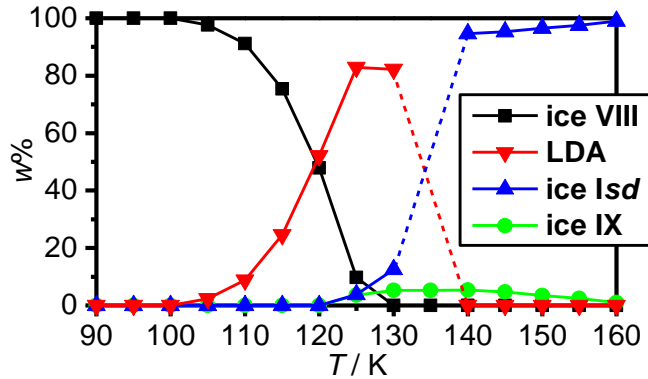
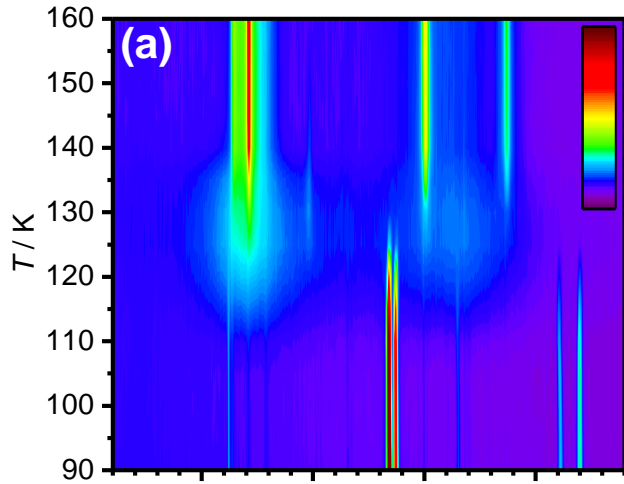
Shortening of the average O-O distance and narrowing of the O-O distance distribution.

LDA from ice VIII



Preparation of ice VIII at 2.5 GPa followed by heating at ambient pressure. LDA forms upon heating at ambient pressure (Klug *et al.*).

A new structural relaxation pathway of LDA



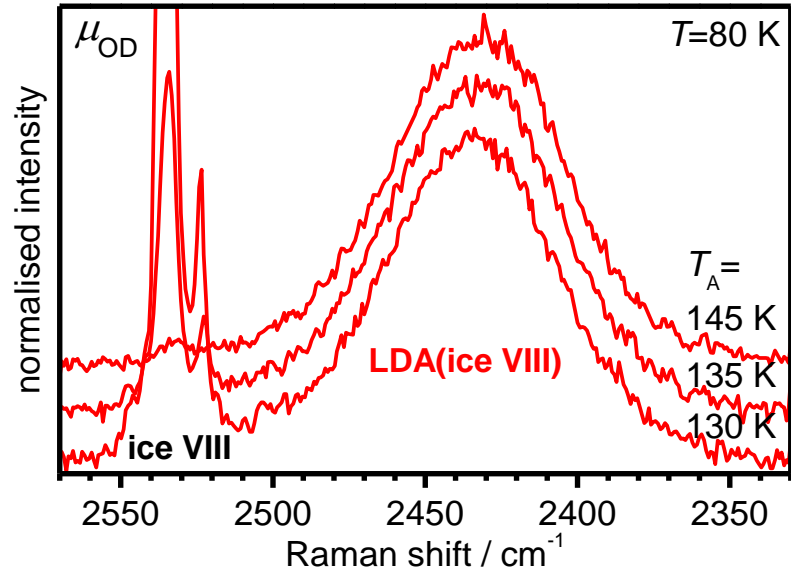
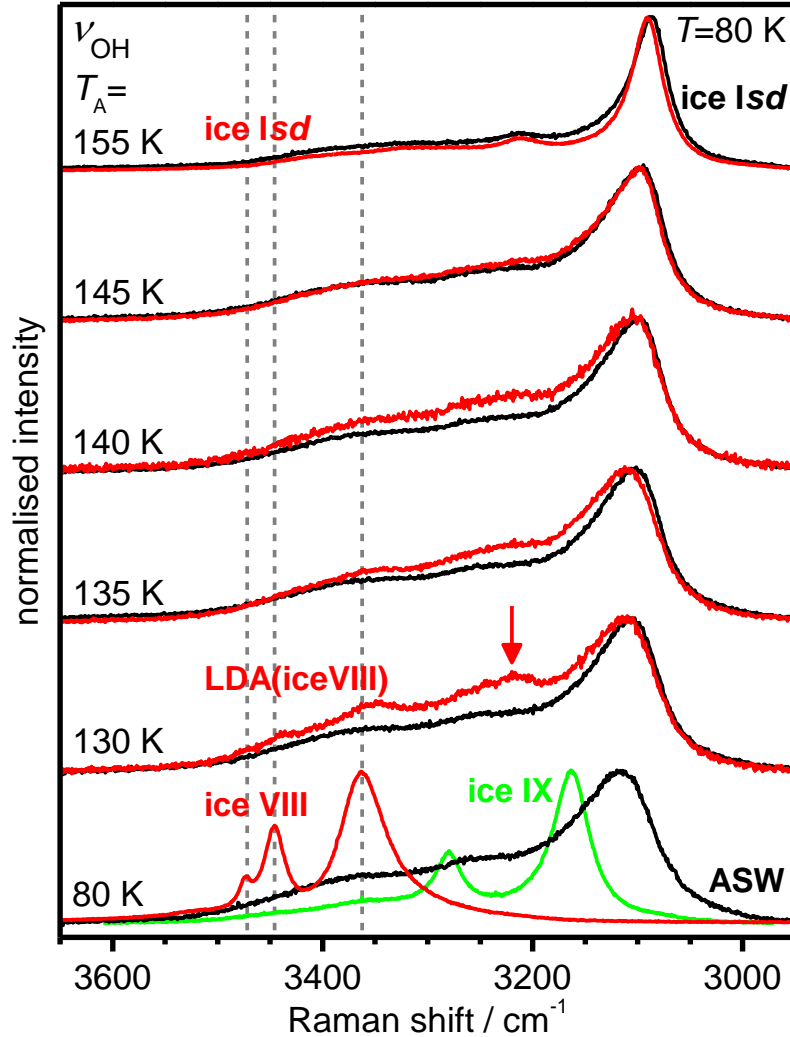
Apart from LDA the formation of ice IX is observed.

LDA from ice VIII is structurally different from LDA from uHDA.

Both kinds of LDA show structural relaxation upon heating.

The relaxation pathways seem to approach each other.

Raman spectroscopy of LDA(ice VIII)



Annealing LDA(ice VIII) leads to an increase in structural order on the intermediate length scale.

Compared to the more 'traditional' forms of LDA, the local structure of LDA(ice VIII) is more ordered initially and becomes more disordered upon heating.

Suspicion that not all degrees of freedom are unfrozen during the glass transition of LDA.

Extension of the glass-transition terminology

Kauzmann: The phenomenon of the glass transition is not restricted to liquids but is, in principle, possible for all noncrystalline materials.

W. Kauzmann, Chem. Rev. 43 (1948) 219.

glassy liquids	translational disorder	rotational disorder
glassy crystal	translation order	rotational disorder
glassy liquid crystals	translation disorder	rotational order

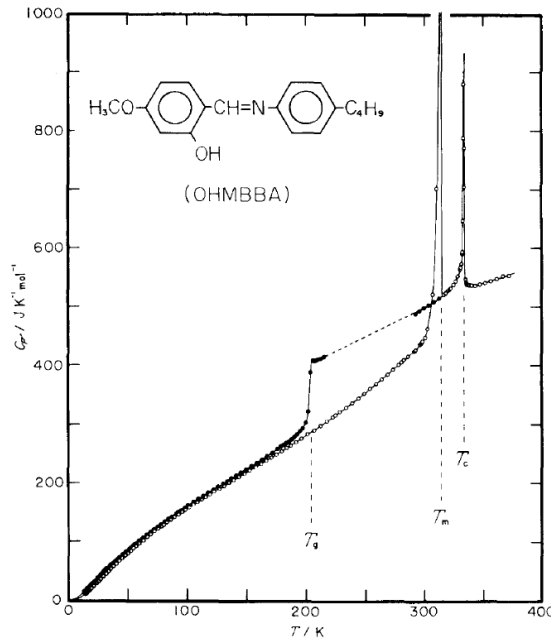
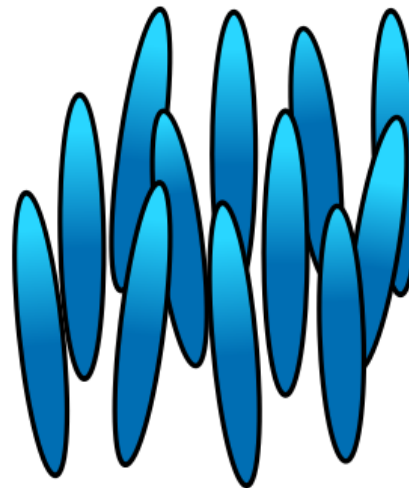
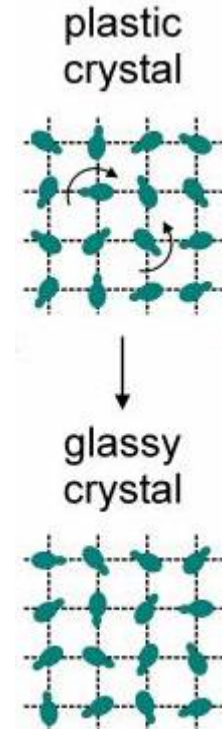


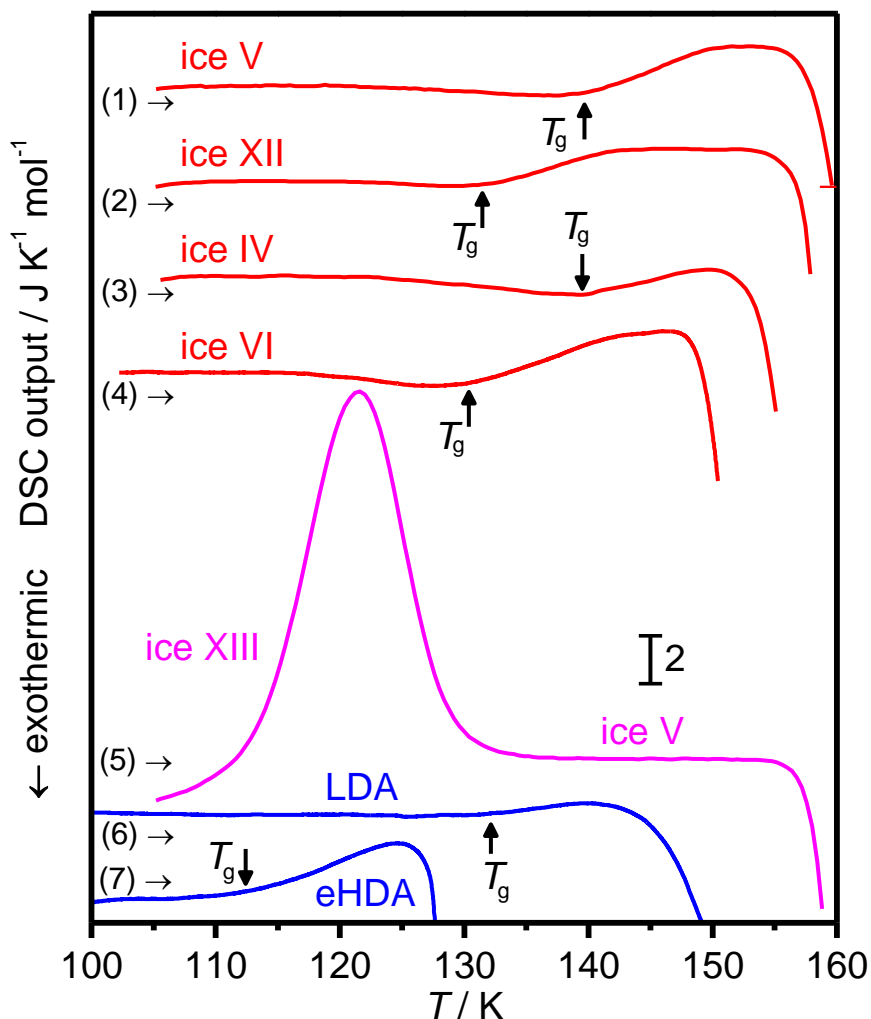
Fig. 12. Heat capacity versus temperature curve of OHMBBA.



Liquid crystal



Glass transitions of hydrogen-disordered ice



The hydrogen-disordered crystalline ices show glass transitions.

Correspond to kinetic unfreezing of reorientation dynamics.

No feature in case of HCl-doped ice V.

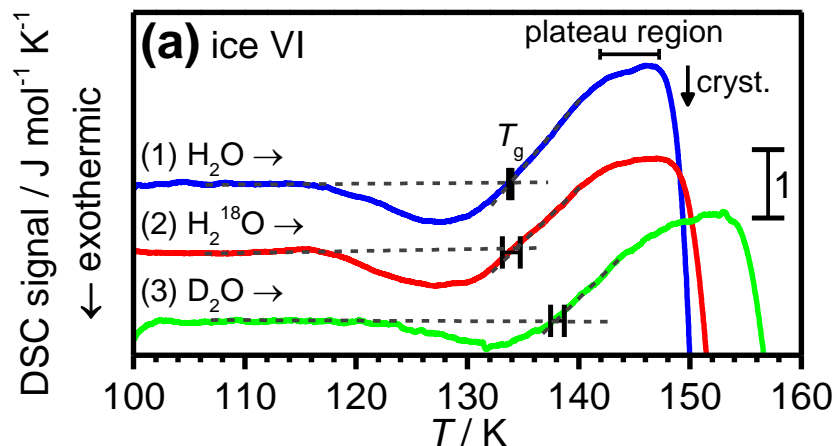
Similar features are observed for the amorphous ices LDA and eHDA.

Have been assigned to the glass-to-liquid transitions.

Glass transitions with similar ΔC_p values have also been observed for inorganic hydrates and clathrate hydrates.

Is the underlying mechanism the same for all these glass transitions?

Molecular reorientation dynamics of ice VI

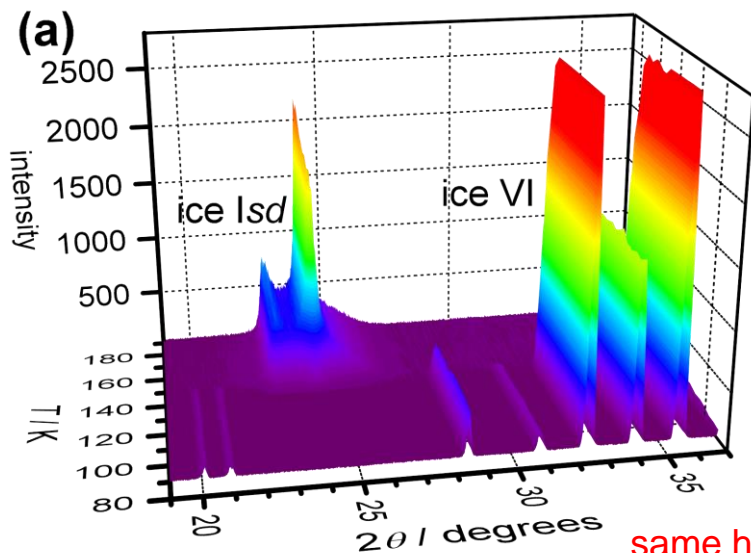


T_g of ice VI stays fixed upon going from H₂O to H₂¹⁸O but shifts towards higher temperature upon going from H₂O to D₂O.

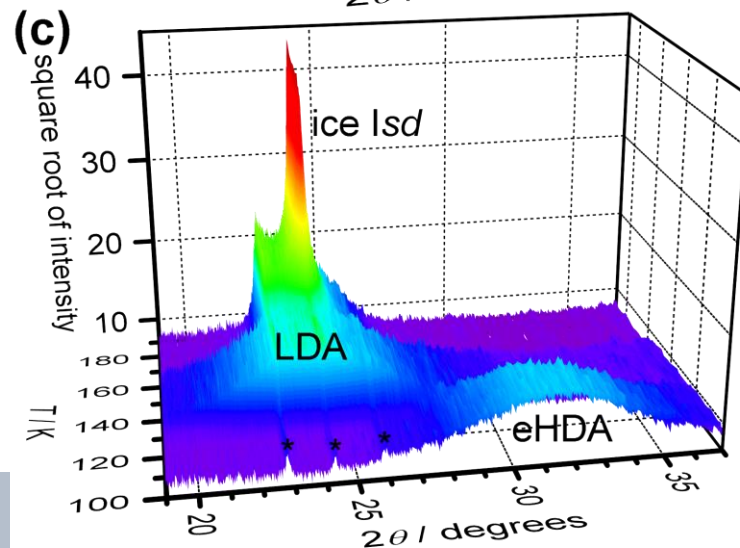
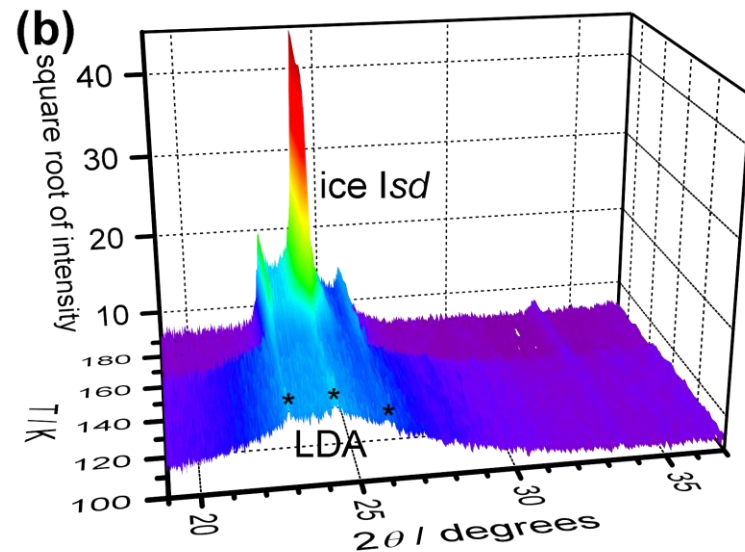
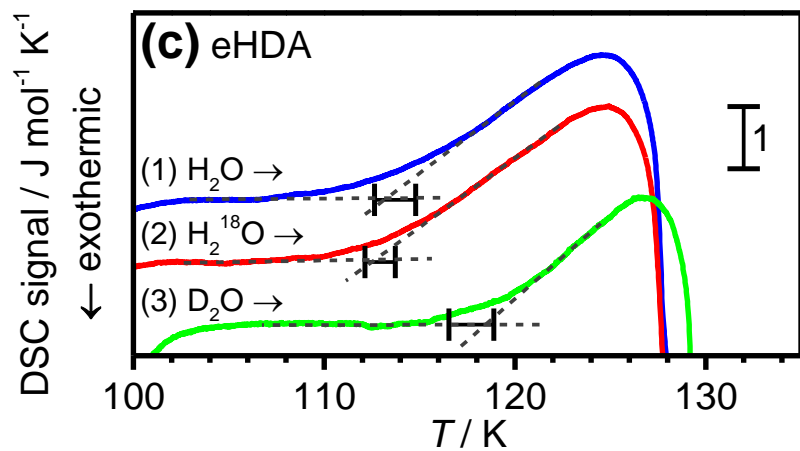
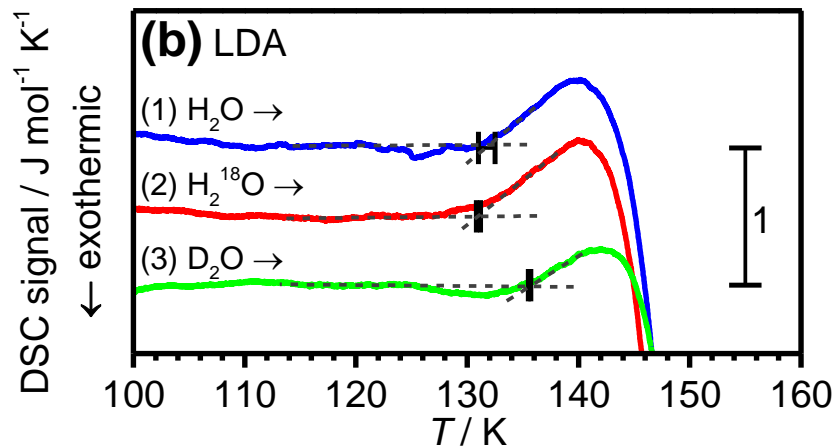
Going from H₂O to H₂¹⁸O or D₂O increases the molecular weight from 18 to 20 g mol⁻¹ in both cases.

The observed isotopic shift pattern is consistent with a change in reorientation dynamics and no translational diffusion.

The absence of translational diffusion at and above T_g is also confirmed by XRD.



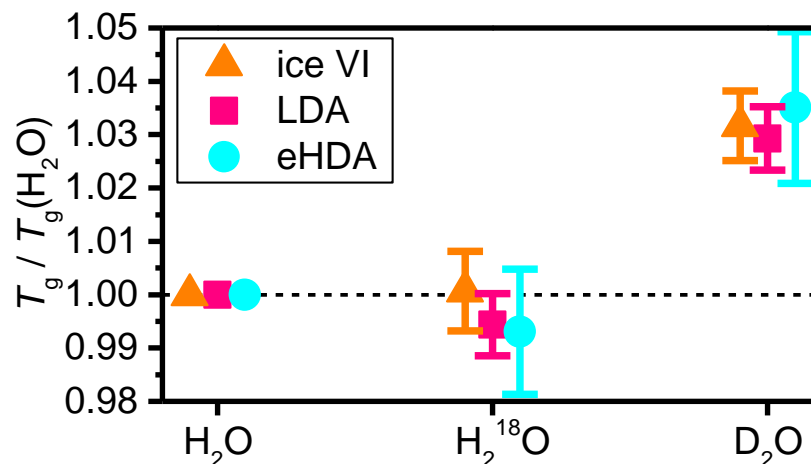
Isotopic shift patterns of LDA and eHDA



Amorphous samples are well-relaxed.
LDA and eHDA show the same isotopic shift
pattern as ice VI.

same heating rate as DSC

Nature of the amorphous ices



The glass transitions of the amorphous ices are governed by molecular reorientation processes.

Mechanism of molecular reorientation in the ices is thought to be defect mediated and therefore highly cooperative.

Diffusion processes in the amorphous ices and liquid water are very different which explains their *strong* and *fragile* properties.

Water is a *fragile* molecular liquid - the amorphous ices are *strong* network materials.

The "reorientation scenario" seems to resolve the previous controversies.

see also: M. Fisher, J.P. Devlin, J. Phys. Chem. 99 (1995) 11584.

Unfreezing of translation diffusion is the *strong* to *fragile* transition.

Acknowledgement

UCL



+ John Finney, Ben Slater, Angelos Michaelides

Leeds: Ben Murray, Tamsin Malkin, Thomas Whale

Durham: Stewart Clarke

Oxford: Paolo Radaelli

Zurich: Peter Hamm, Halina Tran **Innsbruck:** Erwin Mayer

Rome: Carla Andreani, Roberto Senesi, Giovanni Romanelli,
Alexandra Parmentier